

UNIVERSITI TEKNOLOGI MALAYSIA

DECLARATION OF THESIS / ~~UNDERGRADUATE PROJECT PAPER AND COPYRIGHT~~

Author's full name : GAMBO HARUNA YUNUSA

Date of birth : 25TH JANUARY, 1980

Title : INFLUENCE OF RAINFALL INFILTRATION AND EVAPORATION ON
SUCTION DISTRIBUTION IN SOIL MASS AND SLOPE STABILITY

Academic Session : 2010/2011

I declare that this thesis is classified as:

CONFIDENTIAL

(Contains confidential information under the Official Secret Act 1972)*

RESTRICTED

(Contains restricted information as specified by the organization where research was done)*

OPEN ACCESS

I agree that my thesis to be published as online open access (full text)

I acknowledged that Universiti Teknologi Malaysia reserves the right as follows:

1. The thesis is the property of Universiti Teknologi Malaysia.
2. The Library of Universiti Teknologi Malaysia has the right to make copies for the purpose of research only.
3. The Library has the right to make copies of the thesis for academic exchange.

Certified by:

SIGNATURE

201007M10132/A01961279
(NEW IC NO. /PASSPORT NO.)

Date: 12 July 2011

SIGNATURE OF SUPERVISOR

ASSOC. PROF. DR. NURLY GOFAR
NAME OF SUPERVISOR

Date: 19 July 2011

NOTES : * If the thesis is CONFIDENTIAL or RESTRICTED, please attach with the letter from the organization with period and reasons for confidentiality or restriction.

“I hereby declare that I have read this project report and in my opinion this report is sufficient in terms of scope and quality for the award of the degree of Master of Engineering (Civil – Geotechnics)”

Signature :
Name of Supervisor : ASSOC. PROF. DR. NURLY GOFAR
Date : 12th July, 2011

INFLUENCE OF RAINFALL INFILTRATION AND EVAPORATION ON
SUCTION DISTRIBUTION IN SOIL MASS AND SLOPE STABILITY

GAMBO HARUNA YUNUSA

A project report submitted in partial fulfillment of the
requirements for the award of the degree of
Master of Engineering (Civil – Geotechnics)

Faculty of Civil Engineering
Universiti Teknologi Malaysia

JULY 2011

I declare that this project report entitled “*Influence of Rainfall Infiltration and Evaporation on Suction distribution in Soil Mass and Slope Stability*” is the result of my own study except as cited in the references. The project report has not been accepted for any degree and is not concurrently submitted in candidature of any other degree.

Signature :

Name : GAMBO HARUNA YUNUSA

Date : 12th JULY, 2011

*Dedicated to my Mother and my late father Haruna Yunusa, May Allah (SWT)
forgive all his sins and May He makes Jannatul Firdaus to be His final abode
(Ameen)*

And

All my family members, teachers right from childhood up to now and friends

ACKNOWLEDGEMENT

Alhamdu Lillahi Rabbil Alameen, all thanks are due to Allah Who in His infinite mercy gave me the strength, ability and courage to complete my course work and thesis successfully. I would like to express my sincere gratitude and appreciation to my able supervisor; Assoc. Prof. Dr. Nurly Gofar for taken her time to guide, help and encourage me right from the beginning up to the end of this work. I am really very proud to be Your student. Thank You for Your generosity and readiness to help at all time.

Similarly, i want extend my warm regards to Assoc. Prof. Ir. Azman Kassim and Bimo Brata Adhitya for their advice and contributions during the modelling stage. Similarly, Engr. H. M. Alhassan and Engr. Salisu Dan'azumi for their guide and help through out the study period.

I would like to acknowledge the support of Department of Irrigation and Drainage, Kuala Lumpur Malaysia, especially Chik Khairul Fadzila Bint Muhammad Omar for supplying the rainfall and evaporation data used in the analyses.

Lastly, I want thank my wife; Zainab Umar Muhammad and my Daughter Aishah for their patience and understanding through out my stay away from home and all my family members especially Hassana Haruna and all my friends for their support and prayers. May Allah reward all of You.

ABSTRACT

Rainfall infiltration is one of the major factors that lead to slope instability in unsaturated soils. The infiltration leads to the decrease of suction and hence causes the reduction in shear strength of the soil. On the other hand, evaporation dries the soil mass which invariably increases suction resulting in increasing the shear strength of the soil and the factor of safety of the slope. Therefore this study is aimed at determining the combined effect of these two processes on suction distribution and the slope stability. Transient seepage analyses were carried out using commercial finite element software SEEP/W, (GeoSlope, 2007) with rainfall infiltration data as control and then with differences between the rainfall infiltration and evaporation data. Residual water content was assigned at the beginning of all analyses. The pore-water pressure distributions generated from these analyses were transported to SLOPE/W, (GeoSlope, 2007) where the factor of safety of the slope for aforementioned cases were determined. The result shows that there is decrease in soil suction with rainfall infiltration which resulted in decrease in FOS of the slope. On the other hand the suction increases when the difference between the infiltration and evaporation is negative (i.e., drying of the soil) resulting in increasing the FOS but when the difference is positive (i.e., wetting of the soil) the FOS decreases. Evaporation hindered the reduction of soil suction within the soil mass due to rainfall infiltration, thus; gives a positive effect on slope stability. The effect of evaporation is more significant during the wet period than dry period.

ABSTRAK

Penyusupan air hujan ke dalam tanah tidak tepu adalah salah satu faktor utama ketidakstabilan cerun kerana penyusupan menyebabkan pengurangan tekanan sedutan yang menghasilkan penurunan kekuatan ricih pada tanah. Sebaliknya, proses penyejatan akan mengeringkan tanah mengakibatkan kekuatan ricih tanah dan juga faktor keselamatan cerun bertambah. Kajian ini ditumpu pada kesan paduan yang berlaku akibat proses penyusupan air hujan dan penyejatan pada taburan sedutan dan kestabilan cerun. Analisis resipan fana dilakukan menggunakan perisian komersial unsur terhingga SEEP/W (Geo-Slope, 2007) dimana data penyusupan air hujan digunakan sebagai kawalan dan data berikutnya adalah perbezaan antara penyusupan air hujan dan juga penyejatan. Kandungan air baki diwujudkan sebagai keadaan awal bagi setiap analisis. Akhirnya, taburan tekanan air liang yang diperolehi dari analisis ini dipindahkan ke SLOPE/W (Geo-Slope, 2007) dimana faktor keselamatan cerun dapat ditentukan. Keputusan kajian menunjukkan bahawa pengurangan pada sedutan tanah akan mengakibatkan pengurangan faktor keselamatan cerun. Sedutan tanah meningkat apabila perbezaan antara penyusupan dan penyejatan adalah negatif (pengeringan tanah) mengakibatkan kenaikan faktor keselamatan cerun. Sebaliknya, apabila perbezaan ini adalah positif (tanah menjadi basah), sedutan tanah berkurangan menyebabkan faktor keselamatan juga berkurangan. Penyejatan menghalang pengurangan tekanan sedutan semasa proses penyusupan air hujan, sekali gus memberikan kesan positif ke atas kestabilan cerun. Kesan sejatan adalah lebih ketara dalam tempoh basah daripada tempoh kering.

TABLE OF CONTENTS

CHAPTER	TITLE	PAGE
	DECLARATION	ii
	DEDICATION	iii
	ACKNOWLEDGEMENTS	iv
	ABSTRACT	v
	ABSTRAK	vi
	TABLE OF CONTENTS	vii
	LIST OF TABLES	x
	LIST OF FIGURES	xi
	LIST OF SYMBOLS	xiv
	LIST OF APPENDICES	xv
1	INTRODUCTION	1
	1.1 Background	1
	1.2 Problem Statement	3
	1.3 Aims and Objectives	3
	1.4 Scope and Limitations	4
2	Literature Review	5
	2.1 Introduction	5
	2.2 Rainfall Infiltration in Soil	6
	2.2.1 Mechanism of Water Movement at the Wetting Front	7
	2.2.2 Seepage Flow through Unsaturated Soil	8
	2.3 Evaporation	9
	2.3.1 Soil Drying During Evaporation	10
	2.4 Soil Suction	12
	2.4.1 Components of Soil Suction	12

	2.4.2 Matric Suction Profile	13
	2.4.3 Measurements of Suction	15
	2.5 Unsaturated Soil Properties Related to Seepage Flow	15
	2.6 Slope Stability	18
	2.6.1 Slope Stability Analysis	22
	2.6.2 Unsaturated Slope Stability	23
3	Methodology	25
	3.1 Introduction	25
	3.2 Data Collection and Analyses	29
	3.2.1 Rainfall and Evaporation Data	29
	3.2.2 Soil Properties	29
	3.2.2.1 Particle Size Distribution	30
	3.2.2.2 Saturated Permeability of the Soil	31
	3.2.2.3 Soil-Water Characteristics Curve (SWCC) and Hydraulic Conductivity	33
	3.2.2.4 Shear Strength Parameters	33
	3.3 Seepage Analyses	34
	3.3.1 Steady-State Seepage Analysis	35
	3.3.2 Transient Seepage Analysis	40
	3.4 Slope Stability Analysis	41
	3.4.1. Factor of Safety	42
4	Results and Discussions	48
	4.1 Introduction	48
	4.2 Preliminary Data	49
	4.2.1 Rainfall and Evaporation Data	49
	4.2.2 Soil Properties	53
	4.3 Seepage Analysis	57
	4.3.1 Suction Distribution in February	58
	4.3.2 Suction Distribution in June	64
	4.3.3 Suction Distribution in March	70
	4.3.4 Suction Distribution in December	76
	4.4 Slope Stability Analyses	82
	4.4.1 Factor of Safety Variations in February	82
	4.4.2 Factor of Safety Variation in June	84

	4.4.3 Factor of Safety Variation in March	86
	4.4.4 Factor of Safety Variation in December	88
	4.5 Discussion	90
5	Conclusions and Recommendations	977
	5.1 Introduction	97
	5.2 Conclusion	97
	5.3 Recommendations	98
	References	99
	Appendices	103 - 125

LIST OF TABLES

TABLE NO.	TITLE	PAGE
2.1	Summary of Suction Measurement devices	19
2.2	Methods of Slope Stability Analysis	24
2.3	Experimental values of ϕ^b	25
3.1	Station for Rainfall and Evaporation in Johor State	29
3.2	Basic Soil Properties for Slope Stability analyses	42
4.1	Soil Properties for Slope Stability analyses	56

LIST OF FIGURES

FIGURE NO.	TITLE	PAGE
2.1	Typical (a) time dependent rate and (b) cumulative infiltration Curve	7
2.2	Schematic of saturated zone, transmission zone, and wetting front	8
2.5	Typical SWCC for drying and wetting conditions	17
3.1	Flow chart of the study	27
3.2	Geometry of the Slope (infinite slope)	28
3.3	Schematic diagram of falling head permeability test	32
3.4	Keyin of (a) material property of the soil and (b) hydraulic conductivity function	35-36
3.5	Applied region to the geometry of the slope	37
3.6	Assigned materials in the slope	37
3.7	Key-in of (a) boundary conditions to the slope geometry and (b) Positions of the boundary conditions	38
3.8	Verification and Solution windows	39
3.9	Seepage pattern and pore-water head profile	40
3.10	Key-in of material property in Transient analysis (SWCC)	41
3.11	Slip surface option	44
3.12	Entry and Exit Points range	44 - 45
3.13	Key-in of material properties	45 - 46
3.14	Assigned material properties to the geometry	46
3.15	Solve dialog box	47
3.16	FOS of the slope	47
4.1	Yearly intensities (a) Rainfall, (Evaporation) and (c) Difference	50

4.2	Rainfall intensity (a) February, (b) March, (c) June and (d) December	51
4.3	Evaporation intensity (a) February, (b) March, (c) June and (d) December	52
4.4	Particle size distribution curve	54
4.5	Soil Water Characteristics Curve (SWCC)	55
4.6	Hydraulic conductivity curve	56
4.7	Slope model	57
4.8	Seepage patterns and pore-water pressure head profile on (a) 1 st , (b) 4 th , (c) 19 th and (d) 28 th	59
4.9	Suction and infiltration variations with depth and time	60
4.10	Seepage pattern and pore-water pressure profile on (a) 1 st , (b) 4 th , (c) 19 th and (d) 28 th	62
4.11	Suction and infiltration variations with depth and time	63
4.12	Seepage pattern and pore-water pressure head profile on (a) 1 st , (b) 14 th , (c) 22 nd and (d) 30 th	65
4.13	Suction distributions with depth and time for June	65
4.14	Seepage pattern and pore-water pressure head profile on (a) 1 st , (b) 14 th , (c) 22 nd and (d) 30 th	68
4.15	Suction distributions with depth and time for June	69
4.16	Seepage pattern and pore-water pressure head profile on (a) 1 st , (b) 9 th , (c) 15 th and (d) 31 st	71
4.17	Suction distributions with depth and time for March	73
4.18	Seepage pattern and pore-water pressure head profile on (a) 1 st , (b) 9 th , (c) 14 th and (d) 31 st	74
4.19	Suction distributions with depth and time for March	75
4.20	Seepage pattern and pore-water pressure head profile (a) 3 rd , (b) 17 th , (c) 20 th and (d) 31 st	77
4.21	Suction distributions with depth and time	78
4.22	Seepage pattern and pore-water pressure head profile (a) 3 rd , (b) 17 th , (c) 20 th and (d) 31 st	80
4.23	Suction distributions with depth and time	81
4.24	Correlation of Infiltration and Difference and the FOS with time in February	83

4.25	Correlation of Infiltration and Difference and the FOS with time in June	86
4.26	Correlation of Infiltration and Difference and the FOS with time in March	87
4.27	Correlation of Infiltration and Difference and the FOS with time in December	89
4.28	Suction distributions with depth due infiltration and infiltration and evaporation, (a) February, (b) March, (c) June and (d) December	92
4.29	Suction distributions due infiltration and infiltration and evaporation, (a) February, (b) March, (c) June and (d) December	92
4.30	Variation of FOS with time due to Infiltration and Infiltration and Evaporation (a) February, (b) March, (c) June and (d) December	95

LIST OF SYMBOLS

FOS	Factor of Safety
A	Area
D, d	Diameter
c	Cohesion
c'	effective cohesion
ϕ	Angle of internal friction
ϕ'	Effective angle of internal friction
h	depth of water table
ϕ^b	Unsaturated friction angle
γ	Unit weight of soil
u_a	pore air pressure
u_w	pore water pressure
τ	Shear stress
K_s	saturated hydraulic conductivity
θ_r	Residual water content
AEV	Air entry value
k_x, k_y	coefficient of permeability
θ_w	Volumetric water content
ψ	Suction
AE	actual evaporation
PE	potential evaporation
H	height of specimen
L	distance between manometers
V	volume of specimen
PSD	particle size distribution

LIST OF APPENDICES

APPENDIX	TITLE	PAGE
A	Rainfall and Evaporation Data	103
B	Test Results of Soil Properties	111
C	Results of Seepage Analyses	114
D	Results of Slope Stability Analyses	122

CHAPTER 1

INTRODUCTION

1.1 Background

Rainfall infiltration has been identified by many researchers as one of the major factor that contributes to slope failure. The problem of rainfall induced slope failure pose major geotechnical hazards and cause severe damage in many part of the world (Ng and Shi, 1998). Cho and Lee (2001) stated that the slope failure occur most frequently during wet period when there is an increase in moisture content. The increase in moisture content will result in decrease in matric suction and increase in pore water pressure effectively decreases shear strength of the soil making it more susceptible to failure (Rahardjo, 2000). Furthermore, rainfall infiltration increases the disturbing force and decreases the resisting force provided by the additional shear strength induced by matric suction, and this results in slope failure. The consequences of the slope failure can be catastrophic which may result in loss of life and economic losses.

Several researches conducted on the influence of intensity and duration of rainfall on slope stability. Studies carried out by Cho and Lee (2001), Gofar, *et al.* (2006), Kassim, *et al.* (2006), Ng and Shi (1998), Rahardjo, *et al.* (2001), Taik and Vanapalli (2010) and many others have all confirmed the influence of rainfall infiltration as the major triggering factor to slope instability, especially in tropical and sub-tropical countries experiencing abundant of rainfall through-out the year. In tropical and sub-tropical countries where the ground surface is covered by residual soil, the water table is at great depth, thus the subsurface soil is in unsaturated

condition and the near surface soil experience negative pore-water pressure (i.e., suction).

The infiltration of rainwater results in significant changes of pore pressure distribution in unsaturated soil. A Point close to the ground surface will response faster to the infiltration than another point at deeper elevation. However, the point close to the ground surface will also be influenced by evaporation process. The difference between the downward flux (i.e., precipitation) and the upward flux (i.e., evaporation and transpiration) have greater importance on the suction distribution close to the ground surface, this is so because the former saturates the soil while the latter dry the soil mass. In extreme cases, a net upward flux produces a gradual drying, cracking and desiccation of a soil mass, whereas a net downward flux eventually saturates a soil mass. The gradual drying, cracking and desiccation of soil mass resulted from the net upward flux (i.e., evaporation or transpiration) may leads to the formation of tension cracks at the crest of the slope and water can seep through this tension cracks and trigger slope failure (Gofar *et al.* 2006).

Despite of many researches carried out on the influence of rainfall patterns (intensity and duration) on slope stability, the effect of evaporation in gradual drying of the soil mass and reducing the quantity of rain that infiltrates in to the soil slope has not been studied in detail. An attempt has been made by Kassim *et al.* (2011) to look at the effect of evaporation. They used constant evaporation of 5 mm/day in their analysis and concluded that the effect of evaporation is more significant during wet condition than dry condition.

The rate of evaporation from the slope surface may be affected by some factors such as the variation of solar radiation, slope angle etc. Solar radiation is a climatic factor that varies from one region to another. For instance, in tropical countries the temperature remains uniformly hot throughout the year. The days are however not very hot and nights are fairly cool throughout the year. Therefore, the rate of evaporation will be high when the temperature is high and vice versa. Besides, the rate varies between the day and night time, being high during the day time and low during the night time or in the early morning hours. Furthermore, the

actual evaporation from a given soil surface is strongly affected by moisture availability, with more evaporation occurring where there is more moisture available, and it is typical to find higher moisture contents near the toe of a slope than at crest. Therefore, variation of evaporation should be considered for the analysis of suction distribution in soil and its effect on slope stability.

1.2 Problem Statement

It has been established that rainfall infiltration trigger slope failures by inducing the increase in moisture content and reducing or eliminating matric suctions. However, the distribution of matric suction is also known to be influenced by evaporation process. Despite of many works done on the influence of rainfall infiltration on slope stability, not much effort have been given to combine the effect of rainfall infiltration and evaporation on slope stability. The difference between the downward flux (i.e., precipitation) and the upward flux (i.e., evaporation and transpiration) is thought to have influence on the suction distribution in soil especially near ground surface. Therefore, this study gave insight on the combine effect of rainfall infiltration and evaporation on suction distribution and the slope stability.

1.3 Aims and Objectives

The aim of this study is to determine the influence of rainfall infiltration and evaporation on suction distribution in soil mass and the slope stability. The aim can be achieved through the following objectives:

- 1 To investigate the effect of rainfall infiltration and evaporation on pore water pressure distribution in the slope.
- 2 To investigate the seepage pattern in the slope by carrying out transient seepage analyses using rainfall infiltration data as control and the difference between rainfall infiltration and evaporation data using a finite element software; SEEP/W (GeoSlope International Ltd., 2007).

- 3 To determine the factor of safety of the slope using the seepage pattern and pore-water pressure generated from (2) above by using SLOPE/W (GeoSlope International Ltd., 2007).

1.4 Scope and Limitations

This study was conducted with rainfall and evaporation data of Loji Air Sungai Layang station, Johor Bahru for period of one year. The data was provided by Department of Irrigation and Drainage, Kuala Lumpur. Average value was used in place of some missing data.

Soil sample was collected at the respected location to determine soil properties required for data analysis. Particle size distribution curve was used to predict SWCC required for seepage analysis from various curves given in the function library of SEEP/W software. The Hydraulic conductivity function was subsequently predicted based on saturated permeability of the soil and the SWCC by using Fredlund and Xing model.

CHAPTER 2

LITERATURE REVIEW

2.1 Introduction

Rainfall infiltration has been identified by many researchers as one of the major factor that contributes to slope failure. According to Cho and Lee (2001) the slope failure occur most frequently during wet period when there is an increase in moisture content and a decrease in matric suction because the additional shear strength provided by the matric suction can be reduced enough to trigger the slope failure. The infiltration of water from rainfall results in significant changes of pore pressure distribution in unsaturated soil, resulting in decreasing the shear strength of the soil which can lead to slope instability. These problems of rainfall induced slope failure pose major geotechnical hazards and cause severe damage in many part of the world (Ng and Shi, 1998). The problem is more peculiar and more frequent in regions characterized with high amount of rainfall through out the year, because the rainfall infiltration leads to the decrease in soil suction which results in decrease in shear strength of the soil and this can cause slope failure. Thus, rainfall infiltration increases the disturbing force and the resisting force provided by the shear strength will be decrease by decrease in soil suction, and this will result in causing slope failure. The consequences of the slope failure often used to be catastrophic which may result in loss of life and economic losses. Yet, it is impractical to flatten the slope to achieve greater stability. Therefore it is the responsibilities of the engineers to exploit all the major causes of slope failure in order to alleviate these problems.

2.2 Rainfall Infiltration in Soil

When rain water falls on the surface of soil, either some part or even whole of it may penetrate in to the soil as infiltration. The quantity that penetrates and distribute in to the soil mass depends on the moisture condition of the soil prior to the rainfall event, the rainfall pattern (i.e., the intensity and duration) and the hydraulic conductivity of the soil. The remaining water that does not penetrate in to the soil will flow as runoff. If the surface of the soil has some depressions this water will accumulates in the depressions and later penetrate in to the soil mass while some will go back to the atmosphere as evaporation.

When the initial moisture condition of the soil mass is very low, (e.g., initially dry soil) rainfall rapidly enters into the soil mass. But as the duration of the rainfall event get longer, the rate of infiltration decreases until it reaches a constant rate. This constant rate is also termed as steady state or equilibrium infiltration rate. Figure 2.1 presents a typical time dependent infiltration rate and cumulative infiltration curve. The high initial infiltration rate in Figure 2.1(a) can be explained by large suction gradients. When water is supplied to an initially dry soil, the suction gradients across the soil surface become very high, which results in a high infiltration rate. As the wetting front moves downward, the suction gradient across the soil profile decreases, which limits the rate of water infiltration into the soil surface. Eventually, after a long time, the infiltration rate approaches zero. However, in actual practice, if ponding on soil surface continues for a long time, the infiltration rate gradually becomes steady gravity driven flow and is equal to the saturated hydraulic conductivity (K_s) of the homogeneous rigid soil. The decrease in infiltration rate may also be caused by dispersion of aggregates or slaking, soil compaction and surface sealing, or clogging of soil pores. Slaking is a term used to describe the initial fragmentation of soil aggregates several millimeters in diameter, which may disintegrate further to become micro aggregates.

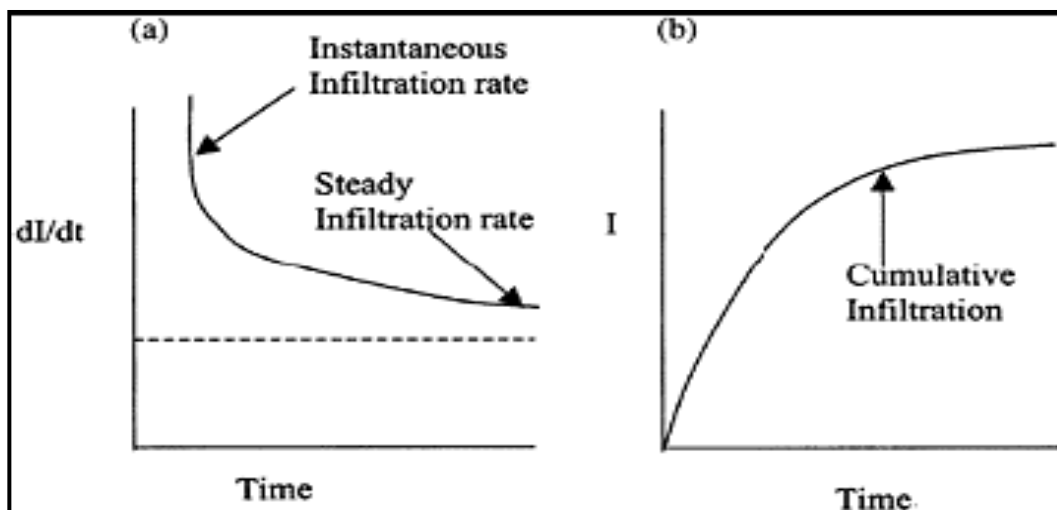


Figure 2.1: Typical (a) time dependent rate and (b) cumulative infiltration curve

2.2.1 Mechanism of Water Movement at the Wetting Front

As long as the rate of water application to the soil surface is less than the instantaneous infiltration rate of soil, all the water infiltrates into the soil profile. Under this circumstance, supply rate determines the infiltration rate and the process of infiltration is called “flux controlled.” On the other hand, if water is applied at a rate higher than the instantaneous infiltration rate of soil, the soil water transmission properties determine the rate of actual infiltration and cumulative infiltration. Under this circumstance, the infiltration is called “profile-controlled.” According to Childs (1969), the infiltration process is dependent upon both hydraulic conductivity (K_s) and the hydraulic gradient ($\Delta H/L$) of the soil profile. Therefore, the entire soil profile rather than just the surface layer governs the infiltration rate in a profile-controlled process. During infiltration, a clear water divide is often seen during the wetted region overlying the drier region. This distinct sharp boundary between wet and dry regions is known as the “wetting front.” A soil-water profile of a homogeneous soil column under ponded infiltration can be divided into three distinct zones: saturated zone ($\theta = s = 1$), transmission zone ($\theta < \theta_s$; $\Delta H/L = 1$), and wetting front as shown in Figure 2.2. The wetting front is a visible wet/dry soil boundary and may be smooth in a clayey soil and a diffused/fingered in a coarse-textured or non-homogeneous soil. The water movement at the wetting front occurs through a condensation-evaporation process. With the advance of the liquid wetting front, the water vapor

moves ahead of the liquid front and condenses. The condensation releases heat of wetting and increases soil temperature in the zone immediately ahead of the liquid wetting front.

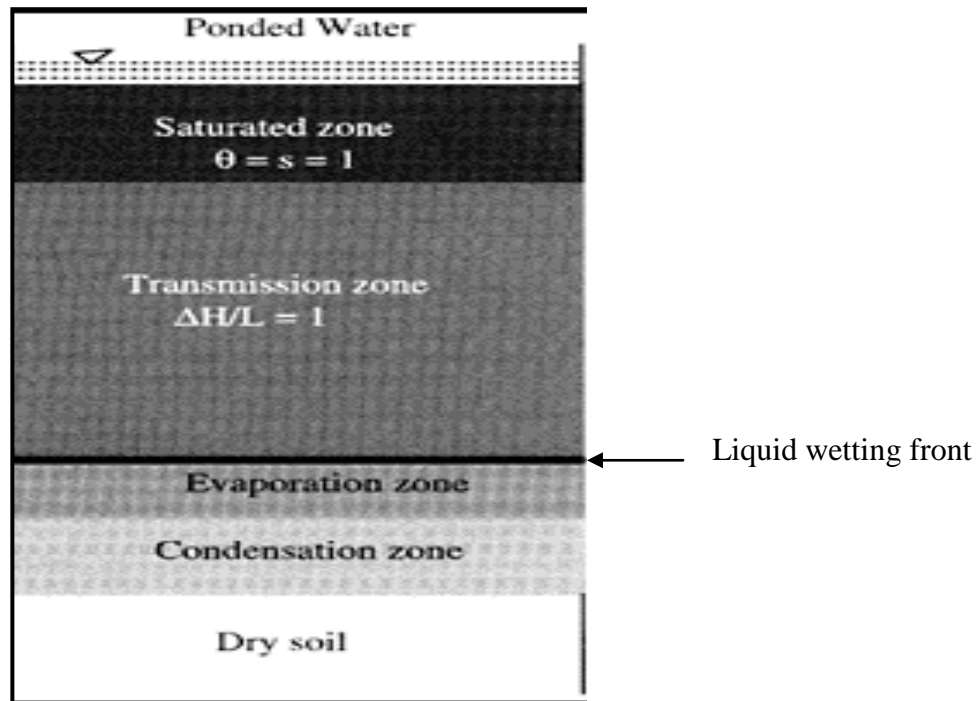


Figure 2.2: Schematic of saturated zone, transmission zone, and wetting front

2.2.2 Seepage Flow through Unsaturated Soil

The flow of water through unsaturated soils can be divided into two; the steady state flow which is a constant water flow and this occurs when the soil is assumed to be either fully dried or fully saturated. This type of water flow is governed by Poisson's equation which combines Darcy's law and continuity equation.

$$\frac{\partial}{\partial x} \left(k_x \frac{\partial h}{\partial x} \right) + \frac{\partial}{\partial y} \left(k_y \frac{\partial h}{\partial y} \right) + q = 0 \quad 2.1$$

Where,

h is the hydraulic head,

k_x, k_y are the coefficients of permeability of the soil along the x and y coordinates, and q is the applied unit flux.

The second type of water flow is called the transient water flow and this is time dependent flow, this type of flow is usually governed by Richard's equation (which takes care of change of volumetric water content with time). This equation is given as:

$$\frac{\partial}{\partial x} \left(k_x \frac{\partial h}{\partial x} \right) + \frac{\partial}{\partial y} \left(k_y \frac{\partial h}{\partial y} \right) + q = m_w^2 \rho_w g \frac{\partial h}{\partial t} \quad 2.2$$

Where; θ_w is the volumetric water content, m_w^2 is the coefficient of volumetric water change with respect to a change in negative pore-water pressure ($u_a - u_w$) and is equal to the slope of the soil-water characteristic curve, ρ_w is the density of water and g is gravitational acceleration.

2.3 Evaporation

Evaporation is the movement of water back to the atmosphere from soil surface or from open water surfaces. Evaporation of water from bare soil (i.e., in the absence of vegetation) is the process by which water is lost from the soil to the atmosphere. The meteorological factors that influence evaporation include; solar radiation, ambient air temperature, humidity, and wind speed. Evaporation is measured by measuring water loss from a pan. Evaporation plays an important role in controlling the water content of soils and is therefore important in variety of geotechnical applications. The accurate prediction of evaporation from sloped soil surface has application for many geotechnical problems, such as evaluating the water balance on sloped soil cover systems, calculating evaporation from earthen dams, and predicting pore-water pressures in soil profile for stability analyses.

Evaporation from a sloped soil surface differs from that over a horizontal surface in at least two regards. First, a sloped surface at a given site will receive a different quantity of net radiation (Q_{net}) over the course of a day. The net radiation received by a soil surface is a major factor controlling the amount of evaporation that will occur, and (Q_{net}) is affected by both the slope steepness and slope direction.

Moisture distribution is a second factor that creates differences in evaporation between sloped and horizontal soil covers. Under a given evaporative demand (as given by the potential evaporation at a site), the actual evaporation from a given soil surface is strongly affected by moisture availability, with more evaporation occurring where there is more moisture available. It is typical to find higher moisture contents near the toe of a slope than at the crest. For sloped soil surfaces, the position along the slope may be related to significant differences in the thickness of the unsaturated zone above the water table and, as a consequence, considerable differences in soil suction. In contrast, the moisture distribution along the length of a horizontal surface is often fairly uniform in engineered soils and is implicitly considered as such when a *I-D* model is used. When evaluating the available methods for the prediction of evaporation from soil surfaces, clear distinctions should be made between the methods for calculating actual evaporation (*AE*), which is the evaporation that actually takes place from the ground surface, and potential evaporation (*PE*), which is the evaporation that could take place if the soil was saturated (i.e., moisture is not limiting). Typically, the moisture availability at a given site will at some point limit the possible rate of evaporation, and the actual evaporation rate will be less than the potential rate.

2.3.1 Soil Drying During Evaporation

Evaporation leads to the loss of water, with attendant drying and depletion of the soil moisture reserves. This process of soil drying occurs in three distinct stages.

Stage 1: Initial Stage

When soil is very wet, evaporation of soil water is governed by external atmospheric conditions rather than soil properties. The soil has enough water; therefore, conductivity and supply of water to soil surface are at the potential rate. The evaporation rate during this stage is denoted as “potential evaporation.” This stage is sustained over time because as the water content of soil profile decreases the hydraulic conductivity also decreases. However, hydraulic gradient increases and

compensates for the reduction in hydraulic conductivity. This situation is analogous to the flux-controlled stage of water infiltration into soil. Some soil properties, which influence the meteorological or atmospheric factors, include soil surface reflectance, mulch, ground cover, etc. The duration of the first stage of the drying process is lower for coarse-textured than fine-textured soils because fine-textured soils retain high water content and have more conductivity than coarse-textured soils.

Stage 2: Intermediate Stage

The evaporation rate during this stage is no longer at the potential rate but starts decreasing gradually with time. Soil starts to heat up and is not able to conduct water to the surface at the potential rate. The water content of the soil profile is decreased further as is the hydraulic conductivity. The hydraulic gradient can no longer increase significantly because the soil water pressure head is close to the partial water vapor pressure. The time at which the decrease in hydraulic conductivity is not compensated by hydraulic gradient denotes the end of first stage of drying. The depth of dry zone increases as does the hydraulic resistance of soil to water transport. The rate of evaporation during this stage is directly proportional to soil water diffusivity.

Stage 3: The Final Stage

The evaporation rate during this stage is relatively steady at a low rate and can continue up to several days. During this stage the liquid-water conductance totally ceases. This stage is also known as the vapor diffusion stage, since water transmission is primarily due to a slow process of vapor diffusion. The evaporation rate is determined by soil properties (affinity of the soil for water) rather than the evaporative demand of the atmosphere.

2.4 Soil Suction

Soil suction is commonly referred to as the free energy state of soil water (Fredlund and Rahardjo, 1993), and it can be measured in terms of the partial vapor pressure of the soil water. The thermodynamic relationship between soil suction and the partial pressure of the pore-water vapor can be written as follows:

$$\psi = \frac{RT}{v_{w0}\omega_v} \ln \left(\frac{\bar{u}_v}{\bar{u}_{vo}} \right) \quad 2.3$$

Where

ψ = Soil suction or total suction (kPa)

R = Universal gas constant [i.e. 8.31432 J/(mol K)]

T = absolute temperature [i.e. $T = (273.16 + t^0)$ (K)]

t^0 = temperature (^0C)

v_{w0} = specific volume of water or the inverse of the density of water

[i.e., $(1/\rho_w)$ (m^3/kg)]

ρ_w = density of water (i.e. $998\text{kg}/\text{m}^3$ at $t^0 = 20^0\text{C}$)

ω_v = molecular mass of water vapor (i.e. $18.016 \text{ kg}/\text{kmol}$)

\bar{u}_v = partial pressure of pore-water vapor (kPa)

\bar{u}_{vo} = saturation pressure of water vapor over a flat surface of pure water at the same temperature (kPa).

From this equation the reference state for quantifying the components of suction is the vapor pressure above a flat surface of pure water (i.e., water with no salts or impurities).

2.4.1 Components of Soil Suction

The soil suction given in the above equation (2.5) which is quantified in terms of relative humidity is called “total suction.” Total suction has two

components; the matric suction and the osmotic suction. The equation of total suction is given as:

$$\psi = (u_a - u_w) + \pi \quad 2.4$$

Where

$(u_a - u_w)$ = matric suction

u_a = pore air pressure

u_w = pore water pressure

π = osmotic suction

Matric suction is known to vary with time due to environmental changes. Any change in suction affects the overall equilibrium of the soil mass. Changes in suction may be caused by a change in either one or both components of soil suction.

The role of osmotic suction has commonly been associated more with unsaturated soils than with saturated soils. However, osmotic suction is related to the salt content in the pore-water which is present in both saturated and unsaturated soils. The role of osmotic suction is therefore equally applicable to both unsaturated and saturated soils. Osmotic suction changes have an effect on the mechanical behavior of a soil.

2.4.2 Matric Suction Profile

Matric suction is closely related to the surrounding environment and is of interest in analyzing geotechnical engineering problems. The *in situ* profile of pore-water pressures (and thus matric suction) may vary from time to time. The variation in the soil suction profile is generally greater than variations commonly occurring in the net normal stress profile. Variations in the suction profile depend upon several factors. Some of these factors are explained below:

- 1. Ground Surface Condition.** The matric suction profile below an uncovered ground surface is affected significantly by environmental changes. Dry and wet seasons cause variations in the suction profile, particularly close to the ground surface. The suction profile beneath a covered ground surface is more constant with respect to time than is a profile below an uncovered surface. For example, the suction profile below a house or a pavement is less influenced by seasonal variations than the suction profile below an open field. However, moisture may slowly accumulate below the covered area on a long-term basis, causing a reduction in the soil suction.
- 2. Environmental Conditions.** The matric suction in the soil increases during dry seasons and decreases during wet seasons. Maximum changes in suction occur near ground surface. During a dry season, the evaporation rate is high, and it results in a net loss of water from the soil. The opposite condition may occur during a wet season.
- 3. Vegetation.** Vegetation on the ground surface has the ability to apply a tension to the pore-water of up to 1-2 MPa through the evapotranspiration process. Evapotranspiration results in the removal of water from the soil and an increase in the matric suction. The rate of evapotranspiration is a function of the microclimate, the type of vegetation, and the depth of the root zone.
- 4. Water Table.** The depth of the water table influences the magnitude of the matric suction. The deeper the water table, the higher the possible matric suction. The effect of the water table on the matric suction becomes particularly significant near ground surface.
- 5. Permeability of the Soil Profile.** The permeability of a soil represents its ability to transmit and drain water. This, in turn, indicates the ability of the soil to change matric suction as a result of environmental changes. The permeability of an unsaturated soil varies widely with its degree of saturation. The permeability also depends on the type of soil. Different soil strata which have varying abilities to transmit water in turn affect the *in situ* matric suction profile.

2.4.3 Measurements of Suction

Suction measurement is very essential when dealing with unsaturated soils (Rahardjo and Leong, 2006). It directly or indirectly affects the engineering properties of unsaturated soils. However, suction is affected more by climatic conditions rather than the loading condition as is the case of positive pore water pressures in saturated soils. Due to the higher uncertainty in climatic conditions, suction is more variable with time than positive pore water pressure. As earlier mentioned total suction consist of matric and osmotic suctions. However, for the case of unsaturated soils the effect of osmotic suction is generally negligible. Table 2.1 summarizes the some of the devices used to measure the soil suction and the range of values of suction the device can measure.

Environmental changes and changes in applied loads produce a change in the water content of the soil. The initial water content of compacted soils appears to have a direct relationship with the matric suction component. On the other hand, the osmotic suction does not seem to be sensitive to the changes in the soil water content. As a result, a change in the total suction is quite representative of a change in the matric suction. Therefore, total suction measurements are of importance, particularly in the high suction ranges where the matric suction measurements are difficult to obtain.

2.5 Unsaturated Soil Properties related to seepage flow

There are two basic soil properties related to flow of water through unsaturated soil. These properties are;

1. The soil water characteristics curve (SWCC) which is the relationship between the volumetric water content and soil suction either for drying or wetting conditions. The typical SWCC for wetting and drying conditions is shown in Figure 2.3. Due to the difficulty of measuring soil suction and due to the fact that the process is time consuming different model where

developed to predict this parameter, some of these models used the particle size distribution curve of the soil. One of these models is Fredlund's model (Fredlund, 2006) which is given as:

$$\theta_w = \frac{\theta_s}{\left\{ \ln \left[e + \left(\frac{\psi}{a} \right)^n \right] \right\}^m} \quad 2.5$$

Where θ_s is the saturated volumetric water content, e is the natural base of the logarithm, ψ is the soil suction, a is the matric suction at the SWCC's inflection point and is closely related to the air-entry value of the soil, m is the fitting parameter related to the residual water content and n is the slope of SWCC at the inflection point.

The soil-water characteristics curve (SWCC) can be obtained directly using different methods such as; pressure plate test, tempe cell, modified tempe cell, tensiometer, etc. but these test methods are time consuming and tedious as well. Therefore, other indirect methods such as filter paper methods can be used to predict the SWCC. The SWCC can also be estimated from grain-size distribution of a particular soil as proposed by Murray, *et al* (2002).

SWCC have two characteristics points; the air-entry value (*AEV*) and the residual water content (θ_r) (Zhang and Ng, 2004). The air-entry value is defined as the matric suction where air starts to enter the largest pores in the soil and the residual water content is defined as the water content where a large suction change is required to remove additional water from the soil. The greater concern in SWCC is what happens between these two points in which both air and water phases are continuous or partially continuous.

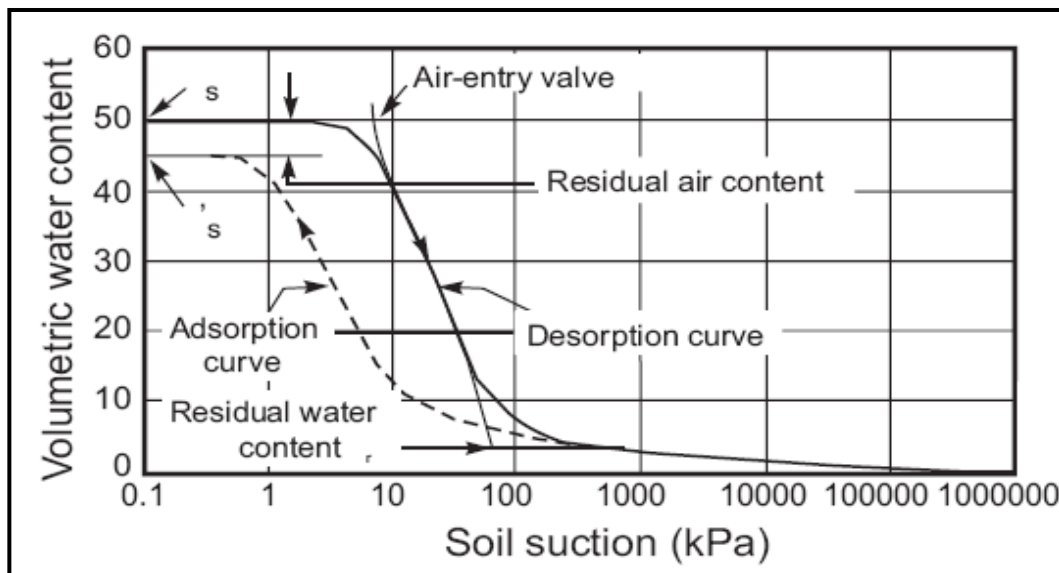


Figure 2.5: Typical SWCC for drying and wetting conditions

2. Hydraulic conductivity of the soil: the hydraulic conductivity of the unsaturated soil is the coefficient of permeability with respect to water content of a soil, and this function is a non-linear function of the volumetric water content of the soil. It later become constant when the soil approaches saturation and will be equal to the saturated coefficient permeability with respect to water, k_{sat} .

The hydraulic conductivity of a soil indicates the ability of the soil to change matric suction as a result of environmental changes (Fredlund and Rahardjo, 1993). For saturated soil the hydraulic conductivity is a function of void ratio (e) only, but for unsaturated soil it is a function of void ratio (e) and the volumetric water content (θ) of the soil. Several prediction methods of this parameter have been outlined by Leong and Rahardjo, (1997). It can also be predicted from the SWCC using some models such as Fredlund and Xing (1994) model and Van Genuchten (1980) model. The equation for Fredlund and Xing model can be written as:

$$k_w = k_s \frac{\sum_{i=j}^N \frac{\theta(e^y) - \theta(\psi)}{e^{yi}} \theta'(e^{yi})}{\sum_{i=1}^N \frac{\theta(e^y) - \theta_s}{e^{yi}} \theta'(e^{yi})} \quad 2.6$$

Where, k_s is the measured saturated conductivity, volumetric water content, y is a dummy variable of integration representing the logarithm of negative pore-water pressure, j is the least negative pore-water pressure to be describe by the final function, N is the maximum negative pore-water pressure to be describe by the final function, is the suction corresponding to the j th interval and is the first derivative and can be obtained through equation 2.4.

2.6 Slope Stability

When the soil surface is not horizontal (i.e., there is difference in height between the two edges), then there is a force of gravity tending to move the soil downward, this type of structure is called a slope. Slopes can either be natural or man-made slopes. Natural slopes are formed by natural causes; such slopes exist in hilly areas. Man-made slopes are designed and constructed by man such as the sides of cuttings, the slopes of embankments constructed for roads, railway lines, canals etc. and the slopes of earth dams constructed for storing water.

The slopes whether natural or artificial may be either Infinite or Finite slopes. The term infinite slope is used to designate a constant slope of infinite extent. The long slope of the face of a mountain is an example of this type, whereas finite slopes are limited in extent. The slopes of embankments and earth dams are examples of finite slopes. The slope length depends on the height of the dam or embankment. Slope stability is an extremely important consideration in the design and construction of earth dams. The stability of a natural slope is also important. The results of a slope failure can often be catastrophic, involving the loss of considerable property and many lives.

Table 2.1: Summary of Suction Measurement Devices

Device	Suction component measured	Measurement range (kPa)	Equilibrium time
Jet fill tensiometer	Matric	0-100	Several minutes
Small-tip tensiometer	Matric	0-100	Several minutes
Null-type axis translation apparatus	Matric	0-1500	Several hours – days
Miniature tensiometer	Matric	0-1500	Several minutes
Filter paper contact	Matric	0-10000	2-5 days
Filter paper non contact	Total	1000-10000	2-14 days
Thermal conductivity sensor	Matric	10-1500	Several hours – days
Electrical conductivity sensor	Matric	0-1500	6-48 hours
Psychrometer	Total	100-10000	Several minutes- several hours

(Source: Rahardjo and Leong, 2006)

The failure of slopes usually occurs when the shear stress developed in the soil exceeds the shear resistance of the soil. Based on the shape of failure surface; the slope failure can be categorized into three i.e., wedge failure, circular and non-circular failures and translational failure. Wedge failure usually occurs on a weak plane or weak joints due to external forces and this type of failure should be evaluated using three dimensional analyses. The circular and non-circular failures are associated with homogenous and non-homogenous conditions respectively. While the translational failure is usually influenced by the presence of weak layer, and usually the failure surface tends to be plane and roughly parallel to the slope surface. The important factors that cause instability in a slope and lead to failure are:

1. Gravitational force
2. Force due to seepage water
3. Erosion of the surface of slopes due to flowing water
4. The sudden lowering of water adjacent to a slope
5. Forces due to earthquakes

The effect of all the forces listed above is to cause movement of soil from high points to low points. The most important of such forces is the component of gravity that acts in the direction of probable motion. The various effects of flowing or seeping water are generally recognized as very important in stability problems, but often these effects have not been properly identified. It is a fact that the seepage occurring within a soil mass causes seepage forces, which have much greater effect than is commonly realized.

Erosion on the surface of a slope may be the cause of the removal of a certain weight of soil, and may thus lead to an increased stability as far as mass movement is concerned. On the other hand, erosion in the form of undercutting at the toe may increase the height of the slope, or decrease the length of the incipient failure surface, thus decreasing the stability. When there is a lowering of the ground water or of a free water surface adjacent to the slope, for example in a sudden drawdown of the water surface in a reservoir there is a decrease in the buoyancy of the soil which is in effect an increase in the weight. This increase in weight causes increase in the shearing stresses that may or may not be in part counteracted by the increase in shearing strength, depending upon whether or not the soil is able to undergo compression which the load increase tends to cause. If a large mass of soil is saturated and is of low permeability, practically no volume changes will be able to occur except at a slow rate, and in spite of the increase of load the strength increase may be inappreciable. Shear at constant volume may be accompanied by a decrease in the inter granular pressure and an increase in the neutral pressure. A failure may be caused by such a condition in which the entire soil mass passes into a state of liquefaction and flows like a liquid. A condition of this type may be developed if the mass of soil is subject to vibration, for example, due to earthquake forces.

Slope stability analyses have become a common analytical tool for assessing the factor of safety of natural and man-made slopes. Any one of numerous two-dimensional, limit equilibrium methods of slices is generally used in practice. These methods are based upon the principles of statics (i.e., static equilibriums of forces and/or moments), without giving any consideration to the displacement in the soil mass. Several basic assumptions and principles used in formulating these limit

equilibrium analyses are outlined prior to deriving the general factor of safety equations. Effective shear strength parameters (i.e., c' and ϕ') are generally used when performing slope stability analyses on soils which are saturated. The shear strength contribution from the negative pore-water pressures above the groundwater table are usually ignored by setting their magnitudes to zero. The difficulties associated with the measurement of negative pore-water pressures and their incorporation into the slope stability analysis is the primary reasons for this practice. It may be a reasonable assumption to ignore negative pore-water pressures for many situations where the major portion of the slip surface is below the groundwater table. However, for situations where the groundwater table is deep or where the concern is over the possibility of a shallow failure surface, negative pore water pressures can no longer be ignored. In recent years, there has developed a better understanding of the role of negative pore-water pressures (or matric suctions) in increasing the shear strength of the soil. Recent developments have led to several devices which can be used to better measure the negative pore-water pressures. Therefore, it is now appropriate to perform slope stability analyses which include the shear strength contribution from the negative pore-water pressures. These types of analyses are an extension of conventional limit equilibrium analyses.

Stability analysis of unsaturated slopes requires an extensive and detailed seepage analysis, because slope failures in unsaturated conditions are closely related to heavy rainfall and infiltration. The mechanism that leads to slope failures is that the negative pore–water pressures start to increase when water starts to infiltrate the unsaturated soil. The loss of negative pore–water pressures decreases the shear strength of the soil below the mobilized shear strength along the potential slip surface. In order to determine the increase of the negative pore–water pressures the relationship between the negative pore–water pressure of the soil and the water content is required. This relationship is called the soil–water characteristic curve and can be obtained in the laboratory with a pressure plate test. The amount of rainwater that infiltrates the slope is also required. It is dependent on the rainfall pattern (i.e. intensity and duration), the permeability of the soil and the initial condition within the soil prior to the rainfall event.

2.6.1 Slope stability analysis

The conventional slope stability analyses are carried out using limit equilibrium methods. These methods includes the ordinary method of slices, Bishop's modified method, force equilibrium methods, Janbu's generalized method, Morgenstern and price's method and Spencer method. Limit equilibrium methods may be fully or partially satisfy all the static equilibrium conditions. Generally speaking the limit equilibrium methods that satisfy all the static equilibrium conditions tend to give a more accurate FOS estimation than those that only partially satisfy the static equilibrium equations. According to Lei *et al*, 2010; "Methods which satisfy all conditions of equilibrium give accurate results for all practical conditions. Regardless of the assumptions they employ, these methods (Janbu's, Spencer and Morgenstern and Price's methods) give values of FOS which differ by no more than $\pm 5\%$ of the correct answer". Table 2.2 shows some of the most frequently used methods of slices used in practice.

In tropical countries like Malaysia the water table is very deep therefore the slope failure is usually shallow, from Table 2.2, the method that is capable of modeling the shallow slope failure is the Morgenstern-Price method because it can analyze slope stability with fully specified failure plane.

A state of limiting equilibrium is said to exist when the shear stress along the failure surface is expressed as:

$$\tau = \frac{S}{FOS} \quad 2.7$$

Where,

τ = average shear stress developed along the potential failure surface

S = average shear strength of the soil

FOS = factor of safety with respect to strength

If the calculated *FOS* is equal to 1, the slope is in a state of impending failure. Generally, a value of 1.5 for the *FOS* with respect to strength is acceptable for the design of a stable slope.

2.6.2 Unsaturated Slope Stability

The negative pore-water pressures (matric suction) have the effect of increasing the shear strength of unsaturated soil. Therefore in unsaturated slope stability it is important to consider this additional shear strength due to matric suction. Fredlund *et al.*, (1978) developed an equation of shear strength of unsaturated soil which includes the additional shear strength due to matric suction. This equation is given as:

$$\tau = c' + (\sigma_n - u_a) \tan \phi' + (u_a - u_w) \tan \phi^b \quad 2.8$$

Where c' is effective cohesion, ϕ' is effective frictional angle, $(\sigma_n - u_a)$ is net normal stress, u_a is pore-air pressure, u_w is pore-water pressure, $(u_a - u_w)$ is matric suction, ϕ^b is internal friction angle due to matric suction.

Table 2.2: Methods of Slope Stability Analysis

Method	Force Equilibrium	Moment Equilibrium	Shape of Slip Surface
Ordinary method of slices (Fellenius, 1927)	Does not satisfy horizontal or vertical forces equilibrium	Yes	Circular
Bishop's Modified (Bishop, 1955)	Satisfy vertical force but not horizontal force equilibrium	Yes	Circular only. Non circular may have numerical problem
			Any shape. More

Janbu's simplified method (Janbu, 1956)	Yes	No	frequent numerical problems than other methods
Morgenstern and Price (Morgenstern and Price, 1965)	Yes permit side forces to be varied	Yes	Any shape
Spencer's method (Spencer, 1967)	Yes side forces are assumed to be parallel	Yes	Any shape

(Source: Duncan, 1996)

The unsaturated friction angle (ϕ^b) depicts the increment rate of shear strength due increase in suction and it can be obtained by performing a series of triaxial compression test under various matric suction conditions where the pore air pressure (u_a) control and transducer are install to measure the matric suction ($u_a - u_w$).

The ϕ^b can be taken as $\frac{1}{2}\phi'$ for practical purposes (Geo-Slope, 2007).

Fredlund and Rahardjo, (1993), presents some experimental values of ϕ^b for soils obtained from various geographical locations as presented in Table 2.3.

Table 2.3: Experimental values of ϕ^b

Type of soil	c' (kPa)	ϕ' (degrees)	ϕ^b (degrees)
Compacted shale	15.8	24.8	18.1
Boulder clay	9.6	27.3	21.7
Dhanauri clay	37.3	28.5	16.2
Dhanauri clay	20.3	29.0	12.6
Dhanauri clay	15.5	28.5	22.6
Dhanauri clay	11.3	29.0	16.5
Madrid grey clay	23.7	22.5	16.1

Undisturbed decomposed granite, Hong Kong	28.9	33.4	15.3
Undisturbed decomposed rhyolite, Hong Kong	7.4	33.4	13.8
Tappen-Notch Hill silt	0.0	35.0	16.0
Compacted glacial till	10	25.3	7-25.5

(Source, Fredlund and Rahardjo, 1993)

The factor of safety (FOS) of a slope is defined as that factor by which the shear strength of the soil must be reduced in order to bring the mass of soil into a state of limiting equilibrium along a selected slip surface. Therefore, the FOS of unsaturated slope can be expressed to include the additional shear strength due to matric suction and can be written as:

$$FOS = \frac{c' + (\sigma_n - u_a) \tan \phi' + (u_a - u_w) \tan \phi^b}{\gamma h \sin \alpha \cos \alpha} \quad 2.8$$

Where c' is effective cohesion, ϕ' is effective frictional angle, $(\sigma_n - u_a)$ is net normal stress, u_a is pore-air pressure, u_w is pore-water pressure, $(u_a - u_w)$ is matric suction, ϕ^b is internal friction angle due to matric suction, γ is the total unit weight of soil, h is vertical depth and α is slope angle.

Since rainfall infiltration have the effect of decreasing the shear strength of unsaturated soils, therefore the FOS of unsaturated slope decreases significantly when the cohesion due to matric suction decreases during wet period.

CHAPTER 3

METHODOLOGY

3.1 Introduction

This chapter describes the methods and procedures followed to achieve the objectives of the study. The flow chart of research methodology is shown in Figure 3.1. The study was divided into three; data collection, seepage analyses and slope stability analyses for the effect of rainfall only and the combined effect of rainfall and evaporation.

The study looks at the influence of rainfall infiltration and evaporation on slope stability, therefore, rainfall and evaporation data are required for the study. These data were obtained from Department of Irrigation and Drainage (DID) Km 7, Jalan Ampang, 6800 Ampang; Kuala Lumpur, Malaysia. Besides, soil properties relevant for seepage and slope stability analysis are required. Thus, collection of soil samples and laboratory test were carried out for this study.

Definition of slope geometry needed to be set at this stage. The geometry of the slope used in this study has a horizontal distance of 47m; this was adopted from previous study by Kassim, *et al.* 2011, and a slope angle of 21° . The slope angle is based on the fact that, the Malaysian slope angles usually varies between 18° to 28° . Figure 3.2 show the geometry of the slope used for this analyses.

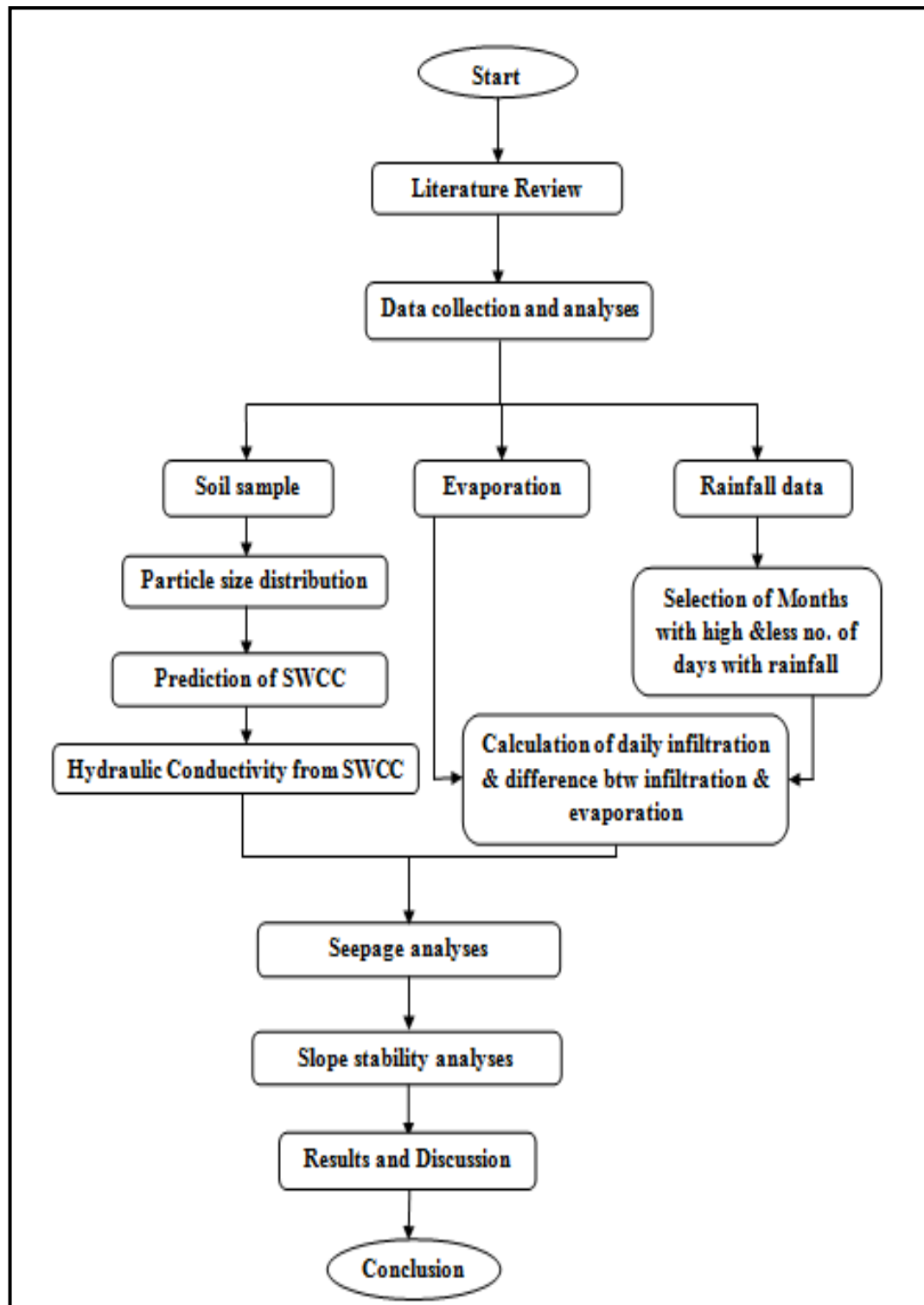


Figure 3.1: Flow chart of the study

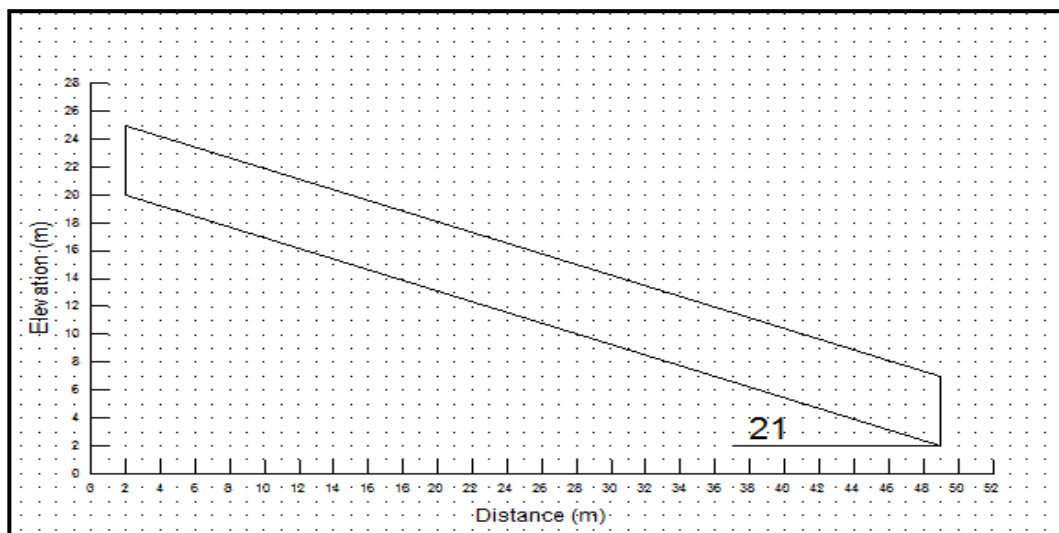


Figure 3.2: Geometry of the Slope (infinite slope)

The second stage of the research involved the seepage analyses for the change of suction distribution in soil due to rainfall infiltration and combined effect of rainfall infiltration and evaporation. Two types of analyses were performed i.e. steady state analysis and transient state analysis. One year data of rainfall and evaporation was collected for transient analysis. The data used in this study was collected for the year 2009. In this stage, analyses were made for two conditions i.e. dry months and wet months based on the number of days with rainfall. February and June was chosen as dry months while March and December was selected as wet months. Comparison was made for suction distribution due to rainfall only and combination of rainfall and evaporation was compared.

The third stage is slope stability analyses. Data obtained from seepage analysis by SEEP/W program was exported to SLOPE/W to evaluate the effect of pore water pressure distribution on the stability of the slope. Detail analysis was made for comparing the effect of rainfall alone and combined effect of rainfall and evaporation. Critical condition should be obtained from this analysis in term of factor of safety.

3.2 Data collection and analyses

3.2.1 Rainfall and Evaporation Data

The data required for this study were divided into three; the rainfall data, the evaporation data and soil sample data. As mentioned in the introduction of this chapter; the rainfall and evaporation data required for the analyses were obtained from DID. According to this department only five stations records these data in Johor state and their names, locations and station IDs were presented in Table 3.1. Before selecting appropriate station; two factors were considered; the nearness of the station to UTM for easy accessibility and preliminary investigation on the type of soils present at the site. Based on these factors Loji Air Sungai Layang was selected.

Table 3.1: Stations for Rainfall and Evaporation in Johor State

S/No	Station ID	Station name	Location
1	1539301	Loji air Sg. Layang	Johor Bahru
2	1632301	Benut di Johor Barat	Pontian
3	2025301	Pintu Kawalan Tg. Agas	Muar
4	2033301	Stn Telemetrik Bnd Kluang	Kluang
5	2636370	Stor Jps Edau	Mersing

3.2.2 Soil Properties

About 5kg of soil samples was taken from the site (Loji Air Sungai Layang). The sample was taken from some where around the area. From the appearance of the sample it has higher percentage of coarse materials (sandy particles); therefore wet sieving is more appropriate for the sample, as given in BS1377 and Head, 2006.

3.2.2.1 Particle Size Distribution

Particle size distribution analysis is important in this study, because from the particle size distribution, the Soil Water Characteristics Curve (SWCC) and the hydraulic conductivity function for the soil (which are the parameters required for seepage analyses) can be predicted. This test is conducted in accordance with the specifications given in BS 1377: Part 2 (1990). The procedures for wet sieving are as follows:

1. The soil sample was prepared and oven dried (allowed to stay overnight in an oven at a temperature of 105°C)
2. It was allowed to cooled and about 500g was measured and recorded as (m_1)
3. A 2mm sieve was nested in the 63micron sieve with other intermediate sieve in between to avoid overloading the 63micron sieve.
4. The soil sample was soaked in a solution of sodium hexametaphosphate for about an hour to ensure separation or dispersion of discrete particles of the soils.
5. The sample was placed over 2mm sieve and washed over with a spray of clean water. The silt and clay passing the 63micron was allowed to run to waste. The washing was continued until the waste water ran as clean as possible.
6. The whole material retained on the sieves was allowed to drain and was carefully transferred to tray and placed in an oven and dried at 105°C overnight.
7. After cooling the whole of the dried material was measured and recorded as (m_4)
8. The dried soil was passed through a nest of completed range of sieves to cover the size of particles present, down to 63micron sieve.
9. The whole range of sieves was placed on mechanical sieve shaker for about 10minutes.
10. The portion retained on each sieve was weighed and the cumulative percentage passing was calculated.

Therefore, the result of this test was used to plot the particle size distribution curve, from which the SWCC was predicted.

3.2.2.2 Saturated Permeability of the soil

The saturated permeability of soil can be determined using two methods depending on the type of soils; either using constant-head permeability test or falling head-permeability test. The constant head-permeability test is recommended for coarse-grained soils and the total hydraulic head remains constant during the duration of the test and the volume of water seeping during a given period of time is measured. It is performed on soils having coefficients of permeability in the range of 10^{-2} to 10^{-5} m/s BS 1377: Part 5 (1990). In the case of falling-head permeability test; it is recommended for fine grained soils and the total head changes during the test. The time it takes the total hydraulic head to drop between two predetermined points is measured. Therefore, based on this information the appropriate test for the type of soil in this study is falling-head permeability test. The schematic diagram of the test set up is shown in Figure 3.3.

Falling-head permeability is not covered in BS 1377: Part 5 (1990) nor by ASTM standards, therefore the procedure is as outlined by Head, (1981) and Fratta, *et al.* (2007). The procedure followed for this test is as follows:

1. Undisturbed soil sample from the site was used for this test and the initial mass of the specimen was determined and recorded as (M_s).
2. The porous stone and the filter paper were placed at the bottom of the permeameter. The soil sample was placed in the permeameter in four layers each of thickness about equal to half the diameter, the first layer was placed on the porous disc, and the subsequent layers on previously leveled soil layers.
3. The diameter (D) of the specimen holder was measured and the cross-sectional area (A) was calculated.
4. The filter paper, porous disc and the spring were placed over the specimen and the permeameter was closed.

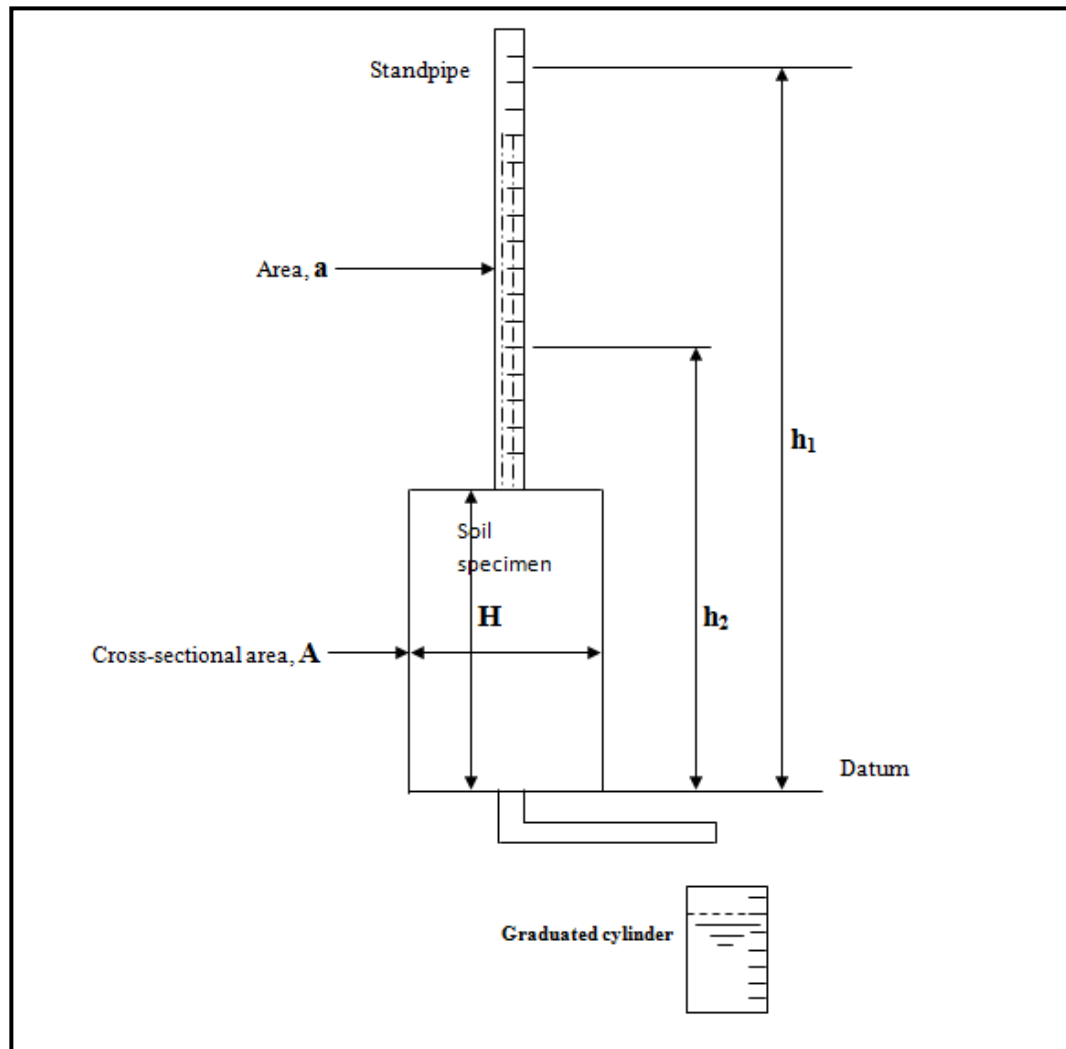


Figure 3.3: Schematic diagram of falling head permeability test

5. The height (H) of the specimen in the permeameter was measured and also the distance (L) between the manometers. The volume of the specimen (V) was then calculated.
6. Water was allowed to rise slowly from the bottom of the specimen.
7. The permeameter was then connected to the standpipe
8. The valve was opened to start the flow and the time required for the water in the standpipe to drop from height h_1 to h_2 was noted.
9. The temperature (T) of the effluent fluid was measured
10. The volume of the seeping water (V_{seep}) was calculated and compared with the volume of the effluent.
11. The permeability of the soil was then calculated.

Details of the calculation are presented in appendix B.

3.2.2.3 Soil-water characteristics curve (SWCC) and Hydraulic Conductivity

The SWCC is the relationship between the volumetric water content and matric suction of a soil. As mentioned earlier, this parameter was predicted from the particle size distribution curve by comparing the type of soil, D10 and D60 of the curve with that given in SEEP/W, (GeoSlope International Ltd., 2007) function library, after selecting the appropriate SWCC the data was then adjusted to suit the appropriate standard shape of the figure. From this curve the *AEV* and *RWC* values were used with saturated permeability test result to predict the hydraulic conductivity function using Fredlund and Xing, (1994) model which was incorporated in to the SEEP/W (GeoSlope International Ltd., 2007) software.

3.2.2.4 Shear Strength parameters

Due to the problems related to acquiring enough samples from site, the shear strength parameters required for slope stability analyses were obtained in accordance with the suggestion given by Holtz and Kovacs (1981). According to these authors; the phi (ϕ') value is usually between 25° and 35° and 30° was used in this study, the effective cohesion (c') ranges between $5 - 10\text{kN/m}^2$ and 7kN/m^2 was used and the angle which relates the increase in shear strength due to matric suction (ϕ^b) was taken as $2/3 \phi'$.

3.3 Seepage Analyses

The seepage analysis is important because the slope failure in an unsaturated soil is usually due to rainfall infiltration. The seepage analyses used in this study was carried out using finite element software SEEP/W; (Geo-Slope, 2007) which can be used to simulate seepage through soils. The SEEP/W has three executing components:

- i. **Define:** Define boundary value problem i.e. input geometry, processes, properties and the boundary conditions.
- ii. **Solve:** Solve the FEM equations
- iii. **Contour:** Visualization of the solution and it involves verifying the input, interpreting the solution and extracting data from the result.

There are two types of seepage analyses; the steady-state seepage analyses in which the analyses does not change with time and it served as initial condition for transient seepage analysis in this study, and the transient seepage analysis which is time dependent analysis. These two types of seepage analyses were used in this study. There are two key processes in seepage analysis, these are:

1. The flow of water through soils which can be represented by Darcy's law:

$$Q = - kiA \quad 3.1$$

Where Q = discharge (m^3), k = hydraulic conductivity (m/s), I = hydraulic gradient and A = cross-sectional area (m^2).

The flow of water depends solely on the hydraulic conductivity value and for unsaturated soils the hydraulic conductivity is a function that depends on degree of saturation, volumetric water content and matric suction (negative pore water pressure).

2. Soil storage: this indicates the amount of water that soil can retain and this depends on the soil water characteristics curve (SWCC) of the soil.

3.3.1 Steady-State Seepage Analysis

This type of analysis is usually performed by assuming that the soil slope is either fully dried or fully saturated as the worst conditions the slope may experienced. In this study; the steady-state analysis was carried out assuming the soil slope was fully dried so that the influenced of the rainfall and evaporation can be simulated in the subsequent transient seepage analyses.

As stated earlier the SEEP/W (GeoSlope International Ltd., 2007) has three executing components, these components were used in this analyses. Under the first component which is Define, the geometry of the slope as shown in Figure 3.2 was defined and the type of analysis was set to steady-state. The most important material properties required for this analysis is the hydraulic conductivity function which was predicted from the SWCC using Fredlund and Xing, 1994 model incorporated in to the software. Figure 3.3(a) and (b) shows how this property of the soil was key-in into the software. Other material properties input required for this analysis are the conductivity ratio (i.e. k_y/k_x) which was set to value of 1, and the conductivity direction which was set to (0^0) i.e. horizontal x-direction.

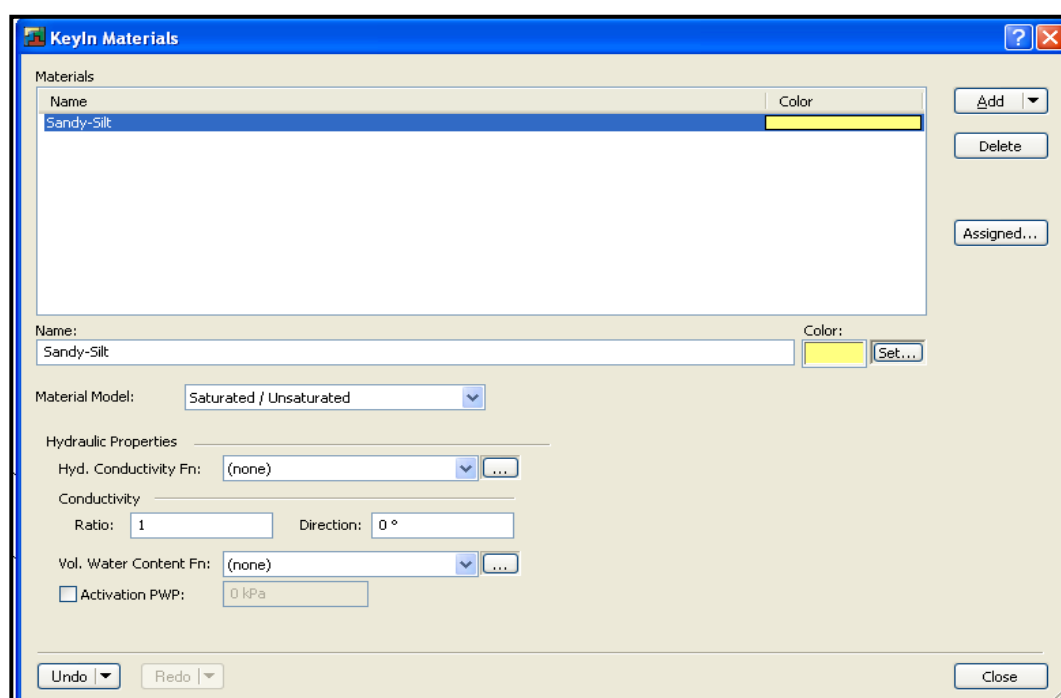


Figure 3.4(a): Keyin of material property of the soil

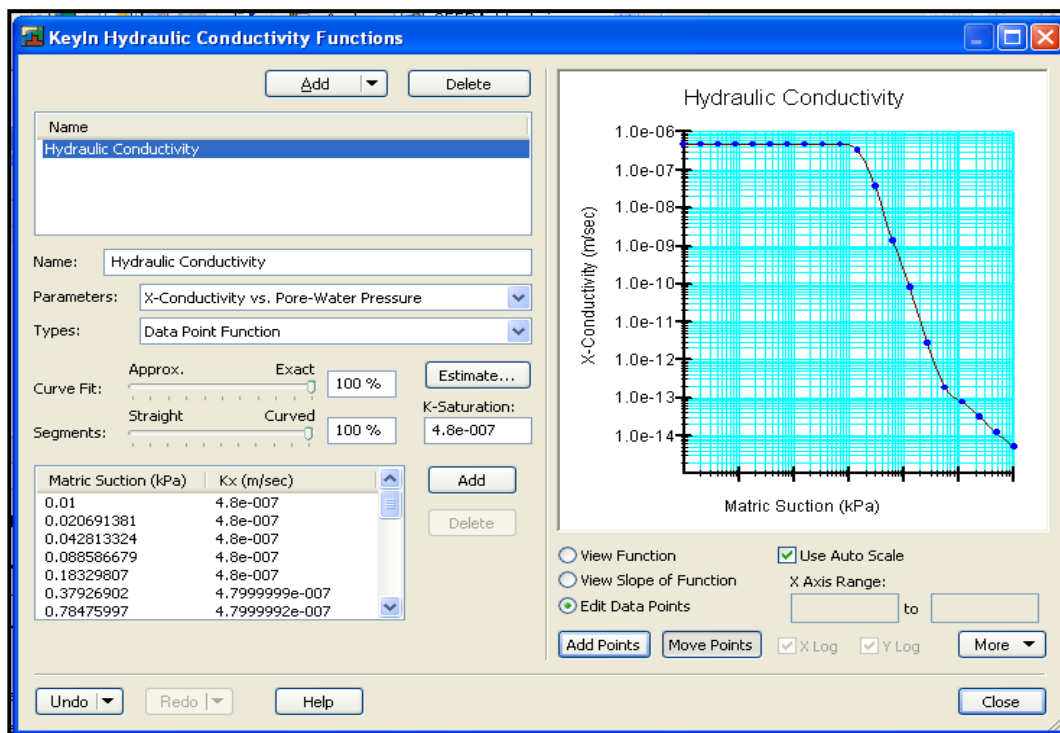


Figure 3.4(b): Keyin of the hydraulic conductivity function

After the materials have been defined then the region to which the material is to be applied was drawn as shown in Figure 3.4 and the materials were assigned to the geometry of the slope as shown in Figure 3.5.

Furthermore, the boundary condition was also defined. Four boundary conditions were defined and they include; the left and right boundary conditions which were defined as Head boundary conditions and were given values of 20m and 2m respectively (based on the geometry of the slope), the bottom boundary condition which was set as potential seepage face boundary and the surface boundary which was set zero unit flux. Figure 3.6(a) and (b) shows the geometry of the slope with assigned boundary conditions.

The next components of the SEEP/W was solve and this component was executed after verifying there is zero warning and zero error, then the FEM equations are then solved. Figure 3.7 shows this component.

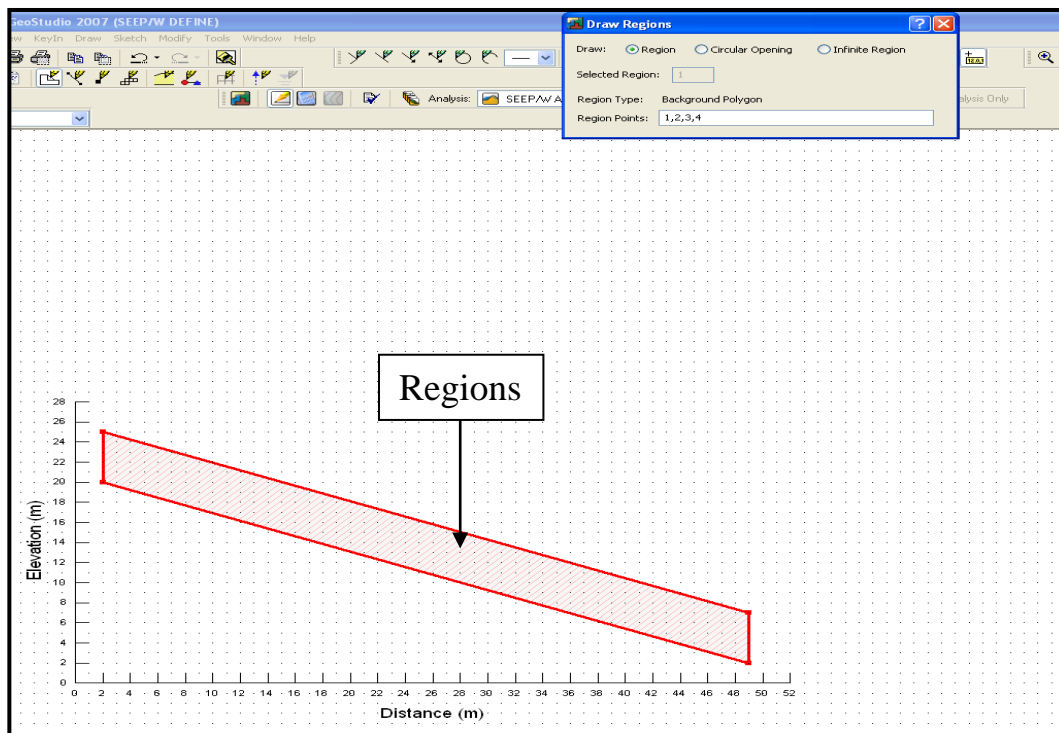


Figure 3.5: Applied region to the geometry of the slope

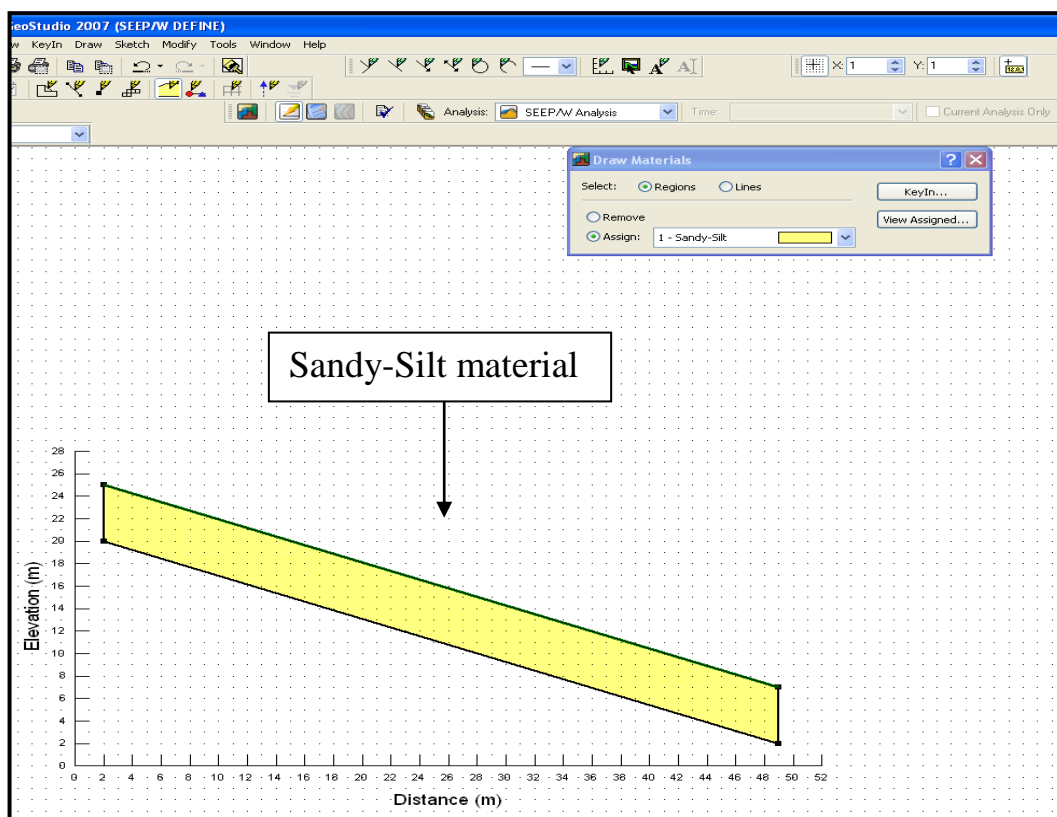


Figure 3.6: Assigned materials in the slope

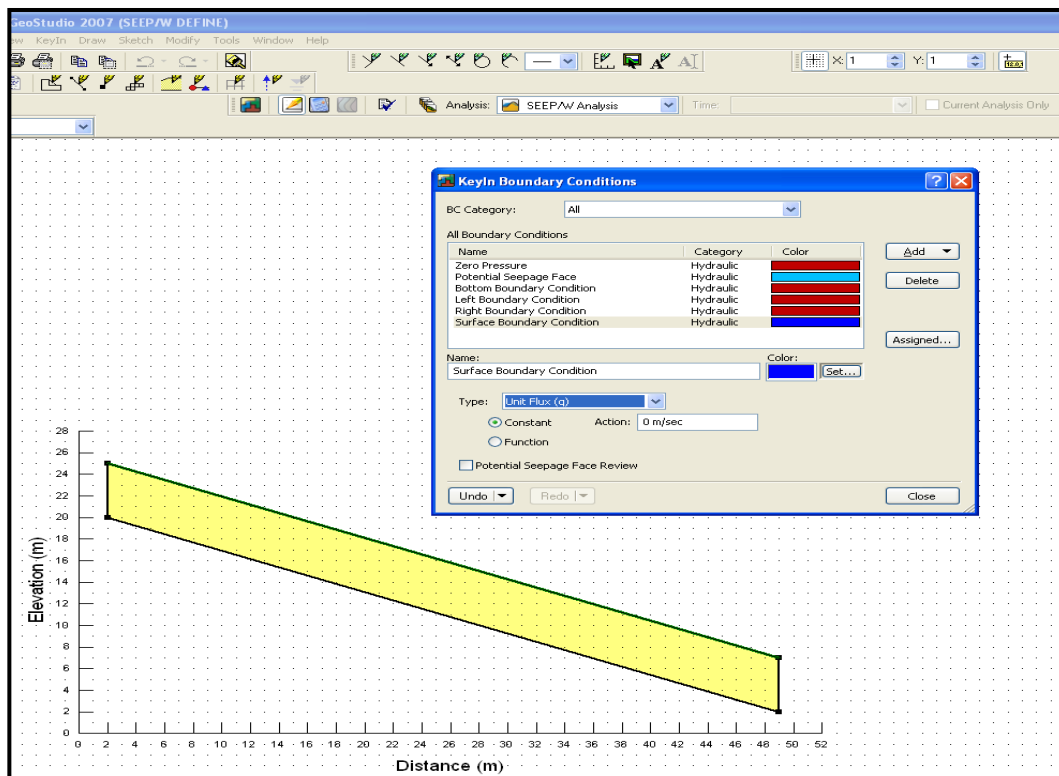


Figure 3.7(a): Keyin boundary conditions to the slope geometry

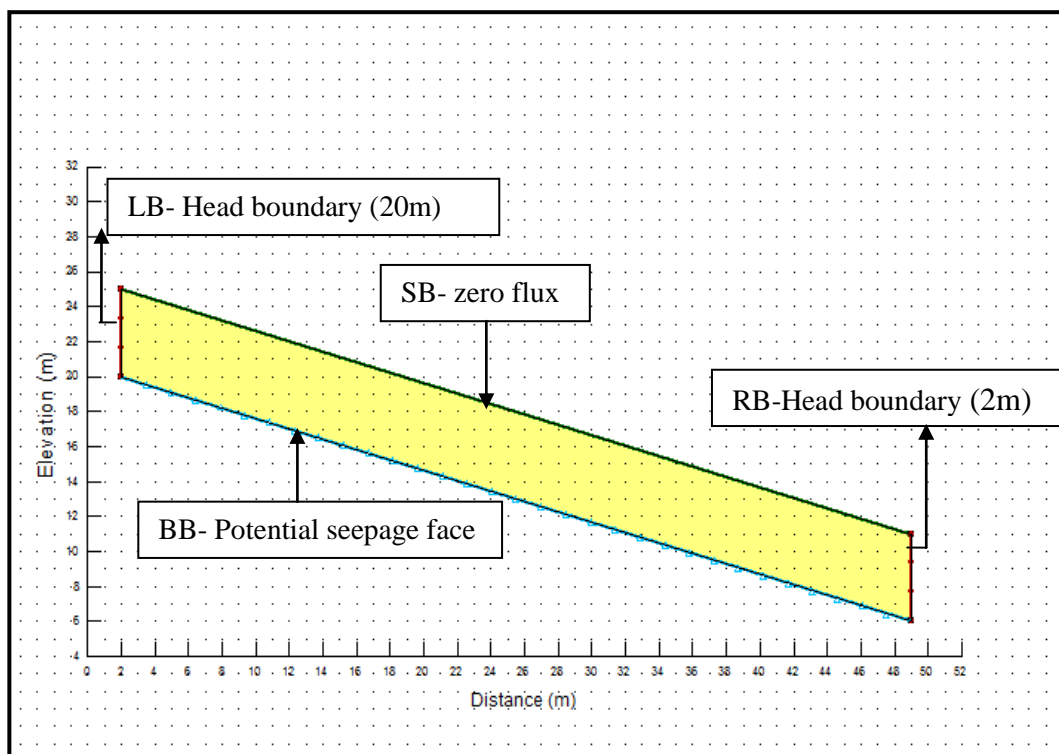
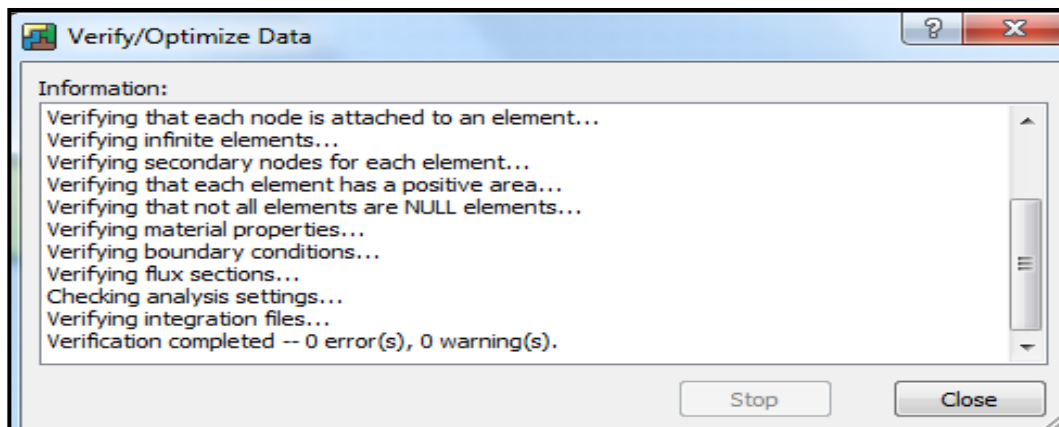
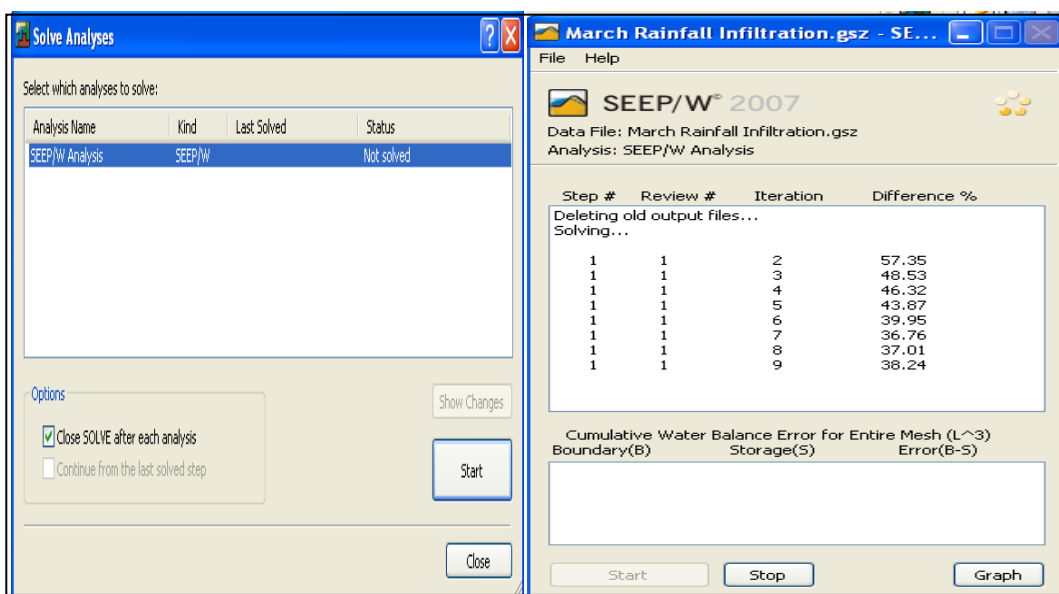


Figure 3.7(b): Positions of the boundary conditions



(a)



(b)

(c)

Figure 3.8: Verification and Solution windows

The last component of the SEEP/W was Contour and under this component the results of the above component are visualized in different forms such as the seepage pattern, pore-water pressure head, total head, etc., as shown in Figure 3.8.

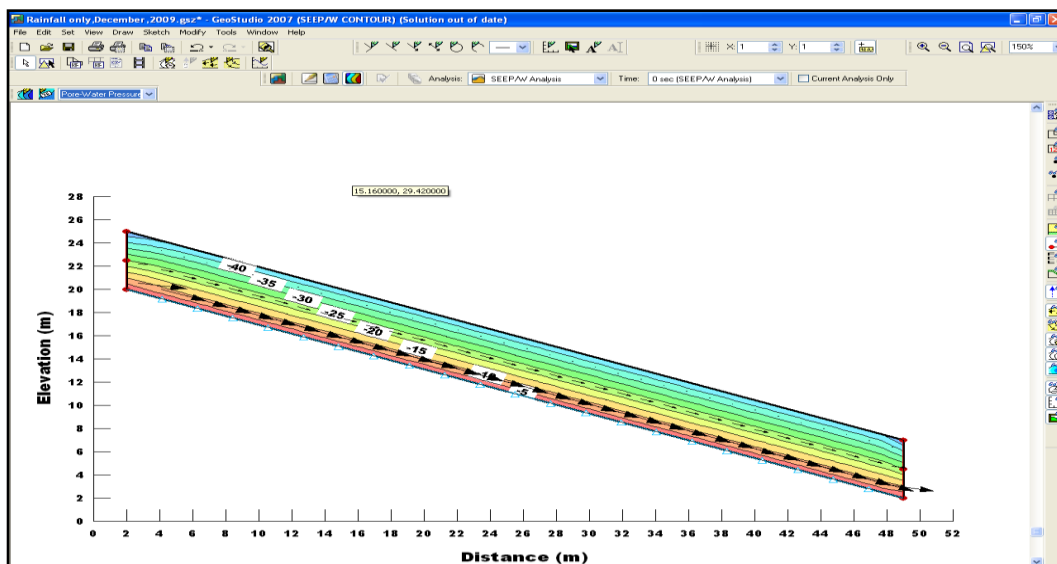


Figure 3.9: Seepage pattern and pore-water head profile

3.3.2 Transient Seepage Analysis

The transient or unsteady-state seepage analysis is defined as a time dependent analysis due to spatial and temporal changes in the environmental conditions (Lu and Likos, 2004). The steady-state analysis described above was set as the parent analysis (initial condition) for the first transient analysis and the analysis type was set transient.

The material used for steady-state analysis was modified and for this type of analysis both SWCC and hydraulic conductivity are required. Therefore the SWCC was included in the modified steady-state analysis as shown in Figure 3.9. Finally, the boundary condition was also modified to include surface boundary condition which is equal to the amount of daily rainfall infiltration in the first analysis and the difference between the rainfall infiltration and evaporation in the second analysis. In the next transient analysis the former was set as the parent analysis continuously like that until all the data were exhausted.

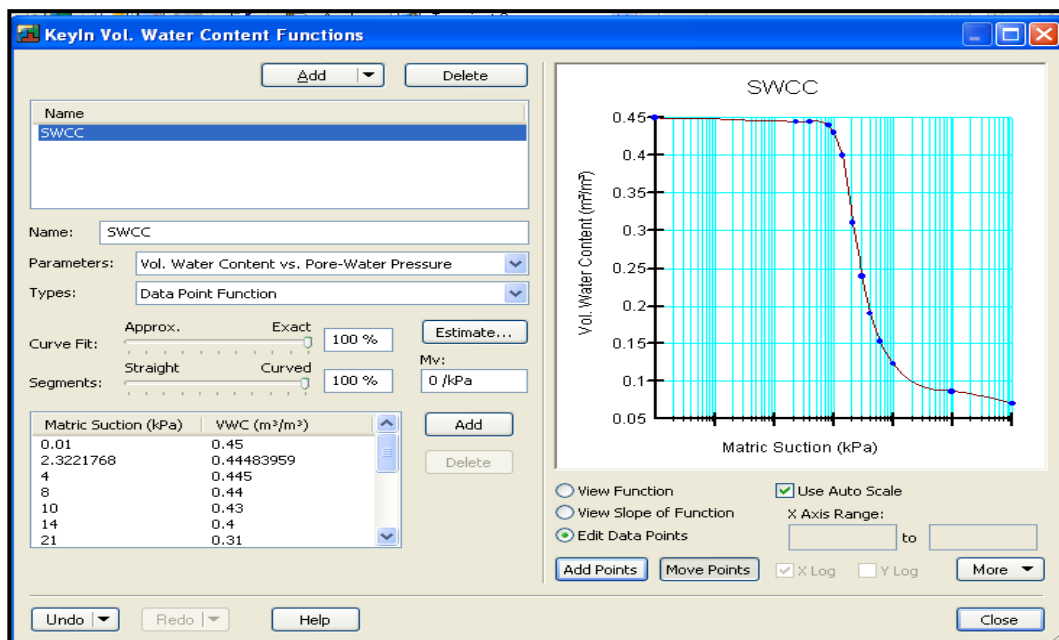


Figure 3.10: Key-in of material property in Transient analysis (SWCC)

3.4 Slope Stability Analysis

The slope stability analysis was carried out using SLOPE/W (Geo-Slope, 2007) software which is based on limit equilibrium. Different methods of analyses such as Janbu's method, Bishop's method, Spencer method, Morgenstern-Price method, etc. were integrated into SLOPE/W software. The results obtained from this study are expressed in terms of factor of safety versus time and the FOS should decrease when the rainfall infiltration increases and vice-versa. Similarly, high FOS is expected with analyses using the difference between rainfall infiltration and evaporation.

The increase in shear strength due to soil suction is usually modeled in two ways in SLOPE/W; the use of constant ϕ^b (which is the angle relating the increase in shear strength due to suction) and the use of volumetric water content function. The former was used in this study and the value of ϕ^b is assumed to be equal to $2/3 \phi'$.

The slope stability analysis was performed using the soil parameters given in Table 3.2. For the unsaturated slope stability analysis, the water table is assumed to

be far below the ground so that effect of suction changes can be explored and also tension crack is not considered in the analysis.

Table 3.2 Basic Soil Properties for Slope Stability Analysis

Soil Property	Value
Unit weight of the soil (γ)	19kN/m ³
Cohesion (c')	7kPa
Angle of internal friction (ϕ')	30 ⁰
Unsaturated soil (ϕ^b)	20 ⁰

3.4.1. Factor of Safety

The factor of safety (FOS) is defined as that factor by which the shear strength of the soil must be reduced in order to bring the mass of soil into a state of limiting equilibrium along a selected slip surface. The FOS was computed using Morgenstern–Price method because of the following reasons:

- i. It considers both shear and normal inter slice forces,
- ii. It satisfies both moment and force equilibrium, and
- iii. It allows for a variety of user-selected inter slice force function.

The SLOPE/W has two executable programs: DEFINE for defining the model and SOLVE for computing the results. The seepage patterns developed in the transient seepage analyses described before was used as the parent analysis to compute the FOS.

In the transient seepage analyses; the pore-water pressure distribution and the seepage pattern in the slope were generated. The seepage patterns generated from the transient analyses were used in the slope stability analyses to compute the factor of safety for the slope.

At the end of every transient analysis, SLOPE/W analysis was key-In so that the name of the analysis is SLOPE/W and the parent analysis is Transient seepage

analysis. The analysis type was set as Morgenstern –Price as stated earlier. In the settings, the side function was set to half – sine function and the pore-water pressure conditions was from the parent analysis as shown in Figure 3.10. For the slip surface the following settings were done.

- i. Direction of movement – is from left to right (from the geometry of the slope)
- ii. Slip surface option – Entry and Exit was chosen this is because the slope is infinite slope and if the Grid and Radius is used the factor of safety is going to be at the edge no matter how the grids were adjusted.
- iii. The tension crack option is not considered the reason was stated earlier.
The settings for the slip surface option and the Entry and Exit points were shown in Figure 3.11 and Figure 3.12(a) and (b) respectively.

In the DEFINE option the materials were key-In as shown in Figure 3.13(a) and (b) and these material were assigned to the geometry of the slope as shown in Figure 3.14. The boundary conditions remained the same as that of the transient seepage analyses (parent analysis). Finally, the analysis was saved and SOLVED as shown in Figure 3.15. Sample of the result of FOS is as shown in Figure 3.16.

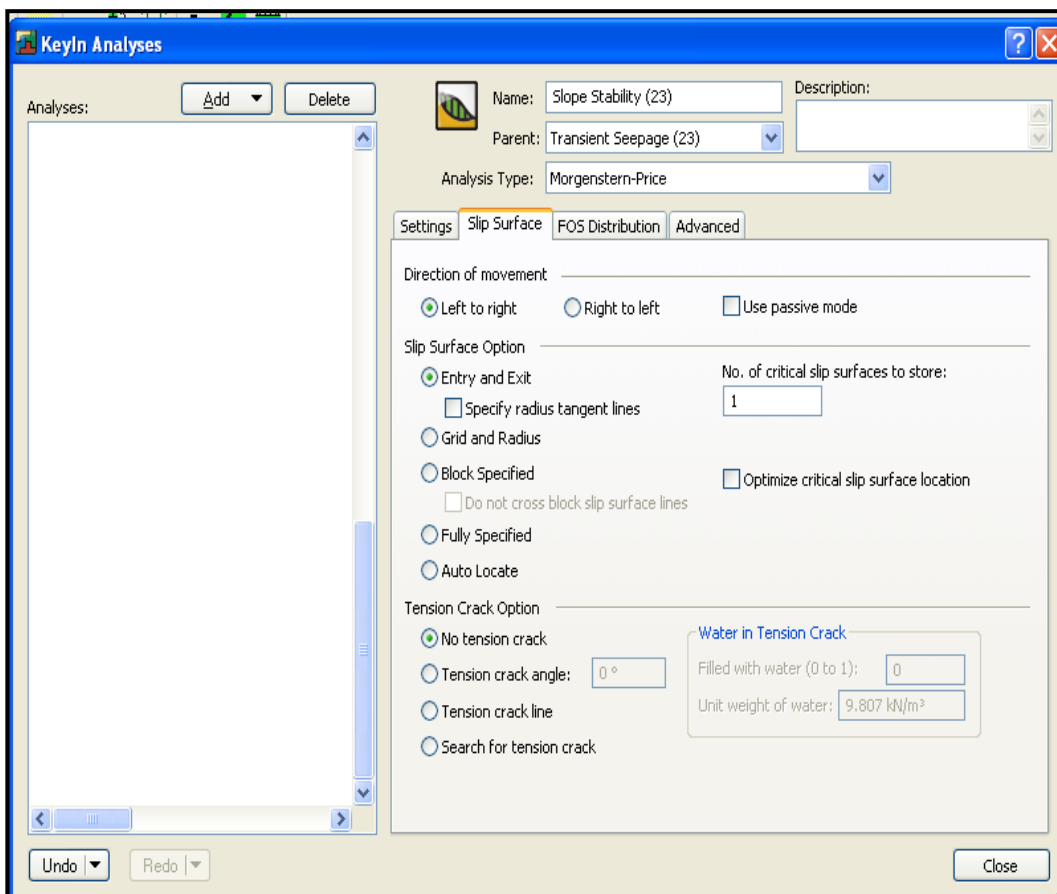


Figure 3.11: Slip surface option

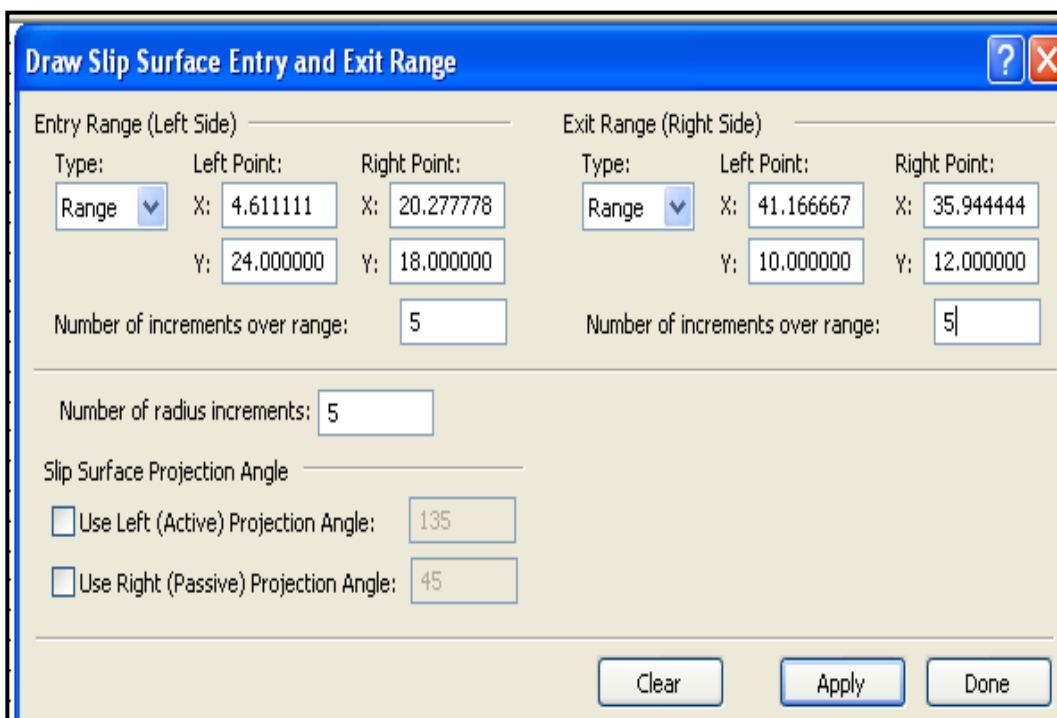


Figure 3.12(a): Entry and Exit Points range

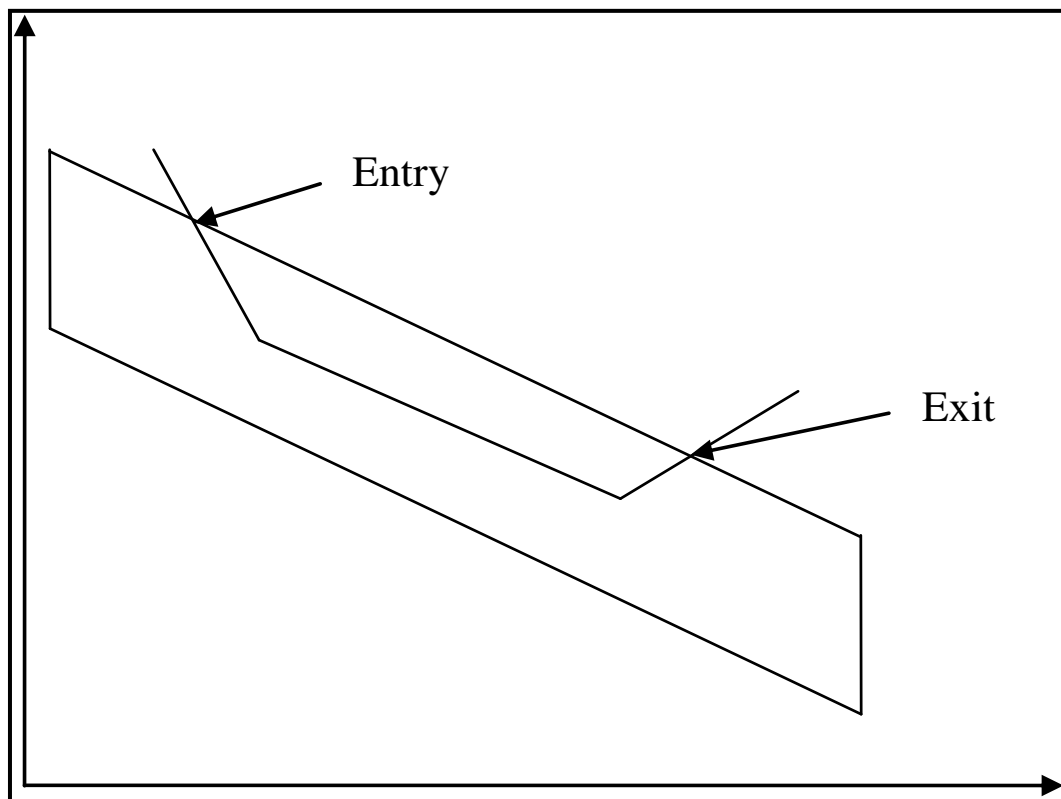


Figure 3.12(b): Entry and Exit Points

The screenshot shows the 'KeyIn Materials' dialog box. The 'Materials' list contains one entry: 'Sandy-Silt' with a yellow color swatch. The 'Name' field is 'Sandy-Silt' and the 'Color' field is yellow. The 'Material Model' is set to 'Mohr-Coulomb'. The 'Basic' tab is active, showing the following properties:

Property	Value
Unit Weight	19 kN/m ³
Cohesion	7 kPa
Phi	30 °

Buttons for 'Add', 'Delete', 'Assigned...', 'Set...', 'Undo', 'Redo', and 'Close' are visible.

Figure 3.13(a): Key-in of material properties

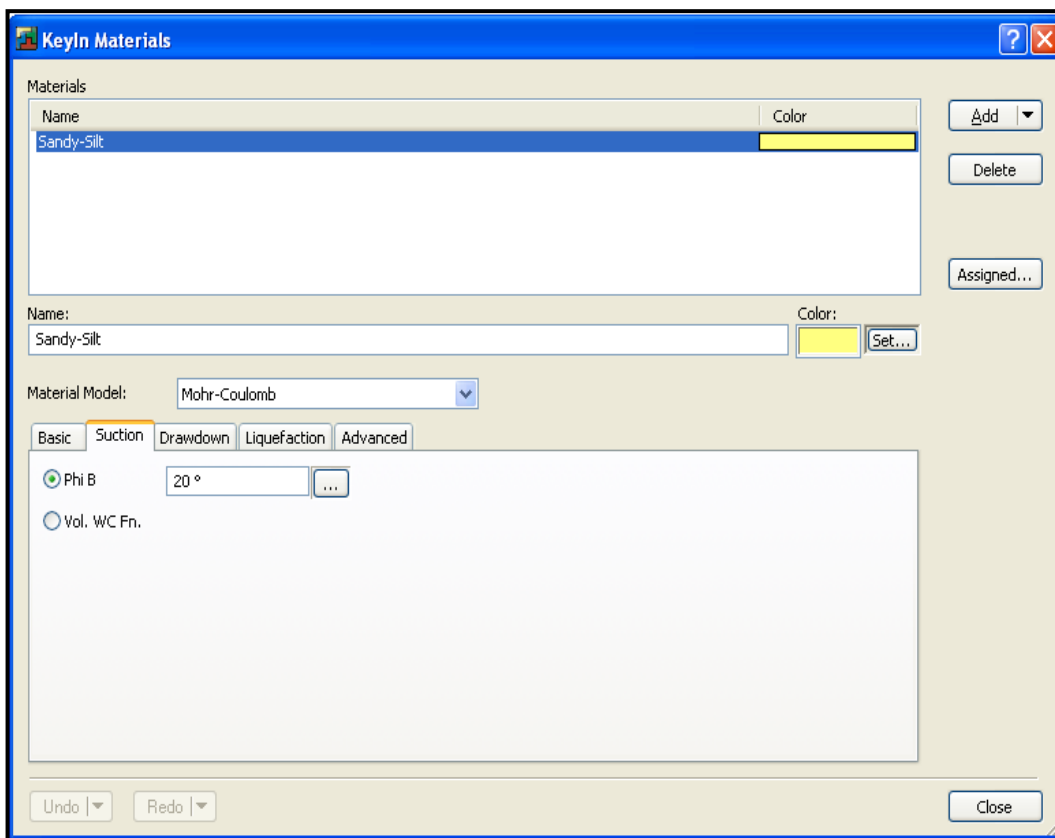


Figure 3.13(b): Key-in of material properties

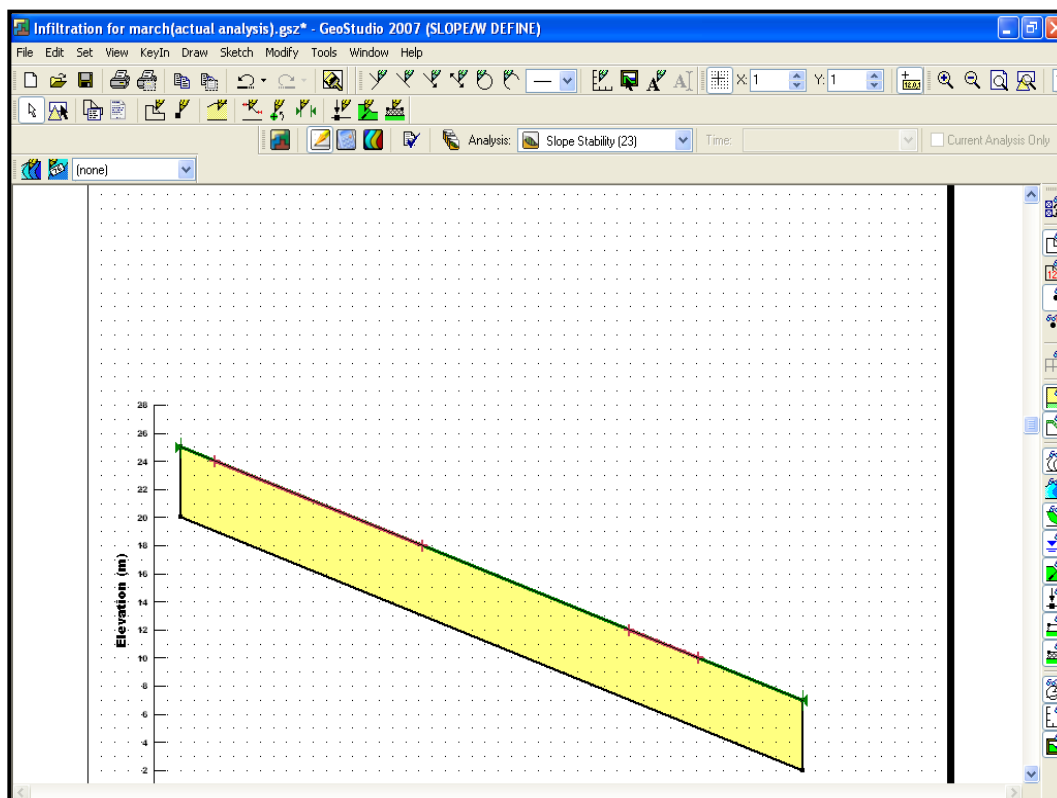


Figure 3.14: Assigned material properties to the geometry

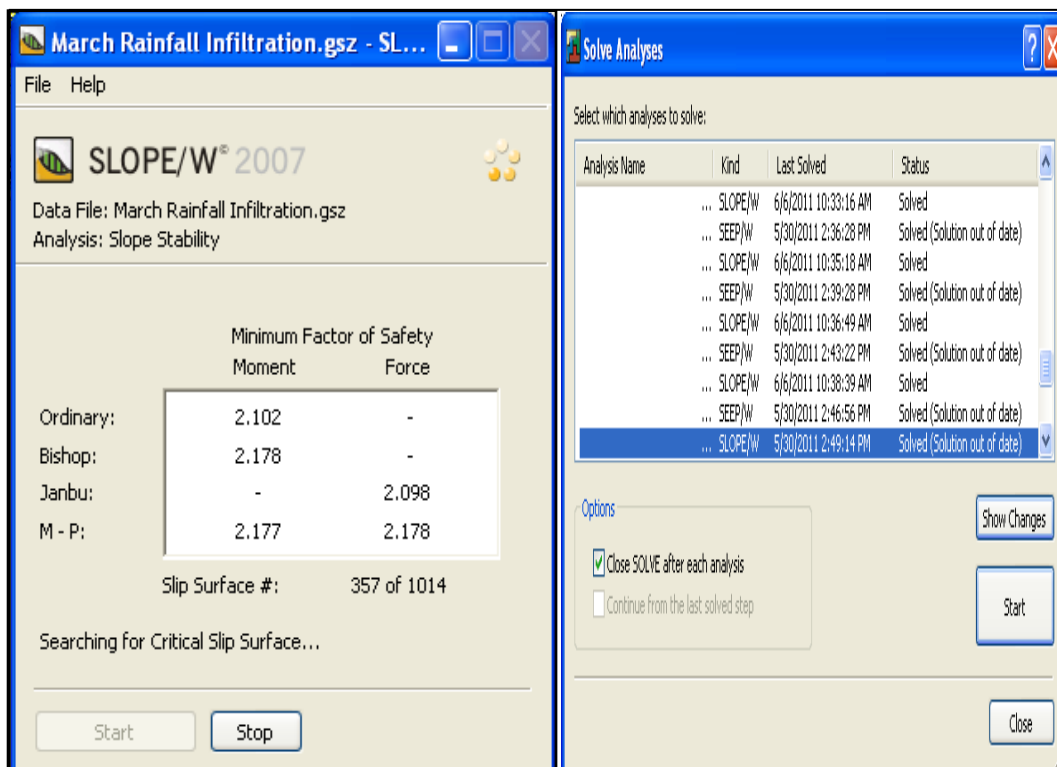


Figure 3.15: Solve dialog box

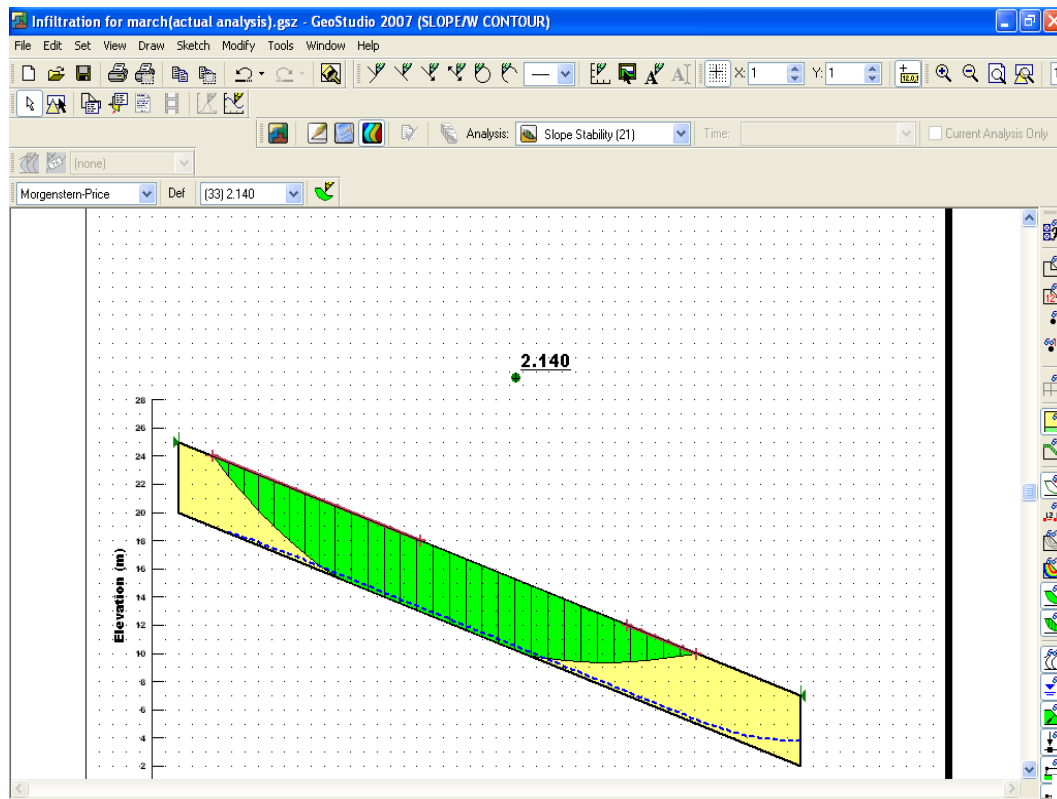


Figure 3.16: FOS of the slope

CHAPTER 4

RESULTS AND DISCUSSIONS

4.1 Introduction

This chapter deals with the analyses and discussion of the results obtained using the procedure described in the previous chapter. The chapter is divided into five sections. Section 4.2 presents the preliminary data needed for the analysis i.e. rainfall and evaporation data as well as soil properties. The rainfall and evaporation data of Loji Air Sg. Layang for complete one year (i.e., 2009) were obtained from Department of Irrigation and Drainage (DID). Two types of data were identified: (1) wet months i.e., the months with more number of days with rainfall, and (2) dry months i.e., months with less number of days with rainfall. Based on these criteria; March and December were found to have more number of days with rainfall (wet) while February and June has less number of days with rainfall (dry). Relevant soil properties required for analysis were also outlined in this Section.

Subsequently, transient seepage analyses and slope stability analyses were performed for months of February, March, June and December. Section 4.3 deals with the analysis of the results obtained from the transient seepage analyses while Section 4.4 presents the results of slope stability analyses. Transient seepage analyses were performed for analysis of suction (negative pore-water pressure) distribution by using SEEP/W software (GeoSlope International Ltd., 2007). Similarly, the factors of safety of the slope were obtained using a computer program SLOPE/W (GeoSlope International Ltd., 2007).

The analyses of the results were used to evaluate the effect of rainfall infiltration and that of difference between rainfall infiltration and evaporation on slope stability where the former was used as control to appreciate how much the latter increase the Factor of Safety (FOS) of the slope. The discussions of the results are presented in Section 4.5.

4.2 Preliminary data

4.2.1 Rainfall and Evaporation Data

The rainfall, evaporation and the difference between rainfall and evaporation intensities for the whole year considered in this study (i.e. 2009) were shown in Figure 4.3(a), (b) and (c). The months considered for analyses in this study were indicated in these Figures. From these Figures the maximum daily rainfall intensity of 86.5mm through out the year occurred on 12th March and it has a value of, while the maximum daily evaporation intensity of 8mm occurred on 15th June. Due to no rainfall on that day the maximum difference between rainfall and evaporation intensity of -8mm occurred on the same day.

The daily rainfall data for months of February, March, June and December were shown in Figure 4.1(a), (b), (c) and (d). The month of February, (Figure 4.1(a)) was one of the dry months and it had only seven days with rainfall and the remaining 21 days of the month without rainfall. The maximum rainfall of 33mm/day was recorded on 19th of February while the minimum rainfall of 0mm/day occurred on those 21 days.

Figure 4.1(b) is for March which is one of the wet months and it had 22 days with rainfall and 9 days without rainfall. The maximum rainfall intensity in the month was 75.20mm/day recorded on 15th of March and there were some other days with low intensities of 0.20mm/day, 0.90mm/day etc. Figure 4.1(c) is for June which was the second dry months and it had only four days of rainfall, but the month started

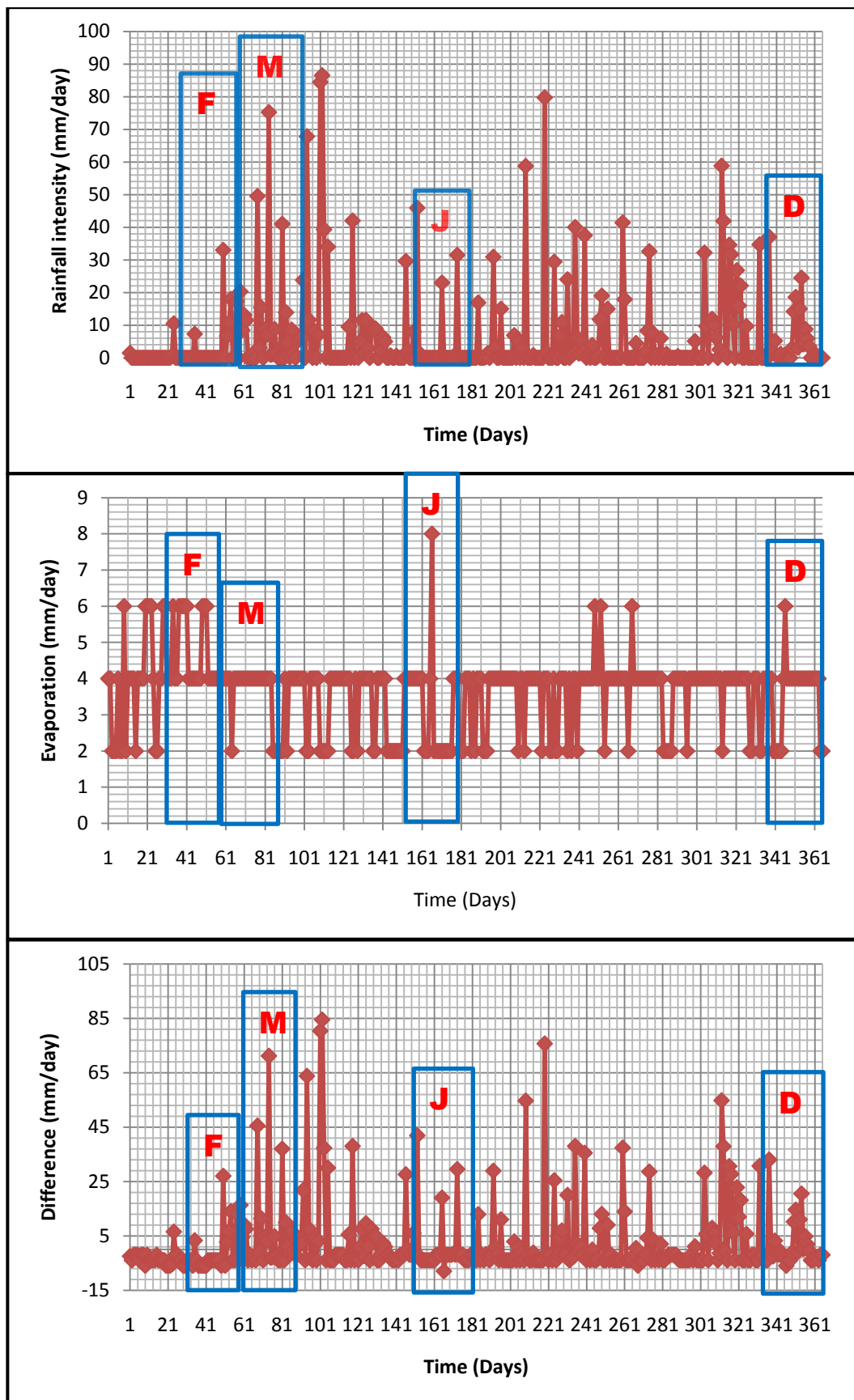


Figure 4.1: Yearly intensities (a) Rainfall, (Evaporation) and (c) Difference
 F – February, M – March, J – June and D - December

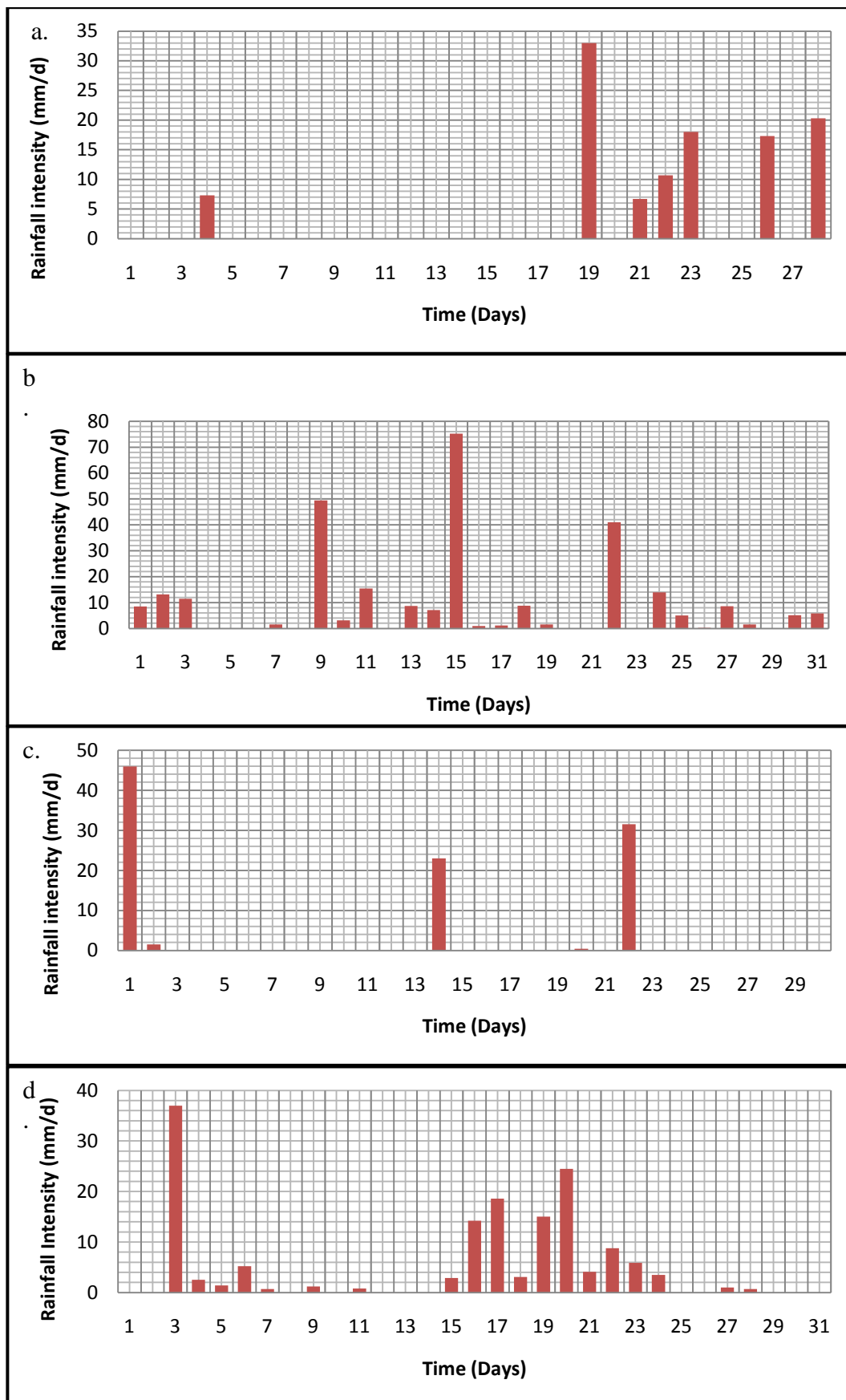


Figure 4.2: Rainfall intensity (a) February, (b) March, (c) June and (d) December

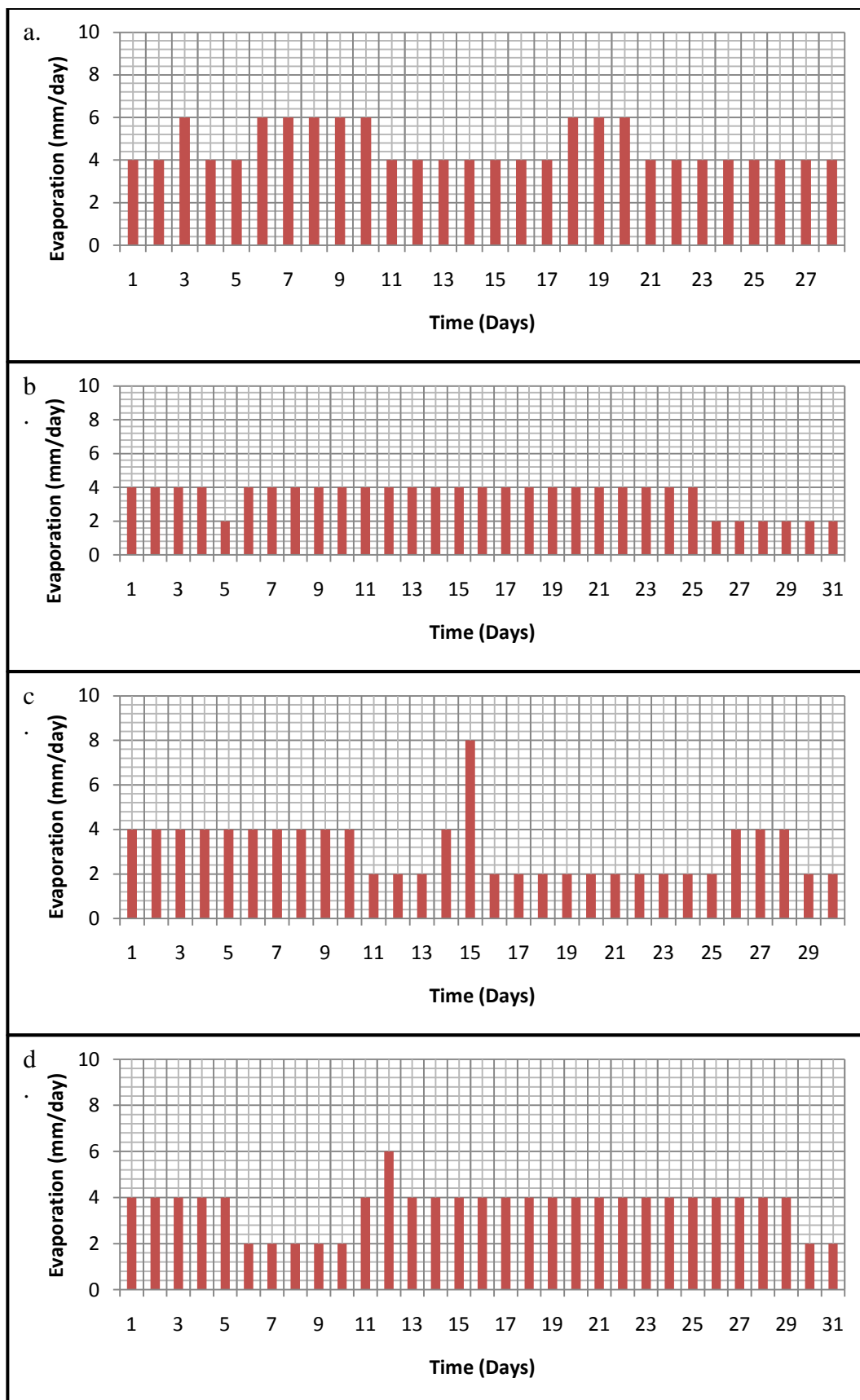


Figure 4.3: Evaporation intensity (a) February, (b) March, (c) June and (d) December

with high rainfall intensity (maximum throughout the month) of 45.90mm/day which had great influence on suction distribution throughout the month. Actually, the rainfall intensities in this month were greater than that of February. Figure 4.1(d) is for December which was the second wet month. It had 19 days of rainfall with maximum rainfall intensity of 37.00mm/day on 3rd December while it has 12 days without rainfall.

The daily evaporation intensities for February, March, June and December were shown in Figure 4.2(a), (b), (c) and (d). From these Figures the maximum daily evaporation is 8mm/day which was recorded on 15th June only and the minimum daily evaporation is 2mm/day. Most of the days have evaporation intensity of 4mm/day.

4.2.2 Soil Properties

Soil properties relevant to the analysis of suction distribution in soil slope are the soil water characteristic curve (SWCC) and Hydraulic conductivity function. Besides, shear strength parameters are required for the analysis of slope stability. Due to the problem with the availability of testing equipment for SWCC (i.e. pressure plate test) at UTM, the SWCC was estimated in this study based on particle size distribution. Subsequently, the hydraulic conductivity curve was predicted based on SWCC and the saturated hydraulic conductivity data through Fredlund and Xing (1994) method.

The procedures followed for wet sieving were explained in Chapter three. Using the results obtained from the sieve analysis; the percentage passing the respective sieves were plotted against the particle size on log scale to obtain the particle size distribution curve of the soil (Figure 4.4). From this curve the soil has only sand and silt content (with some percentage of Silt passing the 63 micron being washed away) and the soil can be classified as SANDY-SILT. From this Figure the

D_{60} was 0.35mm and the curved does not reached the D_{10} because the finer silty particles passing the 63 micron were washed away during the process of washing.

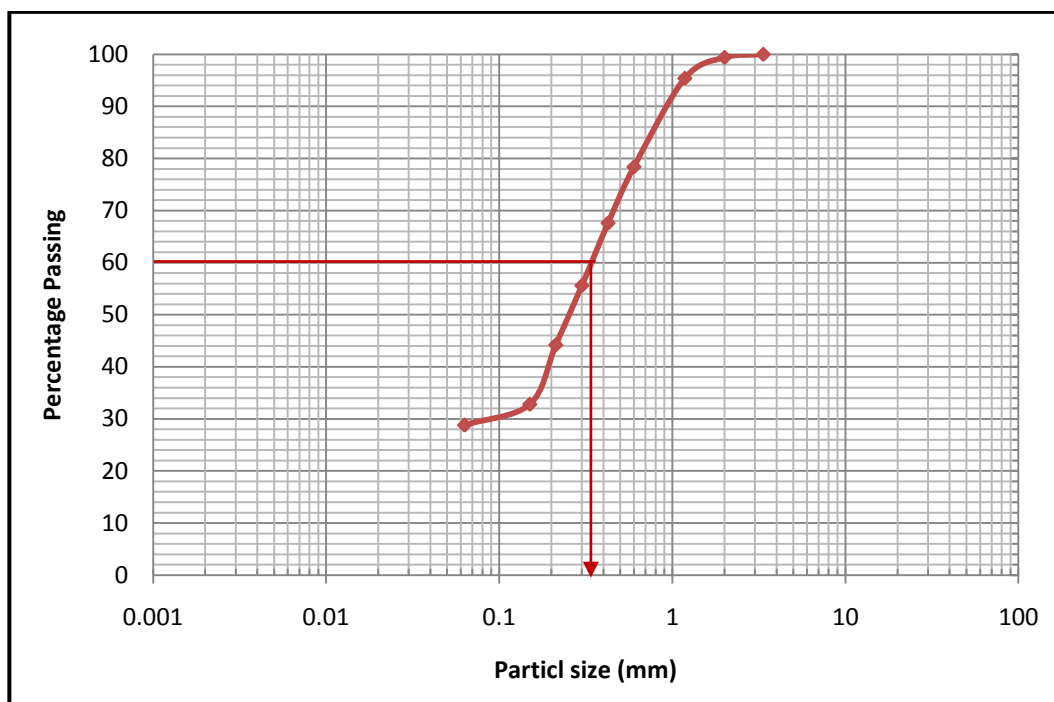


Figure 4.4: Particle size distribution curve

The SWCC used in this study was obtained from SEEP/W function library based on the correlation with particle size distribution (*PSD*) curve. The selected SWCC was modified to cover up to 10000kPa matric suction. Based on the theory that soil sample will be fully dried (i.e., reached zero water content) at 10^6 kPa. Therefore, the curve was extended to 10^6 kPa and the intermediate values between 100kPa (as given in the original curve from the library) to 10000kPa were obtained. Add and move option given in the SEEP/W, 2007 (GeoSlope International Ltd., 2007) software was used to make the curve as perfect as possible. The SWCC curve was shown in Figure 4.5. From this figure the soil has air-entry value (*AEV*) of 12kPa and residual water content (*RWC*) of 12.5%. The saturated hydraulic conductivity of the soil obtained from falling head permeability test was 4.5×10^{-7} m/s. Subsequently, the hydraulic conductivity function was predicted based on the parameters obtained from the SWCC curve and the saturated permeability of the soil using Fredlund and Xing (1994) model incorporated in the SEEP/W (GeoSlope

International Ltd., 2007) software. Laboratory permeability test shows that the saturated permeability of the soil is 4.5×10^{-7} m/sec. Figure 4.6 shows the hydraulic conductivity curve used in the analysis.

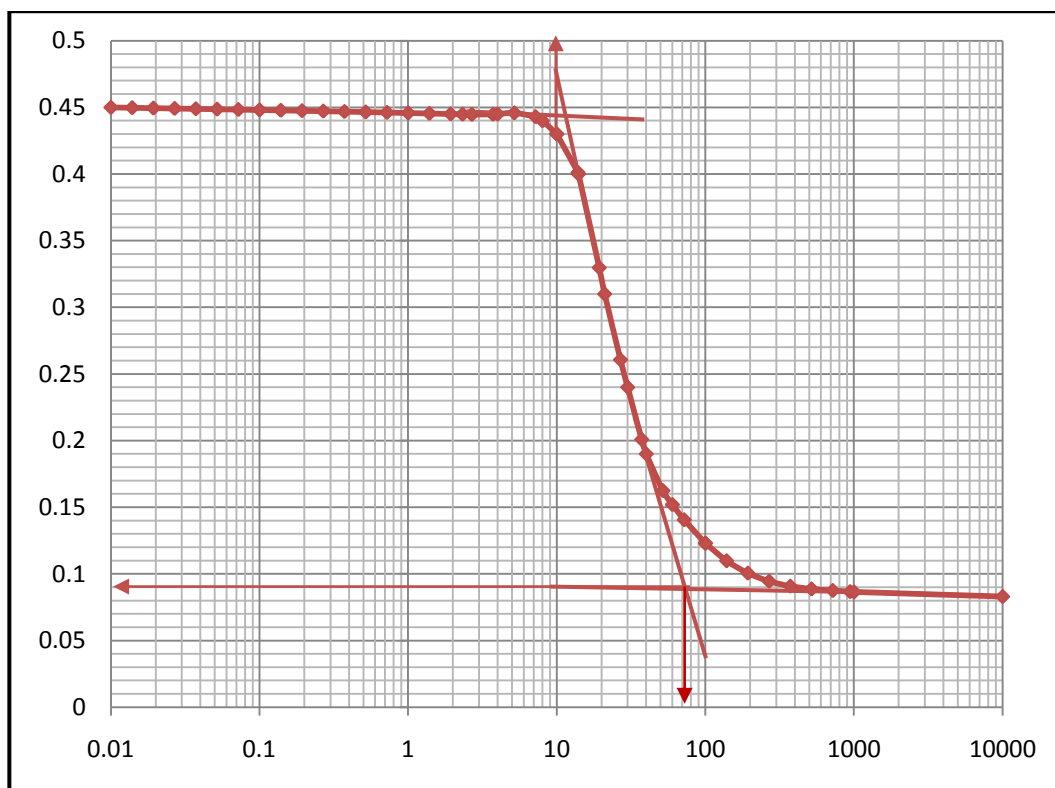


Figure 4.5: Soil Water Characteristics Curve (SWCC)

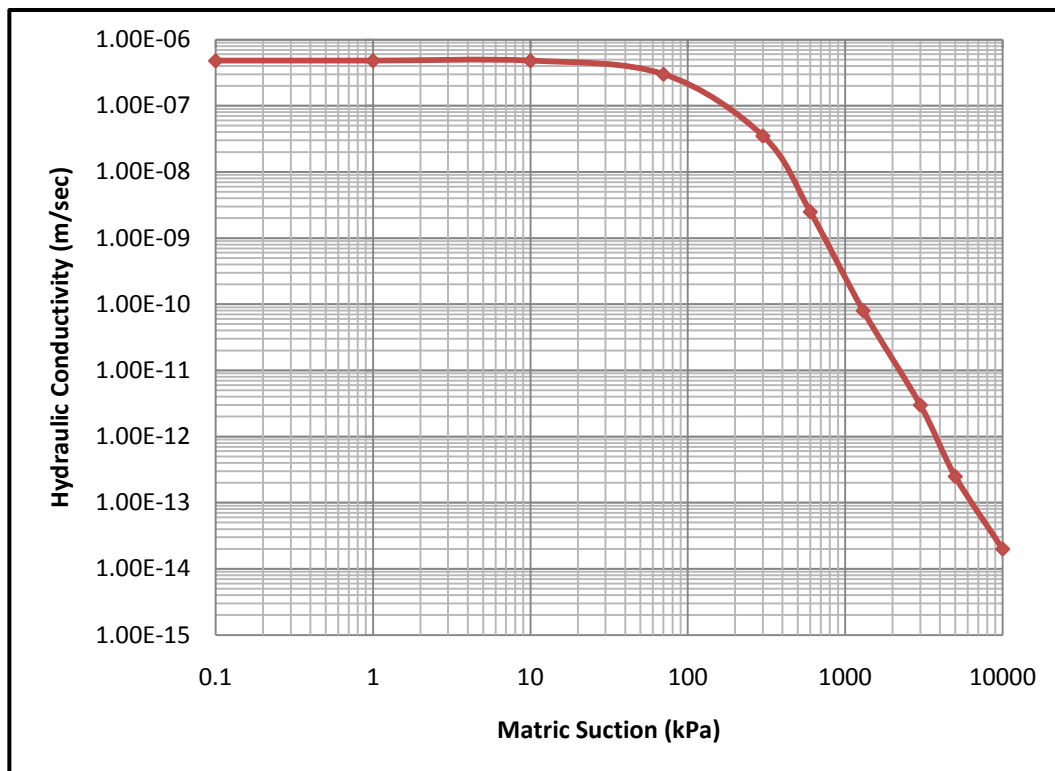


Figure 4.6: Hydraulic conductivity curve

Typical values of shear strength of soil were used for stability analysis. The effective angle of internal friction (ϕ') value for this type of soil ranges between 25° to 30° and may reach up to 35° in some cases, the cohesion (c') ranges from 5-10kPa. Therefore based on this recommendations; the shear strength parameters as shown in Table 4.1 were used for the slope stability analyses and these values were in accordance with those obtained by previous researcher for Sandy - Silt soil.

Table 4.1: Soil Properties for Slope Stability Analysis

Soil Property	Value
Unit weight of the soil (γ)	19kN/m ³
Cohesion (c')	7kPa
Angle of internal friction (ϕ')	30°
Unsaturated friction angle (ϕ^b)	20°

4.3 Seepage Analysis

The seepage analyses were conducted using commercial Unsaturated and Saturated finite element seepage software, SEEP/W (GeoSlope International Ltd., 2007). The simplified model of the slope with slope angle of 21° and 47m horizontal distance was shown in Figure 4.7. The model comprised of 142 elements meshes which have 140 nodes to represent the slope. The initial suction used for the seepage analyses was 65kPa (suction at residual water content).

The suction variation with depth and time was determine for every designated month, and as explained earlier some critical days were selected from each month.

The values of matric suction (i.e., negative pore water pressure) obtained from the transient seepage analysis were taken at five different depths based on the geometry of the slope. These depths are; 0.5m, 1.0m, 1.7m, 3.3m and 5.0m. It was observed at the crest, middle and toe of the slope but because the differences between the values obtained at these three positions were very small; average values were considered for each of the above depths.

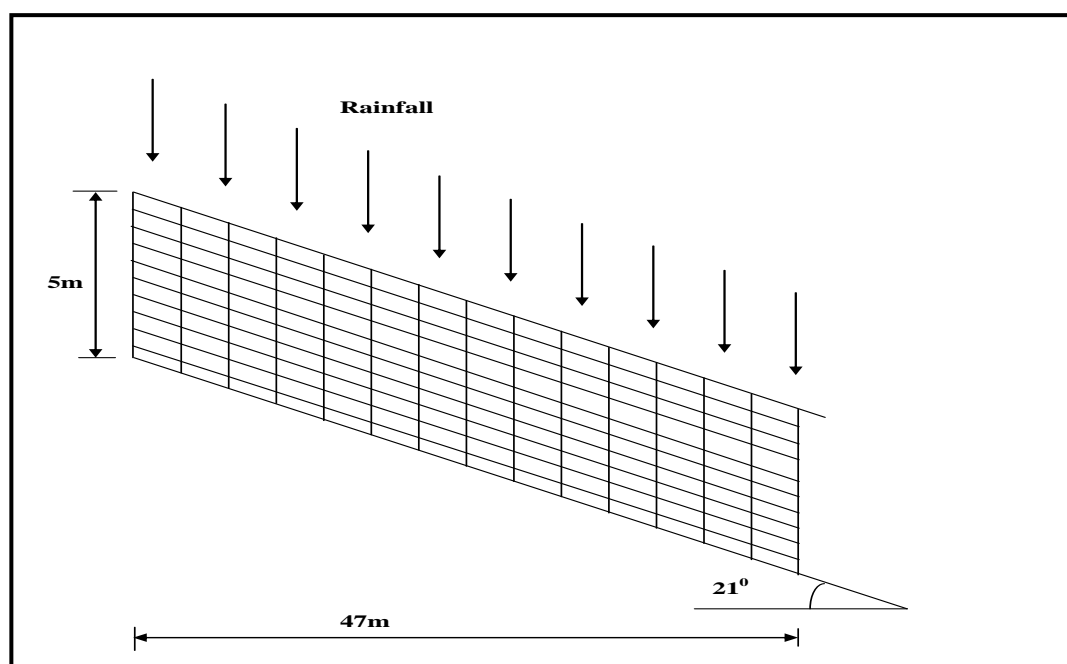


Figure 4.7: Slope model

4.3.1 Suction Distribution in February

a. Due to Rainfall Infiltration

The month of February was one of the dry months considered for the analysis. Four days were considered to explain the effect of rainfall infiltration and evaporation on suction distribution. These days with their corresponding rainfall infiltration are; 1st February (zero rainfall infiltration), 4th February (5.11mm/day), 19th February (23.1mm/day) and 28th February (14.21mm/day). The seepage pattern and pore-water pressure head profile for these days were shown in Figure 4.8(a), (b), (c) and (d).

The seepage direction is from the crest to the toe that is flowing downward which was due to the differences in pressure head gradient between these two points (i.e., 20m at the crest and 2m at the toe). The variation of suction with depths and time for this month is presented in Appendix C. Figure 4.9(a) and (b) shows the variation of suction with depth and time and that of rainfall with time. From these Figures; the changes of suction due rainfall infiltration is more noticeable at depths of 0.5m and 1.0m from the surface of the slope while at depths of 1.7m, 3.3m and 5.0m the changes were insignificant. Furthermore, the negative pore water pressure increases (i.e., decrease in matric suction) as the rainfall infiltrated in to the soil mass. Between 1st – 3rd February, the suction is uniform because there were no rainfall that infiltrated in to the soil but on 4th February the suction decreases due to rainfall infiltration and it then continues to increase at slower rate until on 19th of February where there is another rainfall infiltration which causes decrease in suction. Finally, on 28th of February the suction also decreases due to another rainfall infiltration.

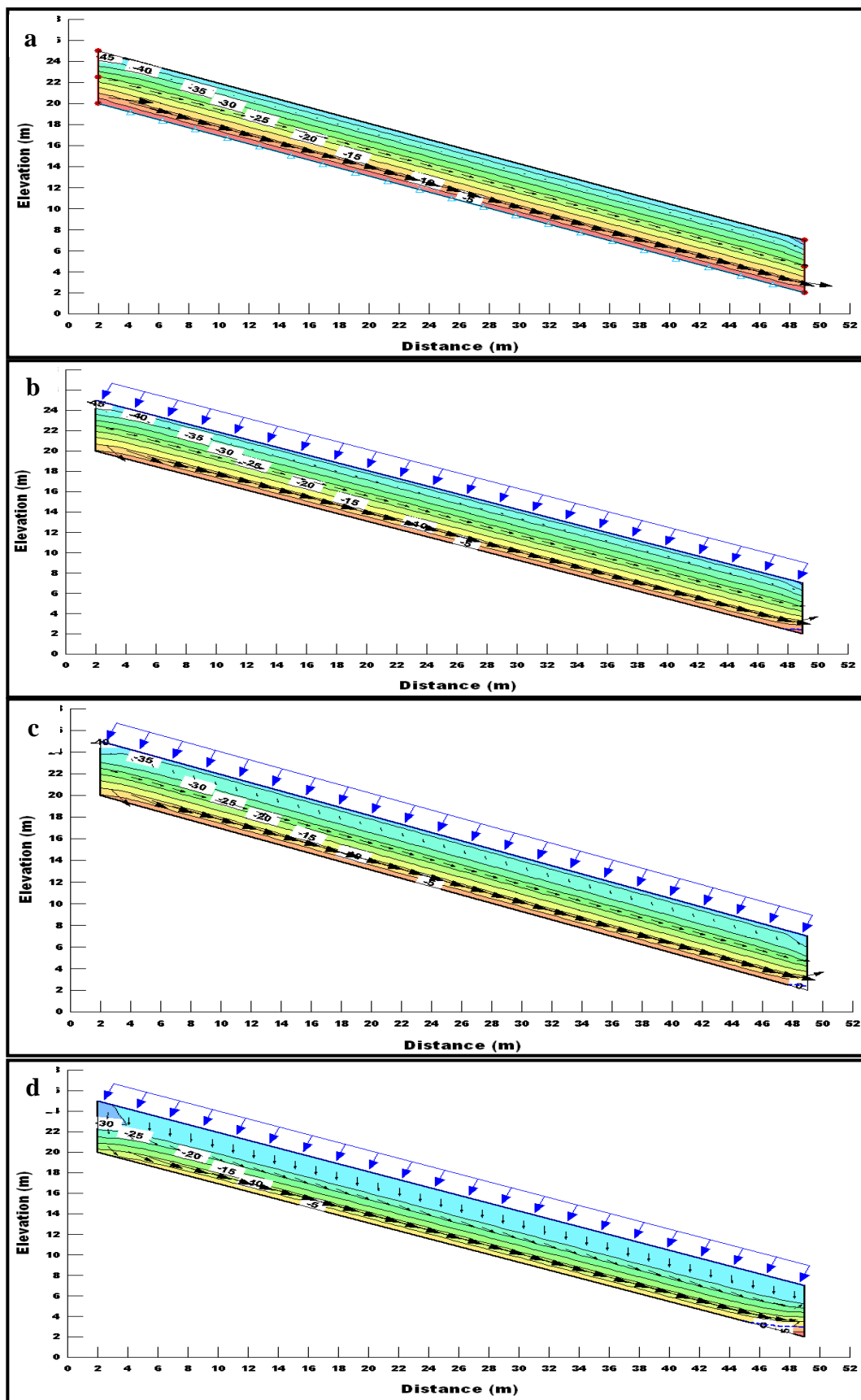
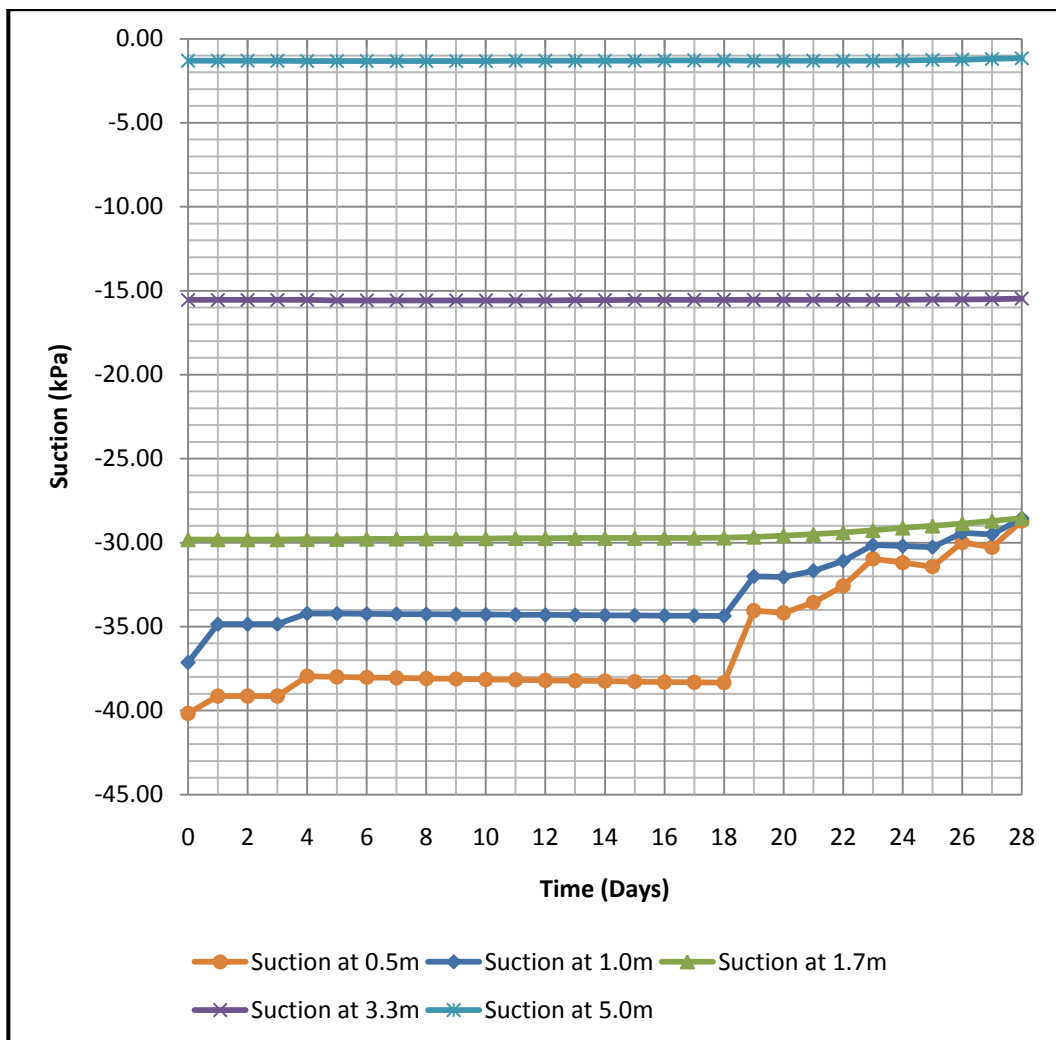
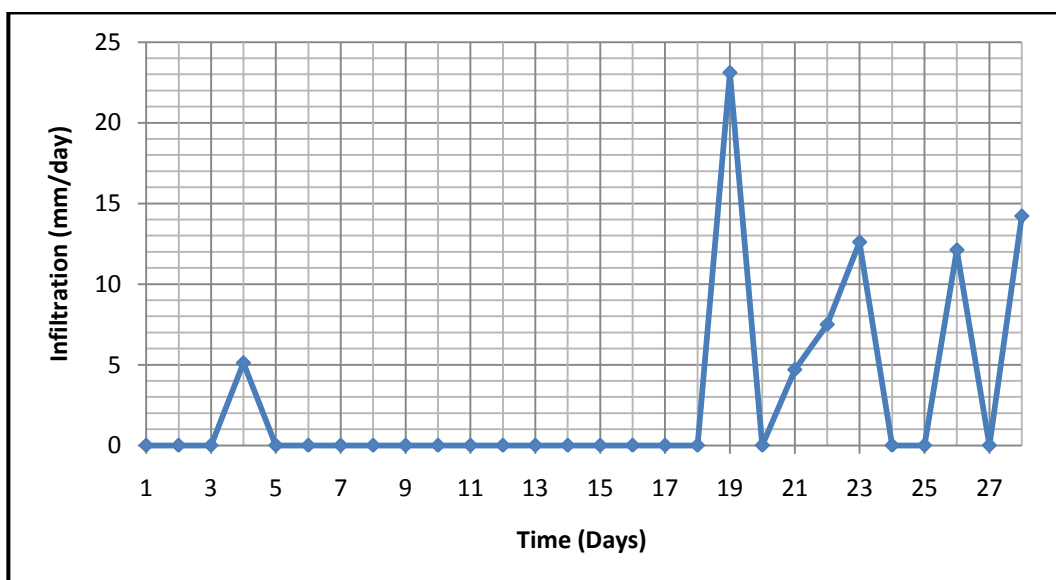


Figure 4.8: seepage patterns and pore-water pressure head profile on (a) 1st, (b) 4th, (c) 19th and (d) 28th



(a)



(b)

Figure 4.9: Suction and infiltration variations with depth and time

b. Due to Rainfall Infiltration and Evaporation

The differences between the rainfall infiltration and evaporation for these days are; 1st February (-4mm/day), 4th February (1.11mm/day), 19th February (17.10mm/day) and 28th February (10.21mm/day). The seepage pattern and pore-water pressure head profile for these days are shown in Figure 4.10(a), (b), (c) and (d).

The variation of suction with depth and time is presented in Appendix C. Figure 4.11(a) and (b) shows the variation of suction with depth and time and that of difference between infiltration and evaporation with time. From this Figures; the changes of suction with depth is also more noticeable at depths of 0.5m and 1.0m from the surface of the slope. The suction increases from 1st – 3rd February due to drying of the soil but on 4th February there was little decrease in suction due to wetting of the soil mass. From 5th – 18th of February the suction increases continuously due to continuous drying of the soil until on 19th when there is wetting which causes decrease in suction. From 20th – 26th the changes in suction continuous alternatively (i.e., decreases when there is wetting and increases when there is drying as shown in that figure. There was final decrease in suction due to rainfall infiltration on 26th of February.

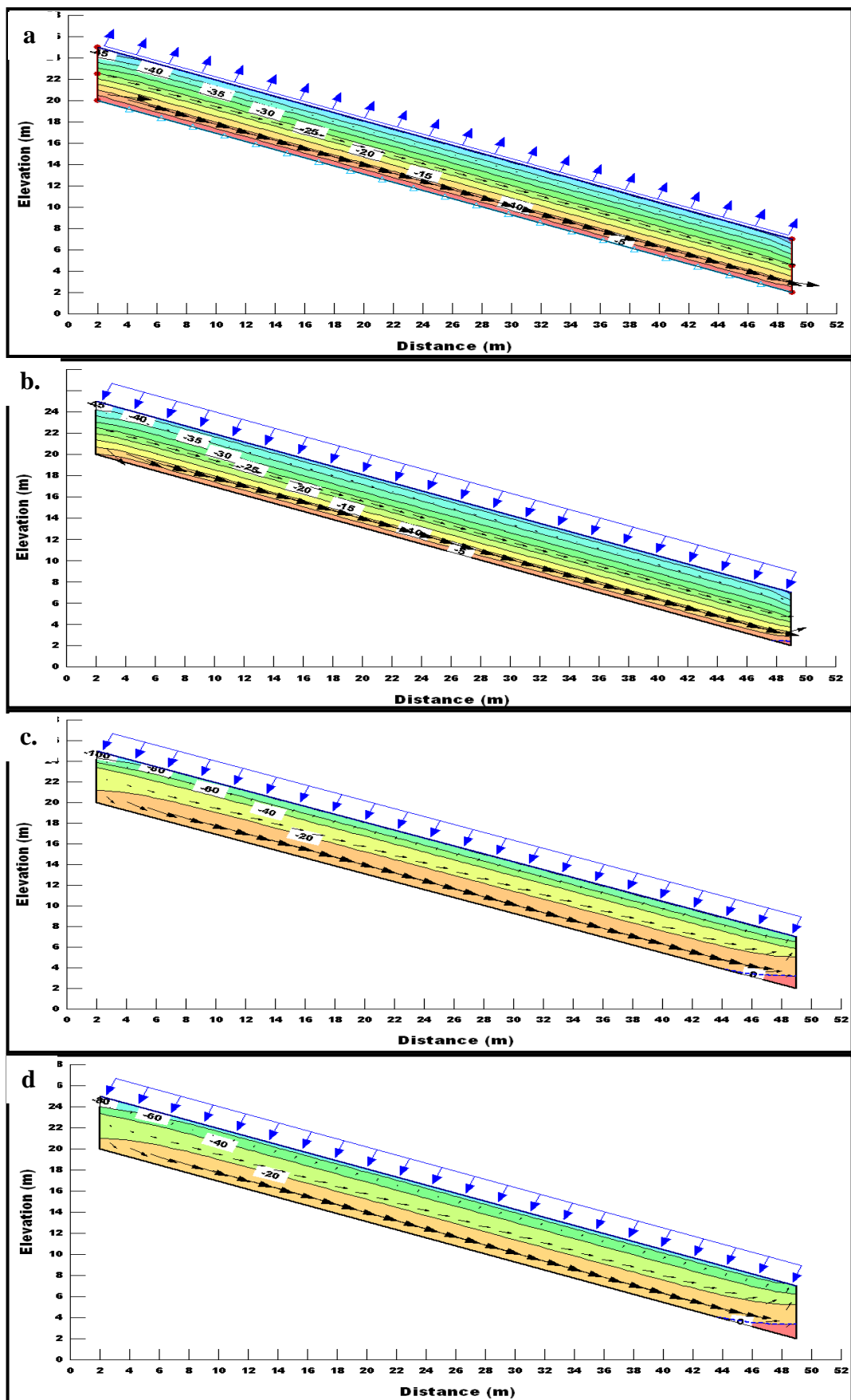
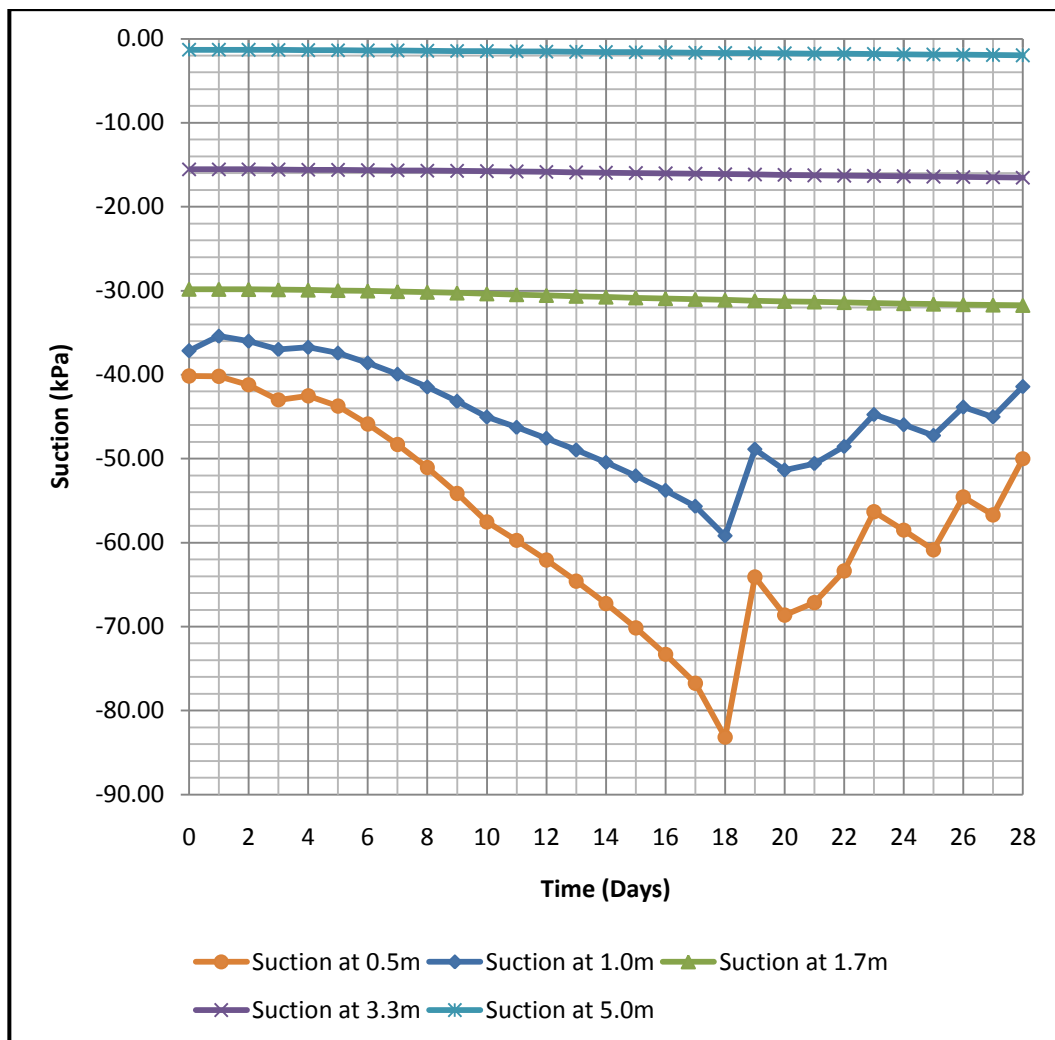
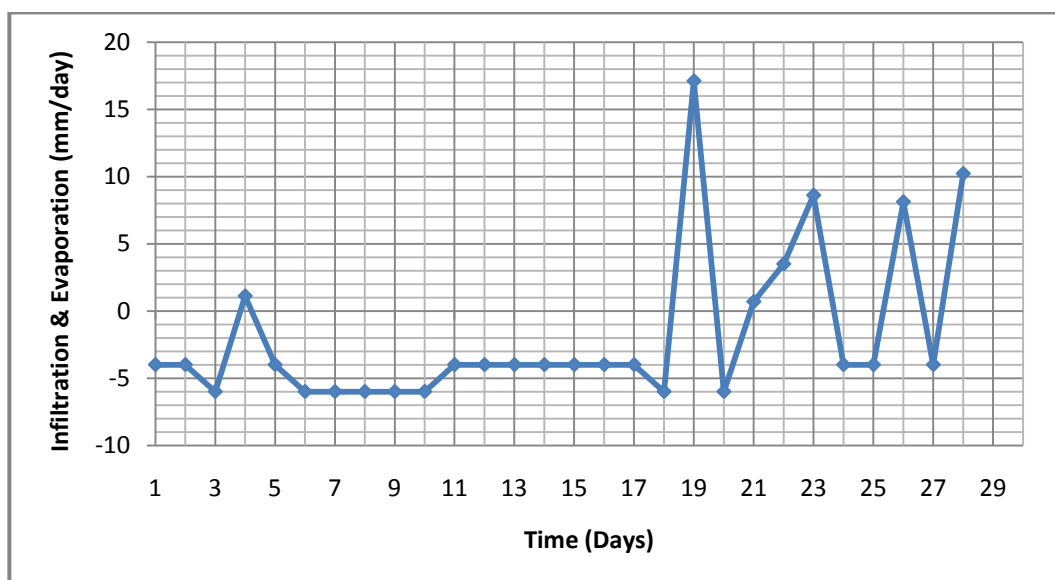


Figure 4.10: Seepage pattern and pore-water pressure profile on (a) 1st, (b) 4th, (c) 19th and (d) 28th



(a)



(b)

Figure 4.11: Suction and infiltration variations with depth and time

4.3.2 Suction Distribution in June

a. Due to Rainfall Infiltration

The month of June is the second dry months considered for the analysis, as in the case of February four days were also considered to explain the variation of suction due rainfall infiltration. These days with their corresponding rainfall infiltration are; 1st June (32.13mm/day), 14th June (16.1mm/day), 22nd June (22.05mm/day) and 30th June (0mm/day). The seepage pattern and pore-water pressure head profile for these days were shown in Figure 4.12(a), (b), (c), and (d).

The suction distribution with depth and time due to rainfall infiltration is presented in Appendix C. Figure 4.13(a) and (b) shows the variation of suction with time and that of rainfall infiltration with time. From these Figures the large suction variation with depth also occurs at 0.5 and 1.0m from the surface of the slope with little variation at other depths. For suction variation with time the initial suction before the rainfall infiltration on 1st June was 39.13kPa which drops to 33.21kPa after rainfall infiltrated in to the soil on 1st June. These suction then increased continuously up to 13th of June (34.72kPa) due to continuous days with out rainfall infiltration. On 14th of June the suction decreases to 32.35kPa due to another rainfall infiltration. Similarly on 22nd of June the suction also drops to 30.49kPa due additional rainfall infiltration. The suction increases until on 30th of June where it reaches a value of 32.21kPa.

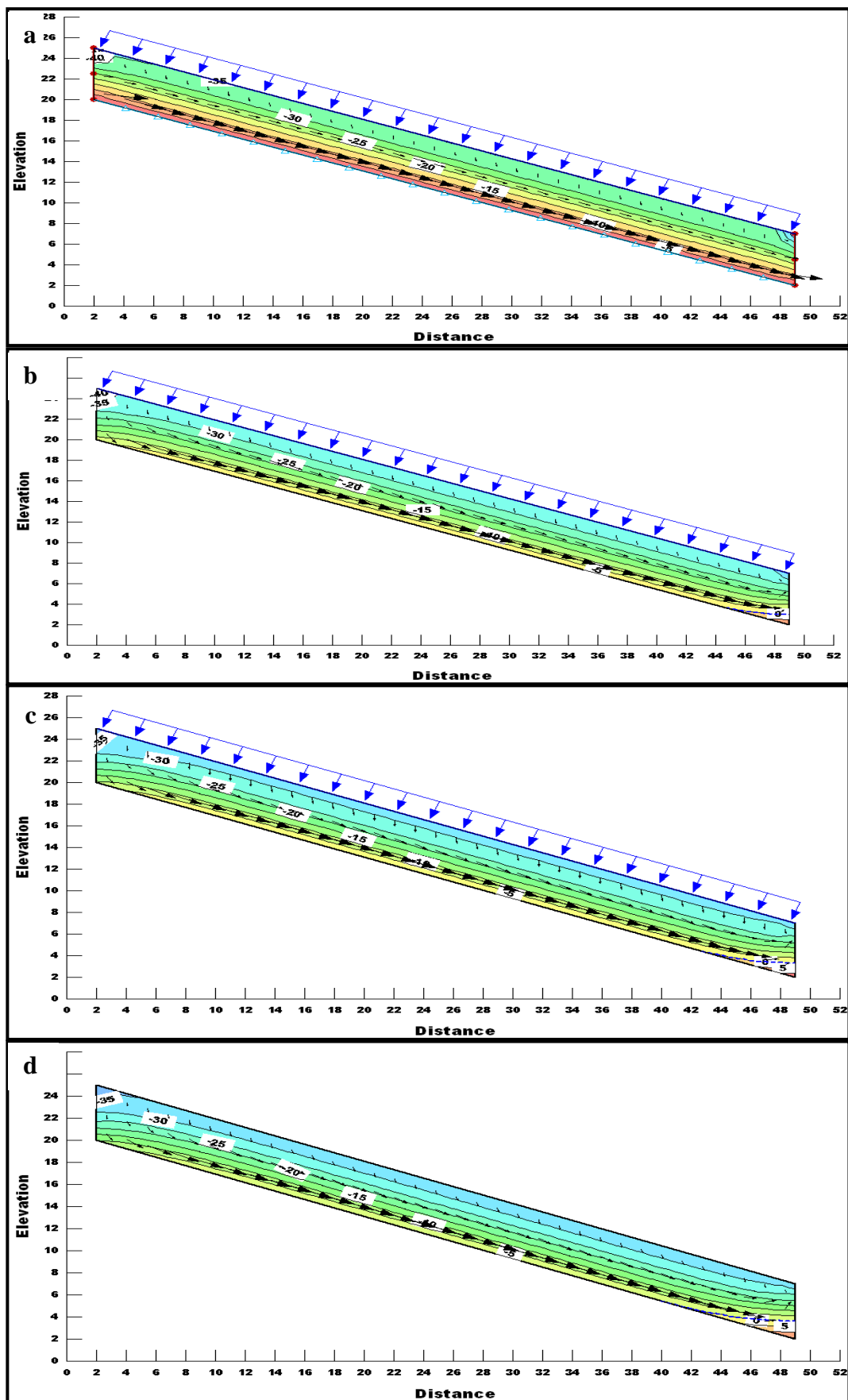
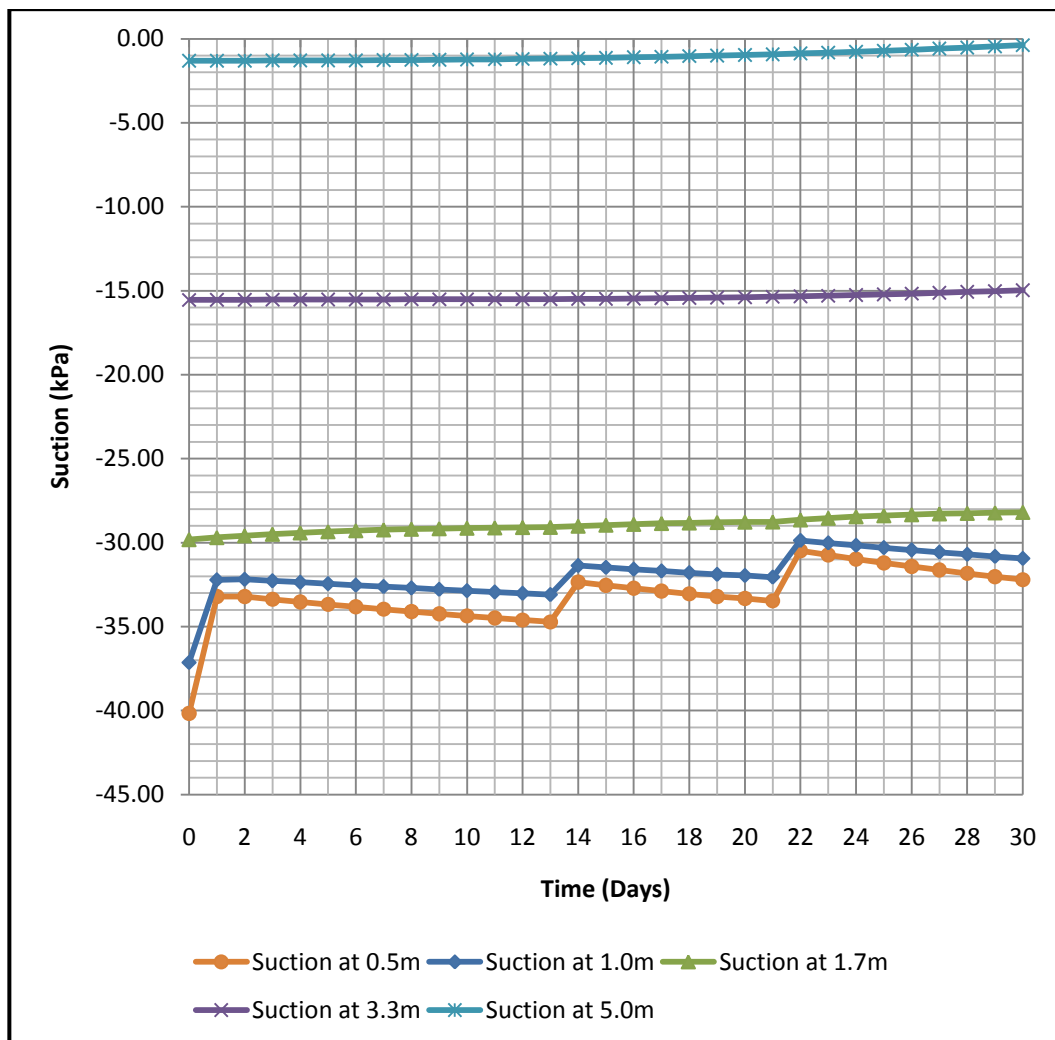
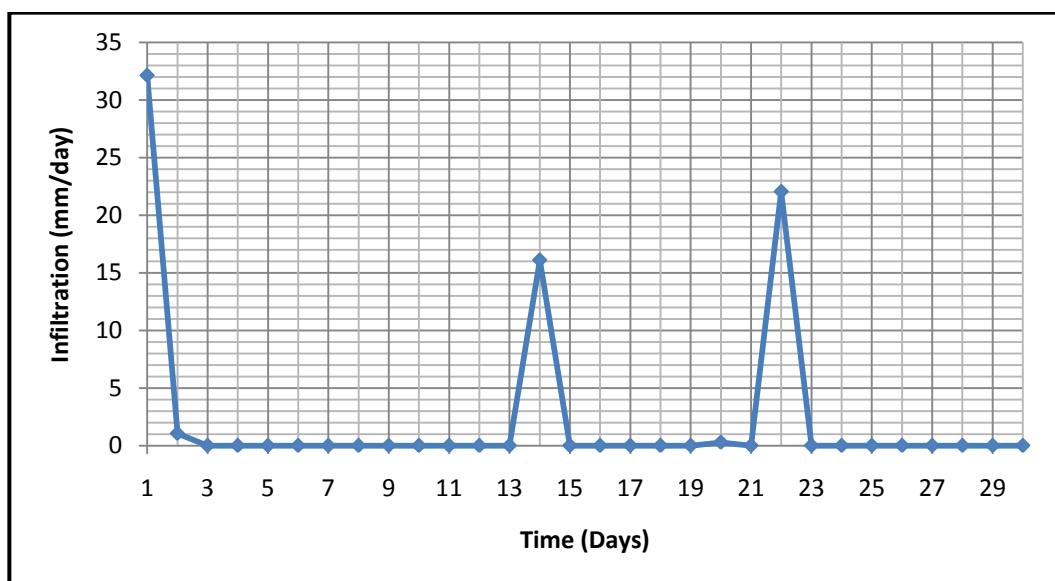


Figure 4.12: Seepage pattern and pore-water pressure head profile on (a) 1st, (b) 14th, (c) 22nd and (d) 30th



(a)



(b)

Figure 4.13: Suction distributions with depth and time for June

b. Due to Rainfall Infiltration and Evaporation

The differences between rainfall infiltration and evaporation for these days were; 1st June (28.13mm/day), 14th June (12.10mm/day), 22nd June (20.05mm/day) and 30th June (-2mm/day). The seepage pattern and pore-water pressure head profile for these days were shown in Figure 4.14(a), (b), (c) and (d).

The suction variation with depth and time is presented in Appendix C. Figure 4.15(a) and (b) shows the variation of suction with depth and time and that of the difference between rainfall infiltration and time. From these Figures the soil suction on 1st June was 33.84kPa which is less than the initial suction before the rainfall infiltration and this value is higher than the value of suction obtained due to rainfall infiltration alone (Figure 4.15). From then, the suction increases continuously due to drying of the soil mass. The suction on 14th and 22nd of June both drops to 39.70kPa and 38.88kPa respectively due to wetting of the soil mass which are all less than the suction values of 43.37kPa and 45.07kPa respectively, observed a day before these days. After 22nd June, there were continuous increase in suction due to continuous drying of the soil and the soil suction on 30th June was 44.94kPa which was higher than the initial suction at the beginning of the month (i.e., 39.13kPa). This really shows that the differences between the rainfall infiltration and evaporation leads to drying of soil mass which causes increase in soil suction.

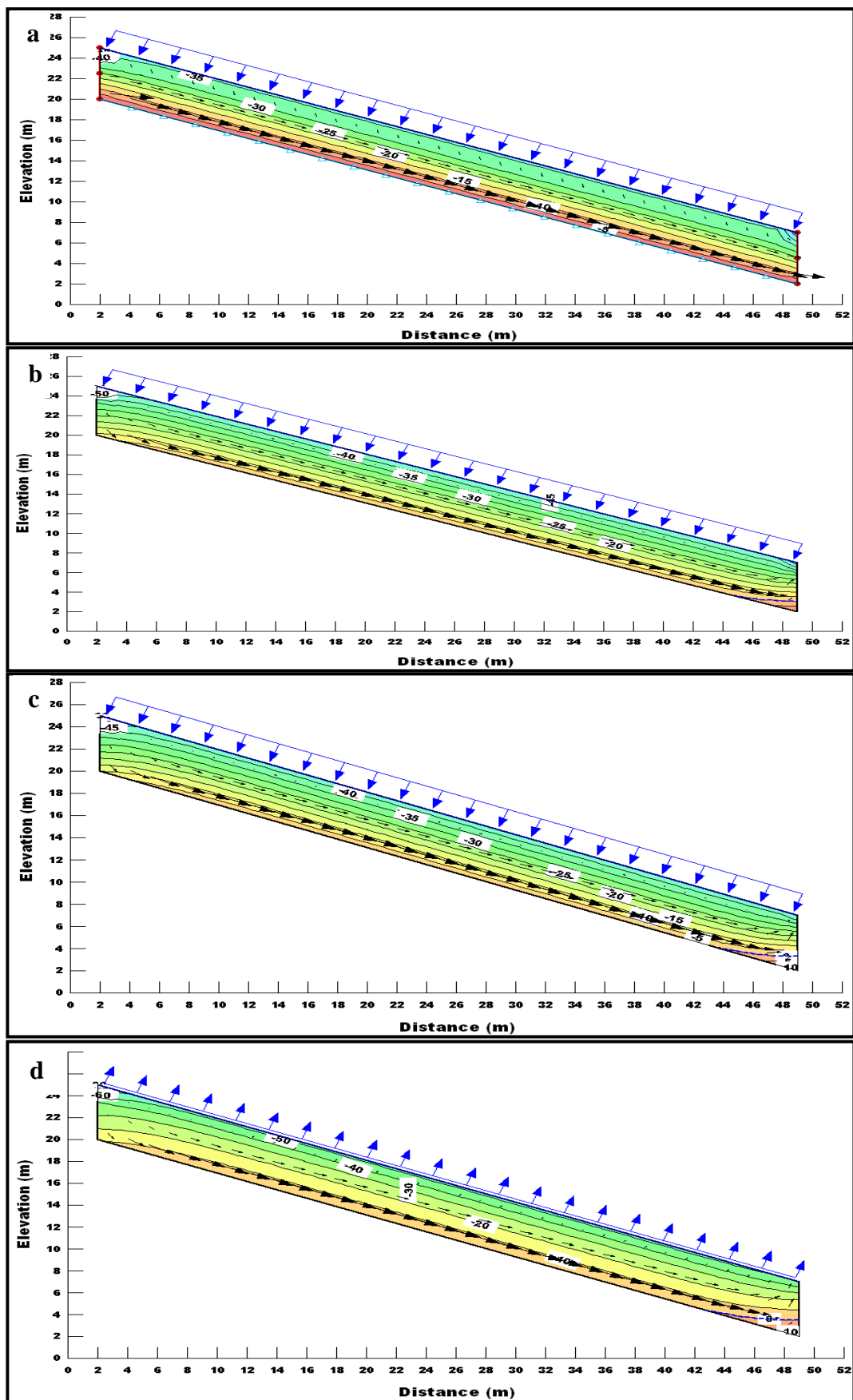
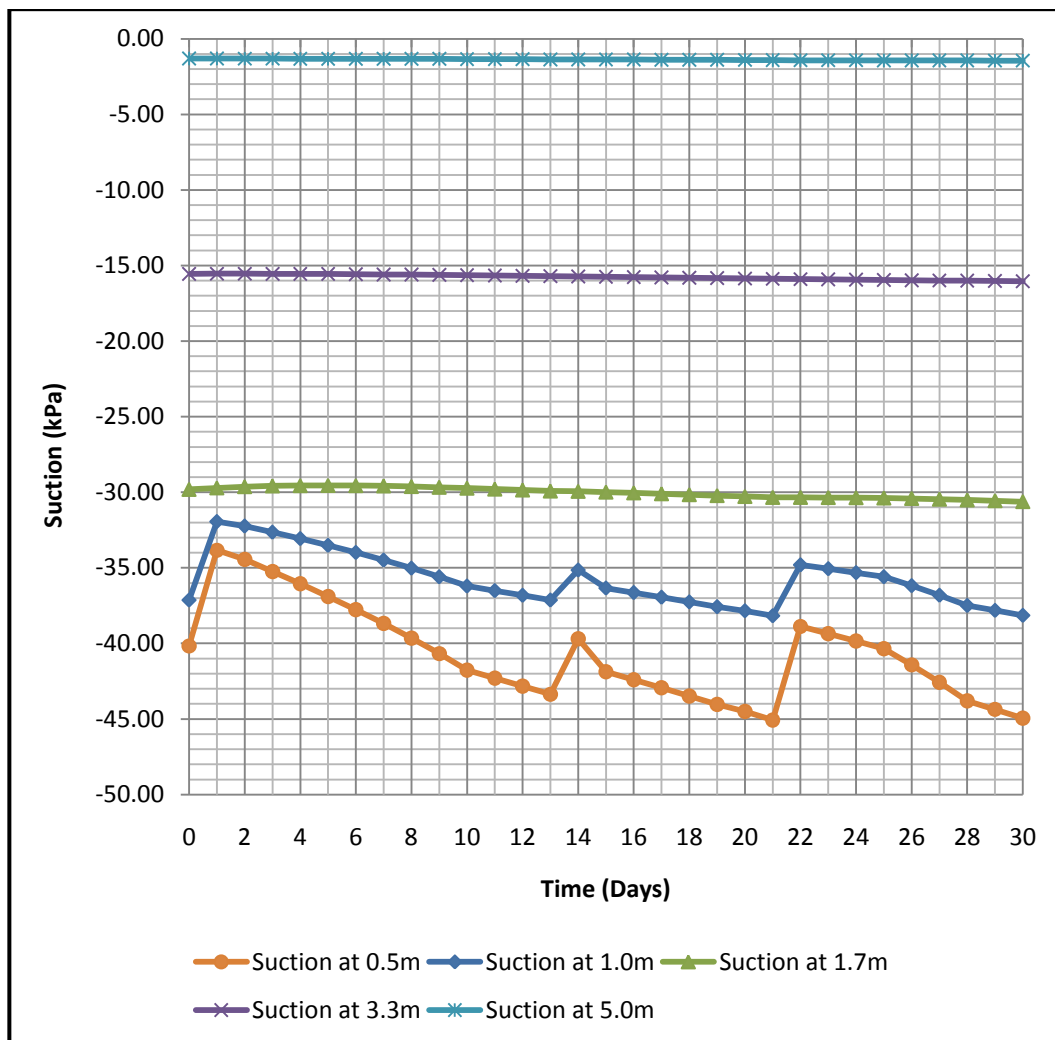
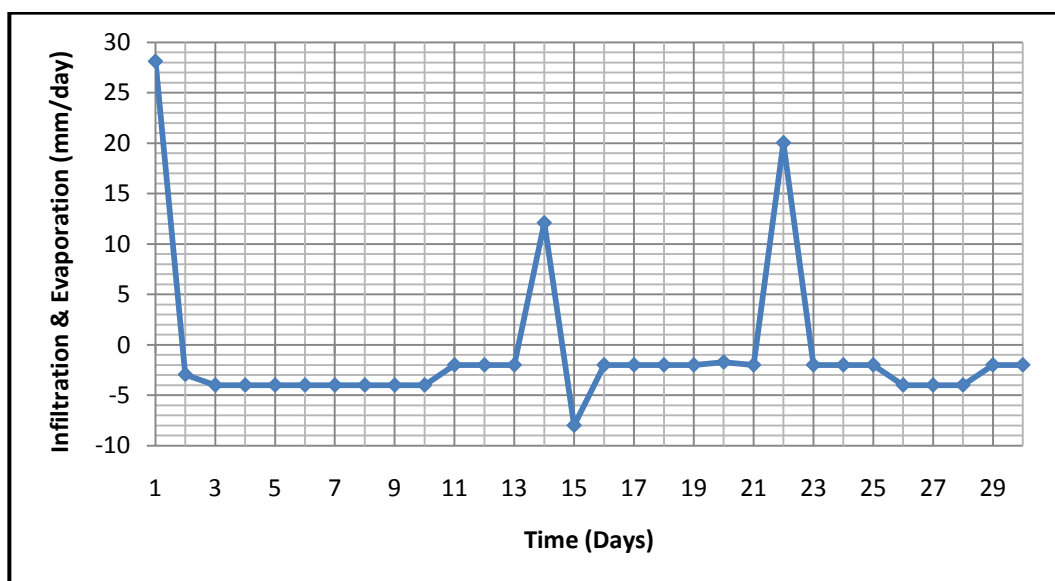


Figure 4.14: Seepage pattern and pore-water pressure head profile on (a) 1st, (b) 14th, (c) 22nd and (d) 30th



(a)



(b)

Figure 4.15: Suction distributions with depth and time for June

4.3.3 Suction Distribution in March

a. Due to Rainfall Infiltration

March is one of the wet months considered for the analysis, as in the case of other months four days were also considered to explain the influence of rainfall infiltration and evaporation on suction distribution. These days with their corresponding amount of infiltrations were; 1st March (5.95mm/day), 9th March (34.65mm/day), 15th March (52.64mm/day) and 31st March (4.06mm/day).

The seepage pattern and pore-water pressure head profile for these days were shown in Figure 4.16(a), (b), (c), and (d). Based on these Figures and the total head gradient the infiltrated water flows in downward direction (i.e., from crest to the toe). The variation of suction with depth and time for this month is presented in Appendix C. Figure 4.17(a) and (b) shows the variation of suction with depth and time and that rainfall infiltration with time. Based on these Figures the initial suction at a depth of 0.5m was 40.01kPa which decreases to 38.56kPa on 1st March after rainfall infiltration. On 9th March the suction also decreases to 30.62kPa against 35.83kPa recorded a day before as a result of rainfall infiltration. The suction also decreases to 23.81kPa due another rainfall infiltration on 15th March this value was also less than 29.20kPa recorded a day before. On 31st March the suction was 26.67 kPa which was slightly less than a value of 26.74kPa recorded a day before (i.e., 30th March). Also from Figure 4.15 the variation of suction with depth and time can be considered significant at all depths due to the effect of wetness, for instance at a depth of 1.0m the suction decreases to 26.51kPa at the end of the month against the initial suction value of 37.13kPa, at 1.7m also the suction drops to 23.63kPa against the initial suction value of 29.79kPa, at 3.3m the suction drops to 11.75kPa against the initial suction of 15.55kPa and finally at the depth of 5.0m the negative pore-water pressure changes to positive (i.e., perched water table has built up at this depth) due to accumulation of rainfall infiltration. This is because of high rainfall infiltration experienced through out the month.

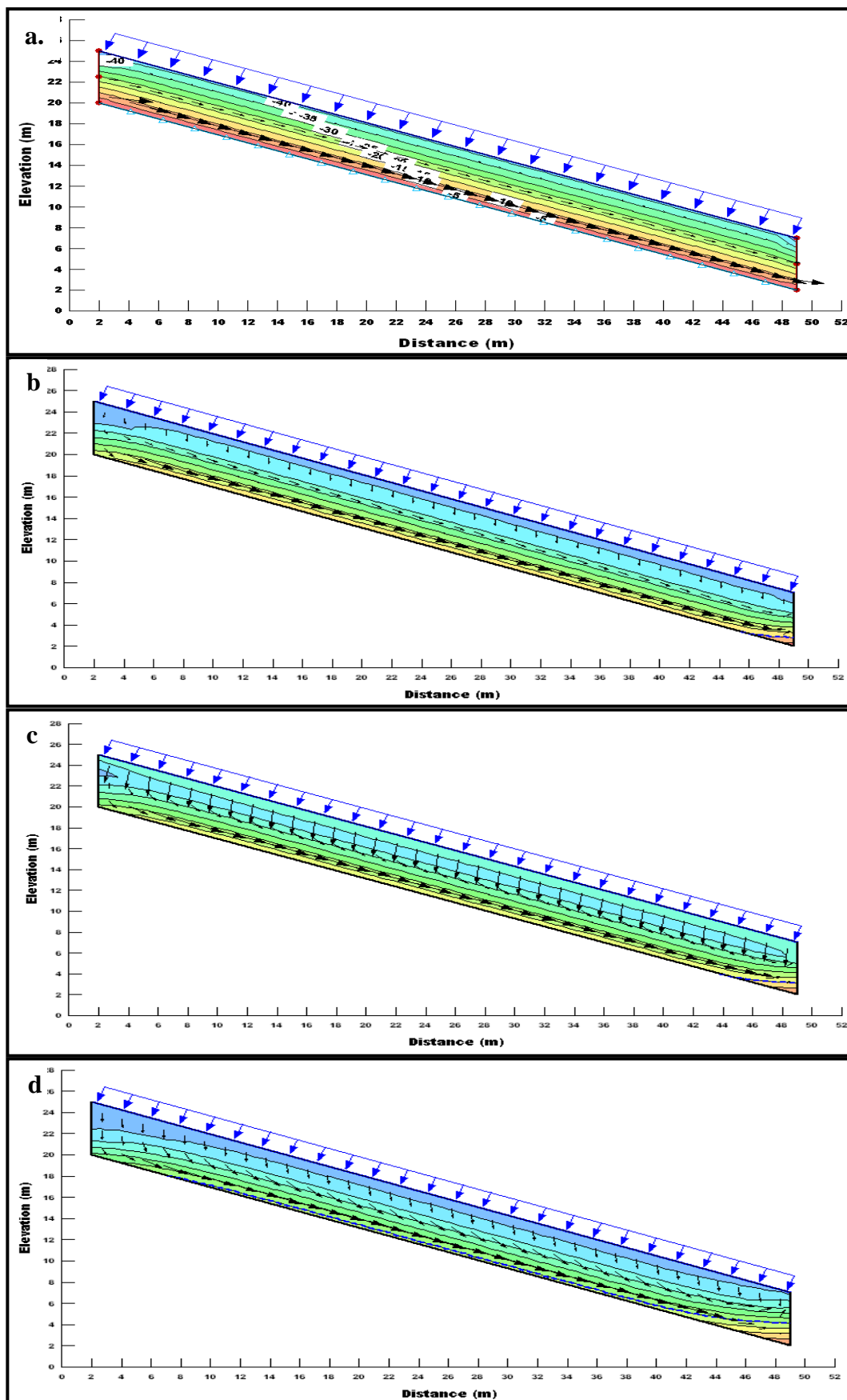
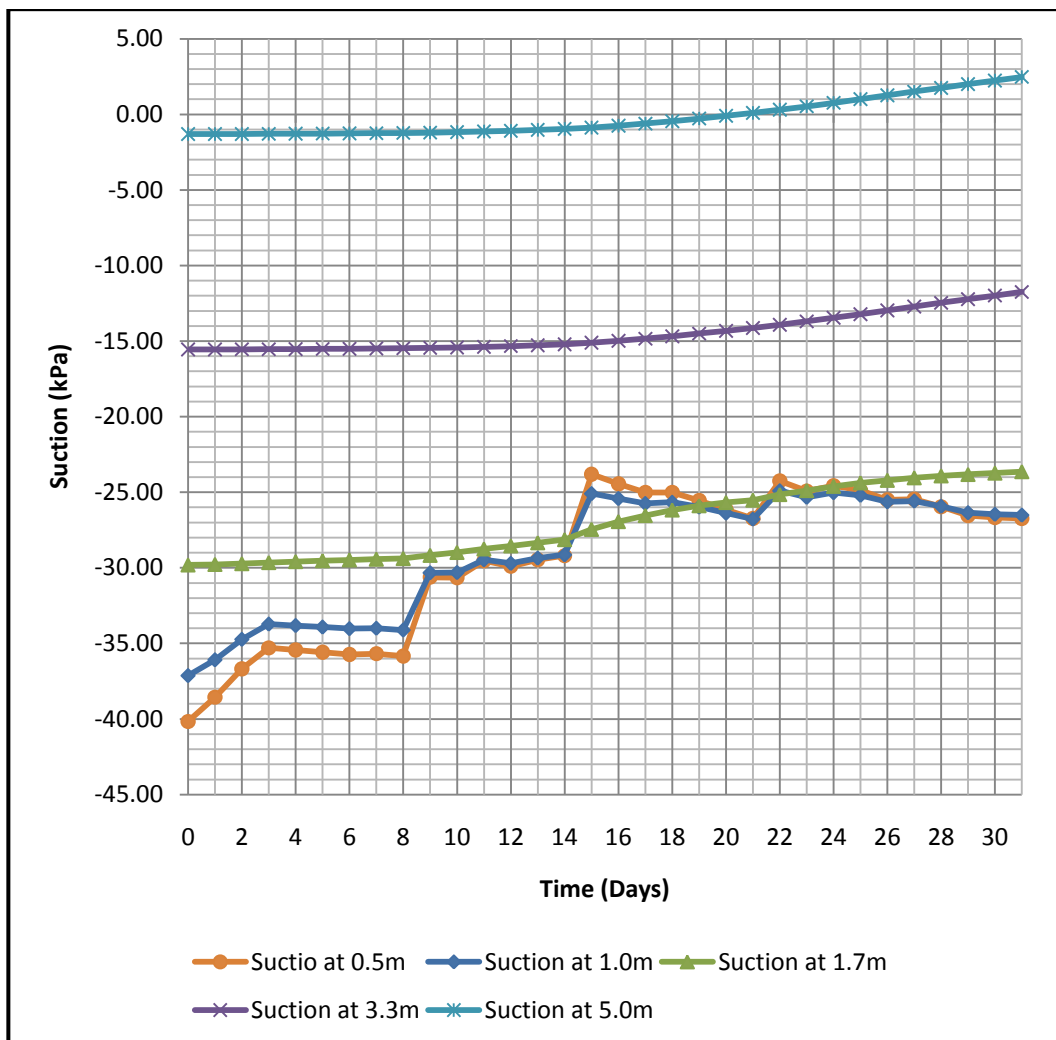
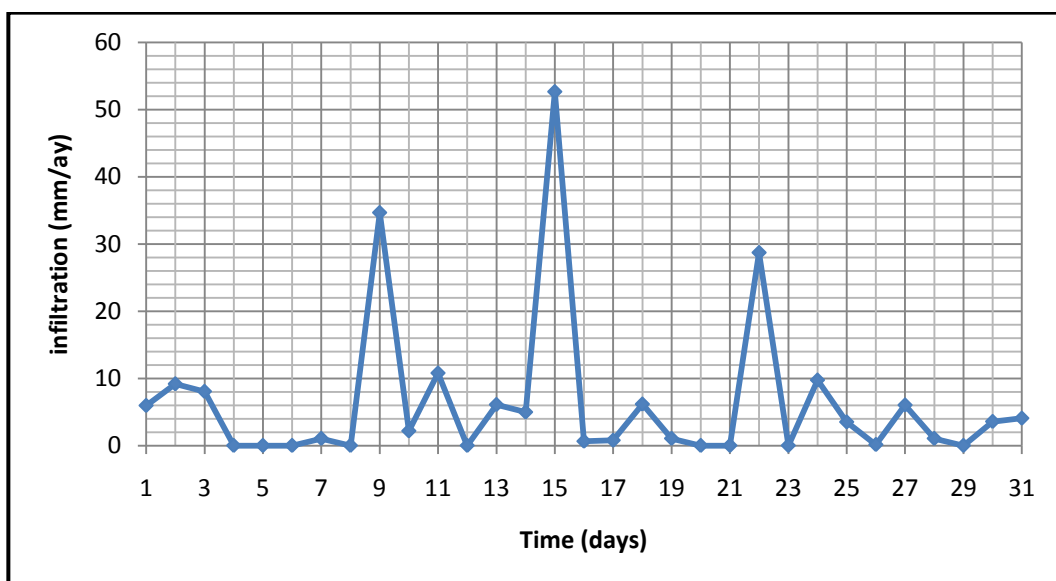


Figure 4.16: Seepage pattern and pore-water pressure head profile on (a) 1st, (b) 9th, (c) 15th and (d) 31st



(a)



(b)

Figure 4.17: Suction distributions with depth and time for March

b. Due to Rainfall Infiltration and Evaporation

The differences between rainfall infiltration and evaporation for these days were; 1st March (1.95mm/day), 9th March (30.65mm/day), 15th March (48.64mm/day) and 31st March (2.06mm/day). The seepage pattern and pore-water pressure head profile for these days were shown in Figure 4.18(a), (b), (c) and (d).

The suction variation with depth and time for this month is presented in Appendix C. Figure 4.19(a) and (b) shows the variation of suction with depth and time and that of difference between rainfall infiltration and evaporation with time. From these Figures; the suction increases when there is drying and decreases when there is wetting, on 1st March the suction was 39.66kPa which is greater than the suction value of 38.56kPa due to rainfall infiltration. On 9th and 15th March the suction values were all less than suction values a day before and were at the same time greater than the suction values due to rainfall infiltration. The suction value on 31st is also greater than that due to infiltration but is the same as that of a day before (i.e., 31.80kPa) this is because the difference between the rainfall infiltration and evaporation is smaller enough to cause any change.

The response of suction due to differences between rainfall infiltration and evaporation was noticed for all depths but is more at 0.5m and 1.0m. The negative pore-water pressure changes to positive value at a depth of 5.0m due to accumulation of rainfall infiltration but the observed values of positive pore-water pressure were less than that of rainfall infiltration only. In the case of rainfall infiltration the negative pore-water pressure changes to positive on 21st of March but in the case of difference between rainfall infiltration and evaporation it changes to positive on 26th March i.e., 5 days later and this was due to the influence of the differences between rainfall infiltration and evaporation on suction distribution.

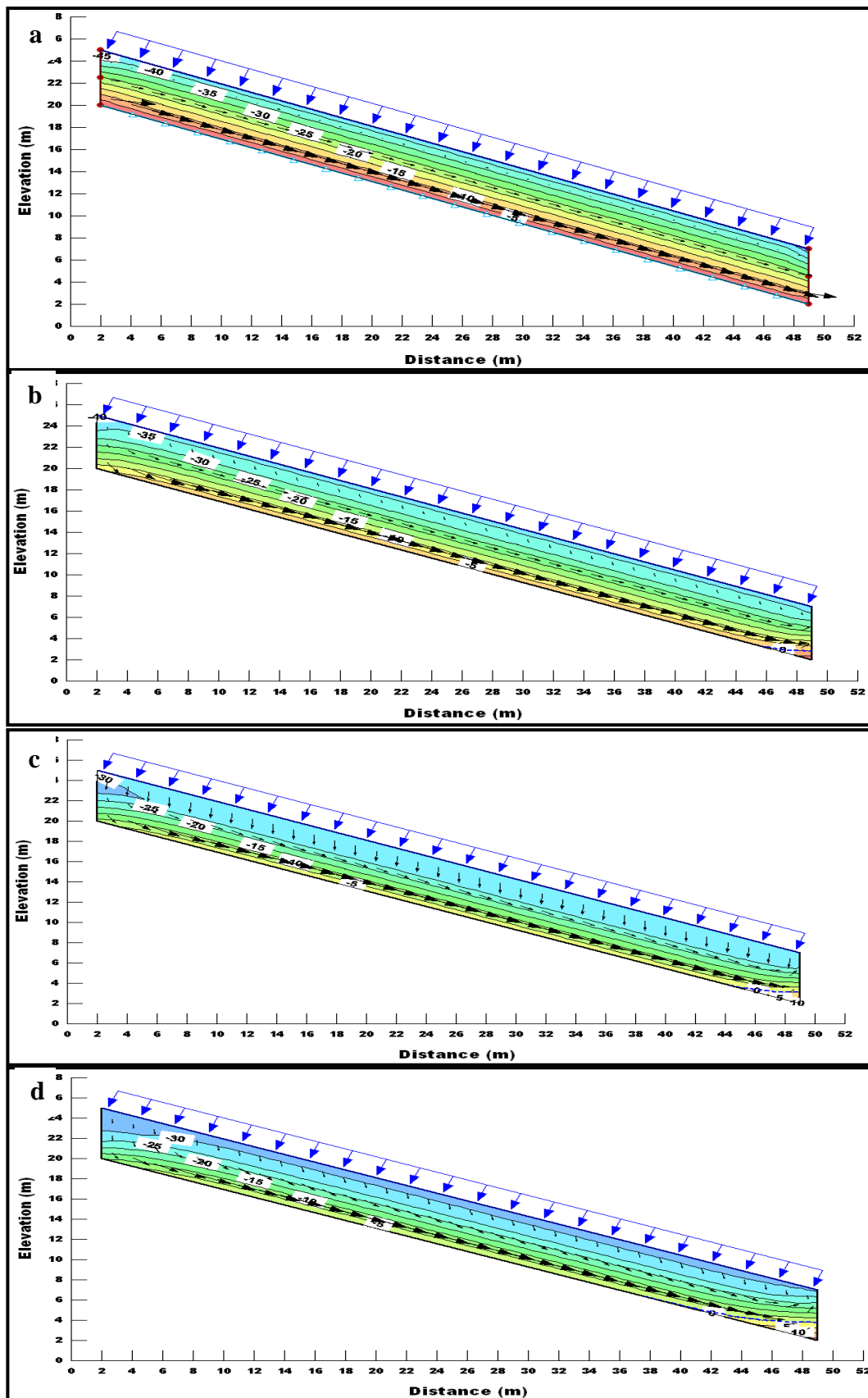
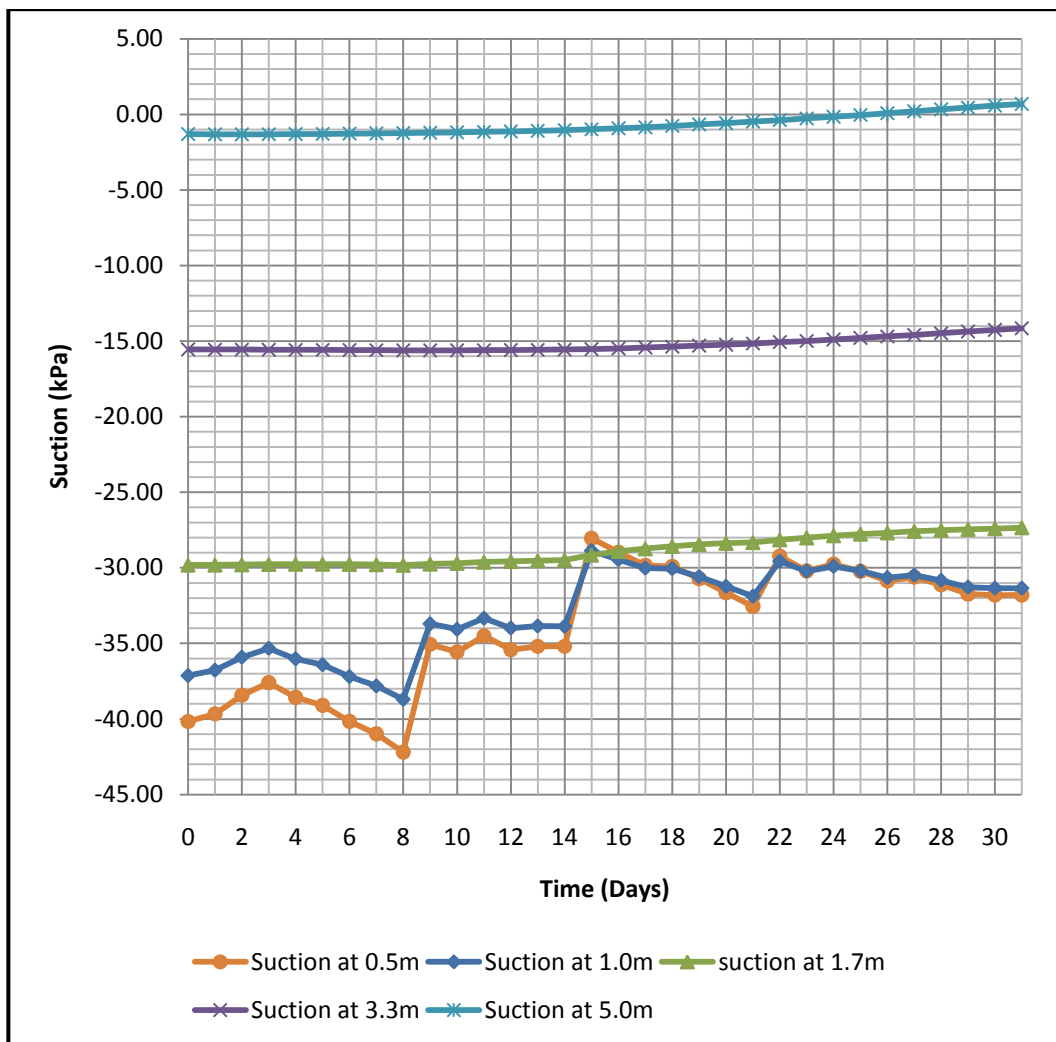
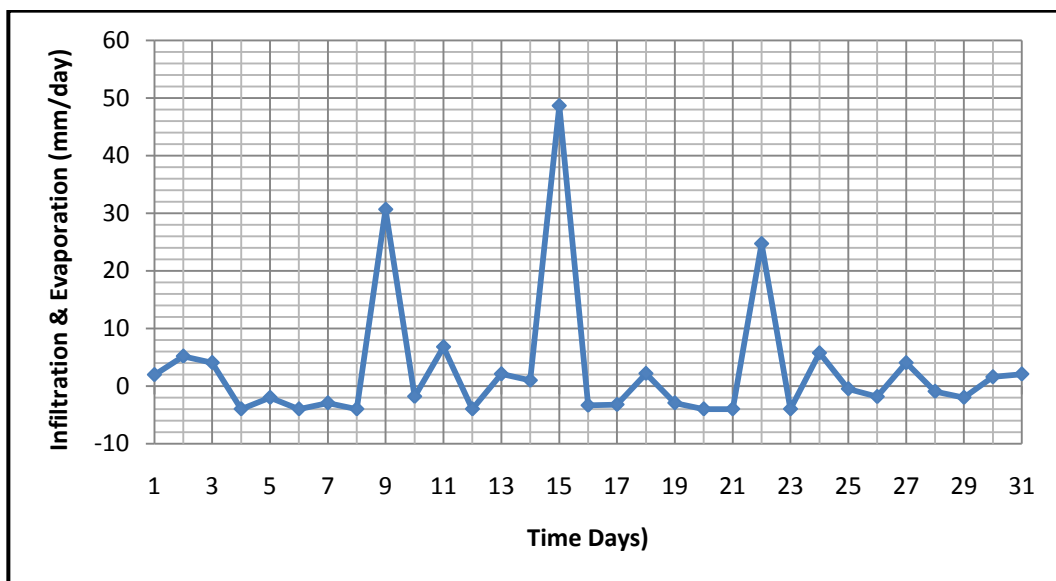


Figure 4.18: Seepage pattern and pore-water pressure head profile on (a) 1st, (b) 9th, (c) 14th and (d) 31st



(a)



(b)

Figure 4.19: Suction distributions with depth and time for March

4.3.4 Suction Distribution in December

a. Due to Rainfall Infiltration

December was the second wet months considered for the analysis. In the same way as done in other months four days were also selected to explain the influence of rainfall infiltration and evaporation on suction distribution. These days with their corresponding amount of rainfall infiltration are; 3rd December (25.9mm/day), 17th December (13.02mm/day), 20th December (17.15mm/day) and 31st December (0 mm/day). The seepage pattern and pore-water pressure head profile due to rainfall infiltration for these days were shown in Figure 4.20(a), (b), (c), and (d).

Similarly, the suction variation with depth and time is presented in appendix C. Figure 4.21(a) and (b) shows the variation of suction with depth and time and that of rainfall infiltration with time for this month. Based on this Figure the value of suction at 0.5m falls drastically on 3rd December to 34.63kPa against 40.17kPa observed in the previous days. This was due to high rainfall infiltration on 3rd December. From then the suction continues to decrease at very slow pace on days with rainfall (because the amounts were small) and increase on days without rainfall infiltration until 16th December. On 17th December the suction was 31.50kPa which was less than 33.37kPa recorded on 16th because the magnitude of rainfall infiltration on 17th is higher. Similarly, on 20th December the suction also drops to 28.11kPa due another rainfall infiltration. The soil suction on 31st December was 30.47kPa which was less than the initial suction recorded at the beginning of the month.

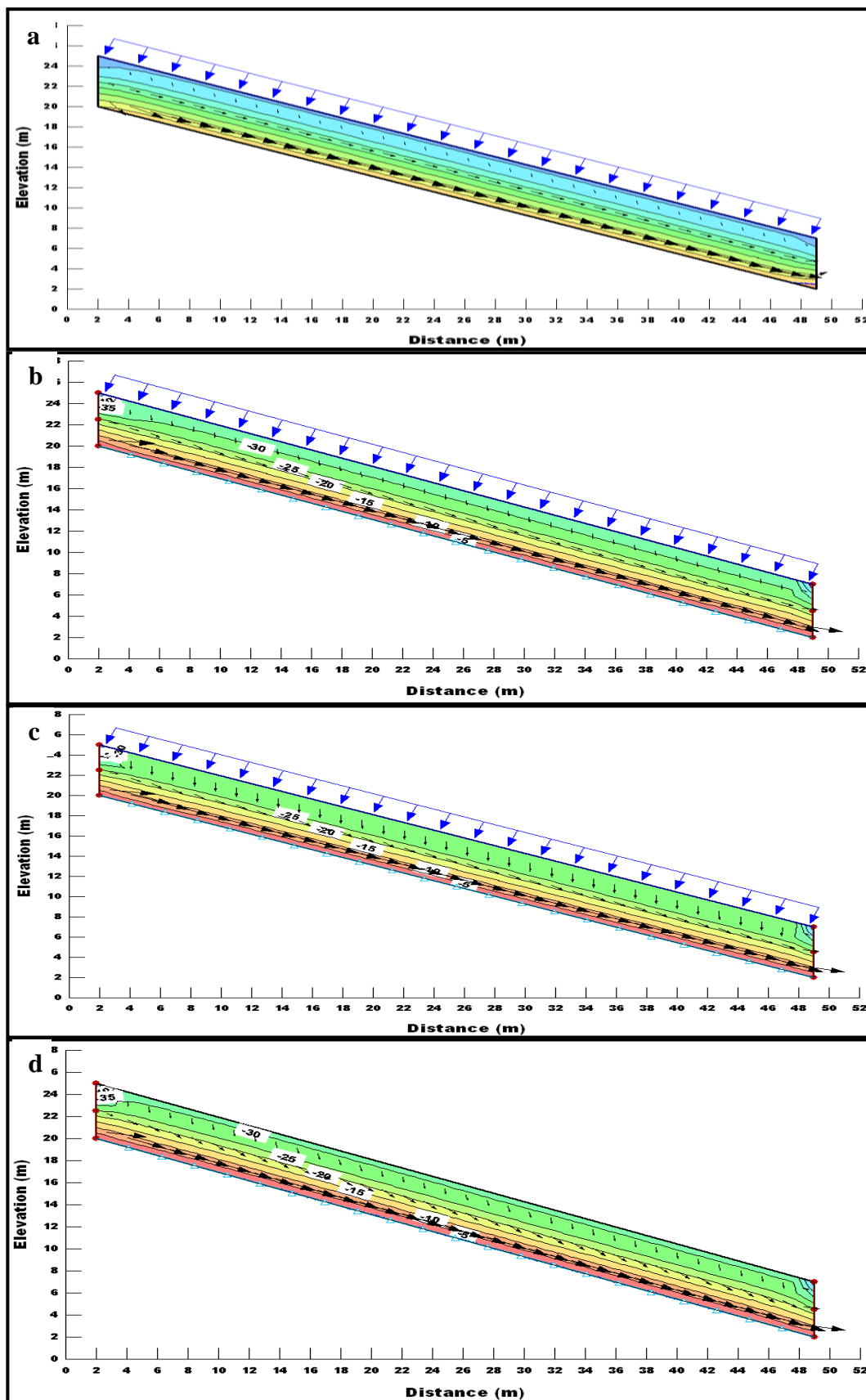
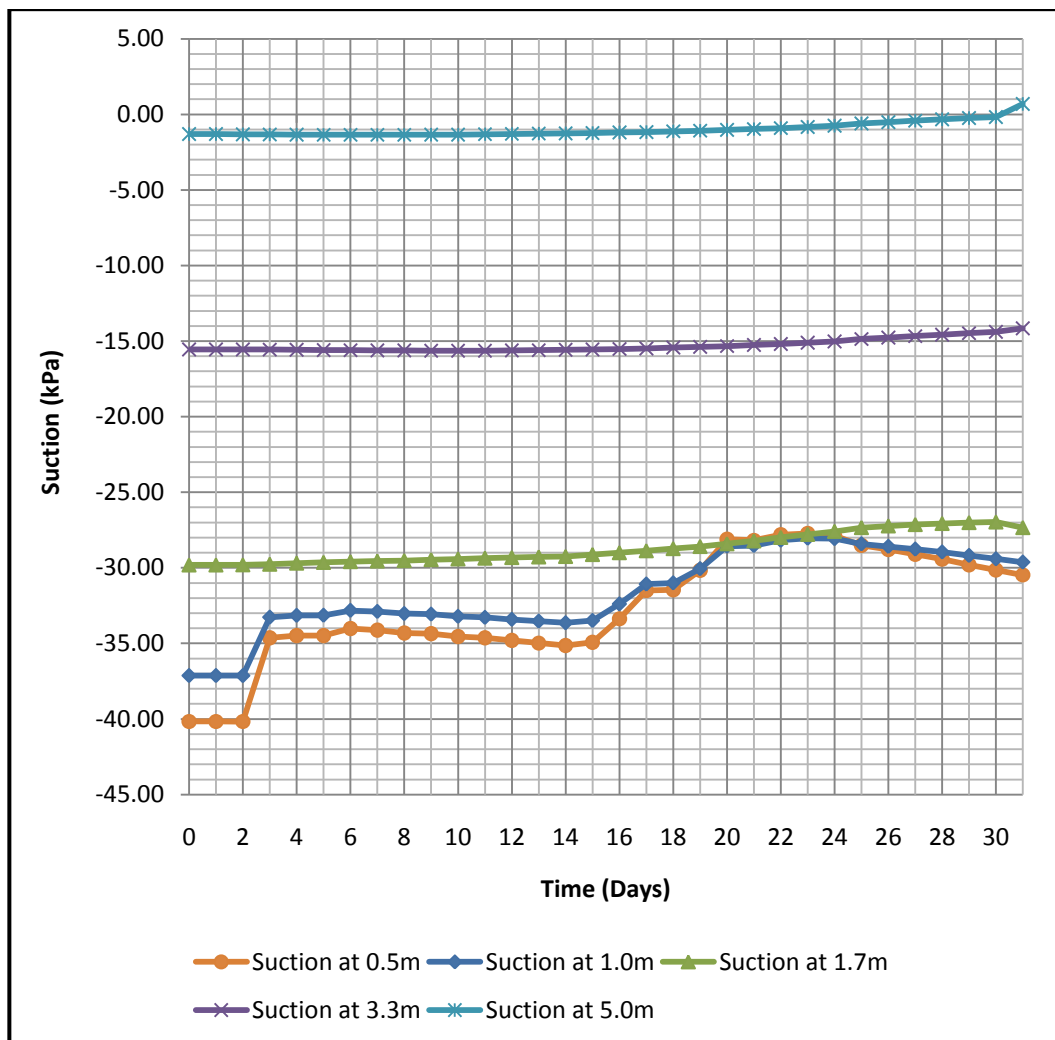
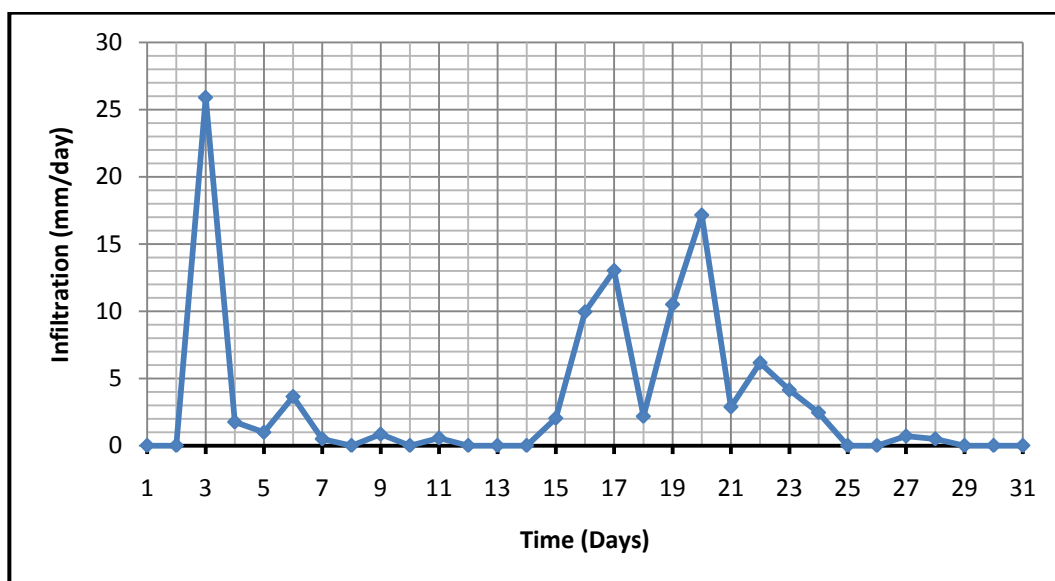


Figure 4.20: Seepage pattern and pore-water pressure head profile (a) 3rd, (b) 17th, (c) 20th and (d) 31st



(a)



(b)

Figure 4.21: Suction distributions with depth and time

b. Due to Rainfall Infiltration and Evaporation

The differences between rainfall infiltration and evaporation for these days were; 3rd December (21.9mm/day), 17th December (9.02mm/day), 20th December (13.15mm/day) and 31st March (-2.00mm/day). The seepage pattern and pore-water pressure head profile due to the differences between rainfall infiltration and evaporation for these four days were shown in Figure 4.22(a), (b), (c), and (d).

The variation of suction with depth and time for this month is presented in Appendix C. Figure 4.23(a) and (b) shows the variation of suction with depth and time and that of differences between rainfall infiltration and evaporation with time for this month. Based on these Figures the suction recorded on 3rd December was 36.97kPa due to wetting of the soil and this value is less than the values recorded on 1st and 2nd which have increase due drying of the soil. Similarly, the suction recorded on 17th and 20th December were 40.44kPa and 36.37kPa which were higher than the values recorded due to rainfall infiltration on the same days and they are also less than the suction values of 43.28kPa and 39.19kPa recorded a day before. The suction on 31st December was 43.17kPa and is greater than 42.52kPa recorded a day before.

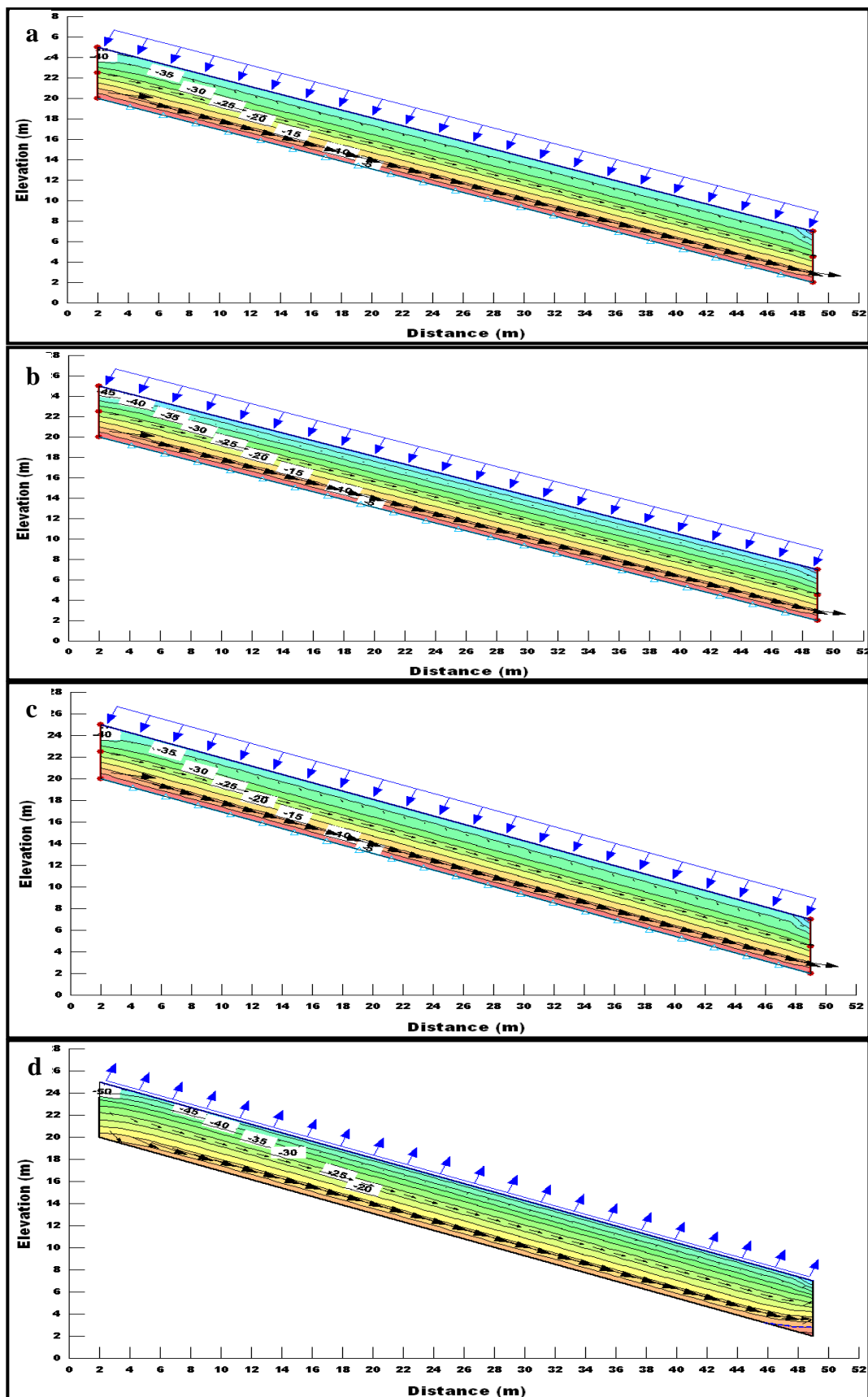
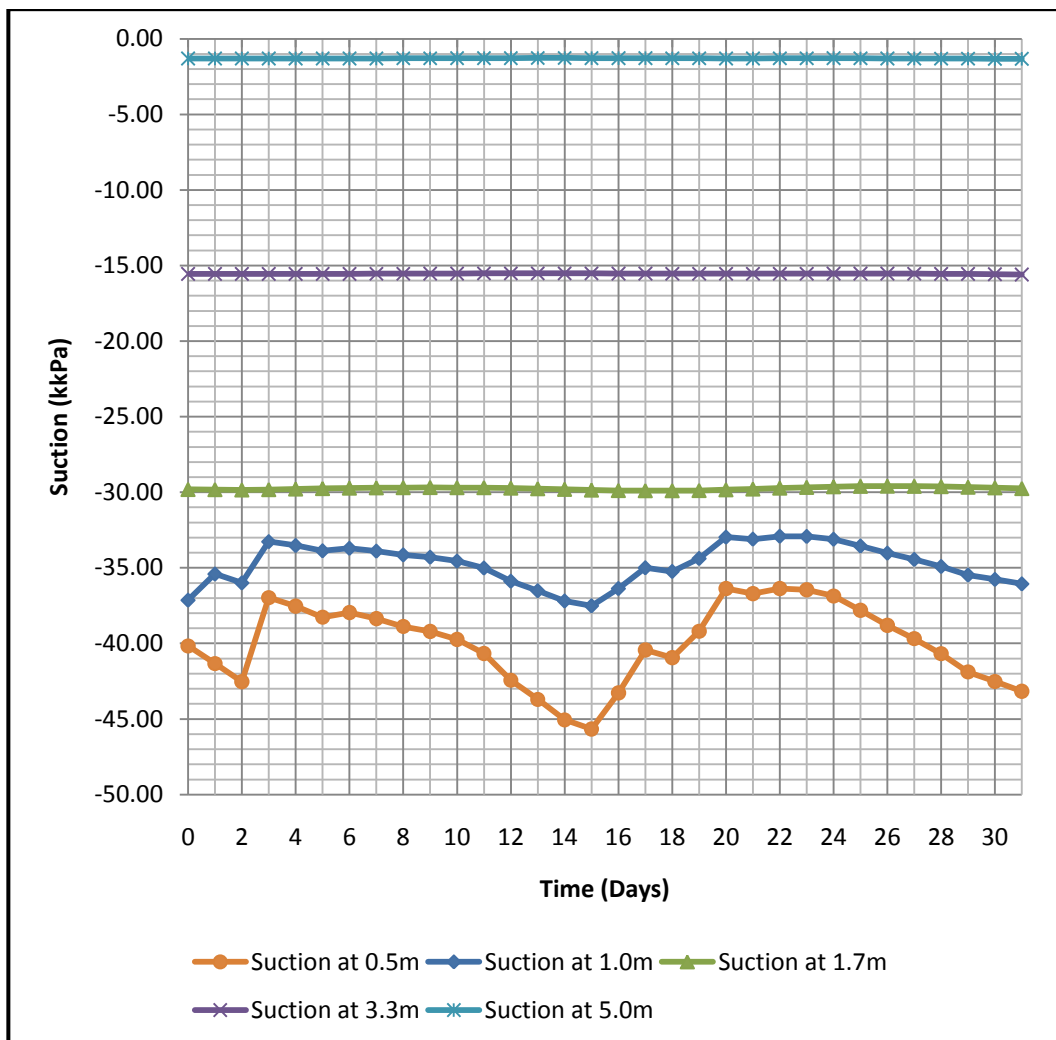
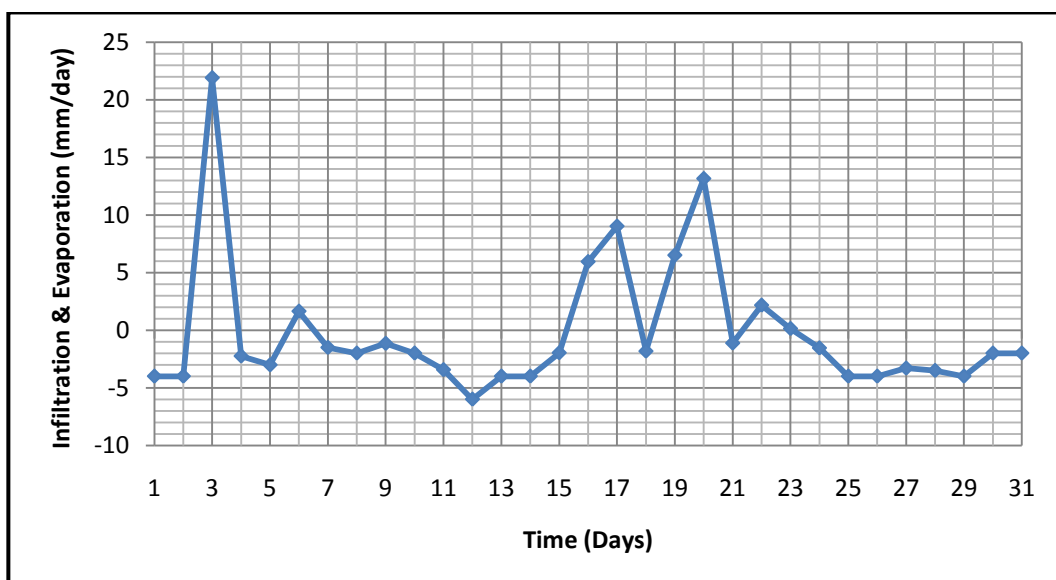


Figure 4.22: Seepage pattern and pore-water pressure head profile (a) 3rd, (b) 17th, (c) 20th and (d) 31st



(a)



(b)

Figure 4.23: Suction distributions with depth and time

4.4 Slope Stability Analyses

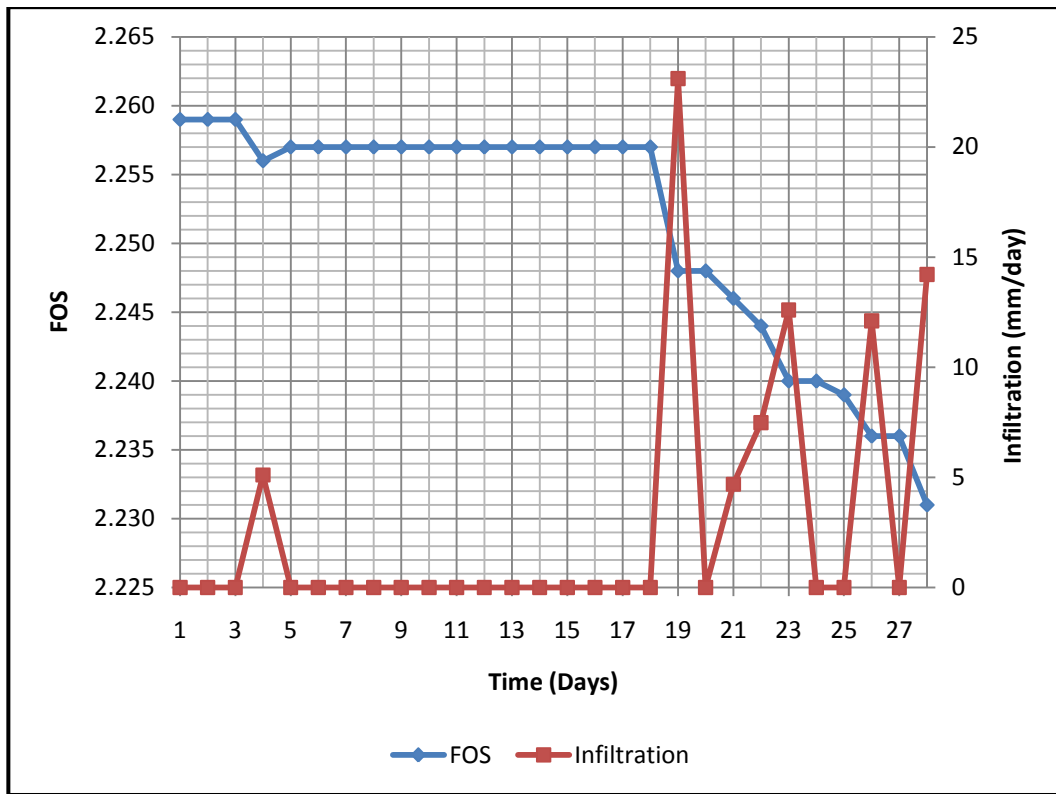
The slope stability analysis was performed based on the seepage pattern and the suction distribution obtained from the transient seepage analysis. The analyses were performed using a computer program SLOPE/W (GeoSlope International Ltd., 2007). Morgenstern-Price method integrated into the software was used to compute the FOS by using Entry and Exit method to specify the slip surface. The slope stability analysis can be used to access how much rainfall infiltration decreases the factor of safety of the slope and how much the difference between rainfall infiltration and evaporation increases the factor of safety of the slope.

4.4.1 Factor of Safety Variations in February

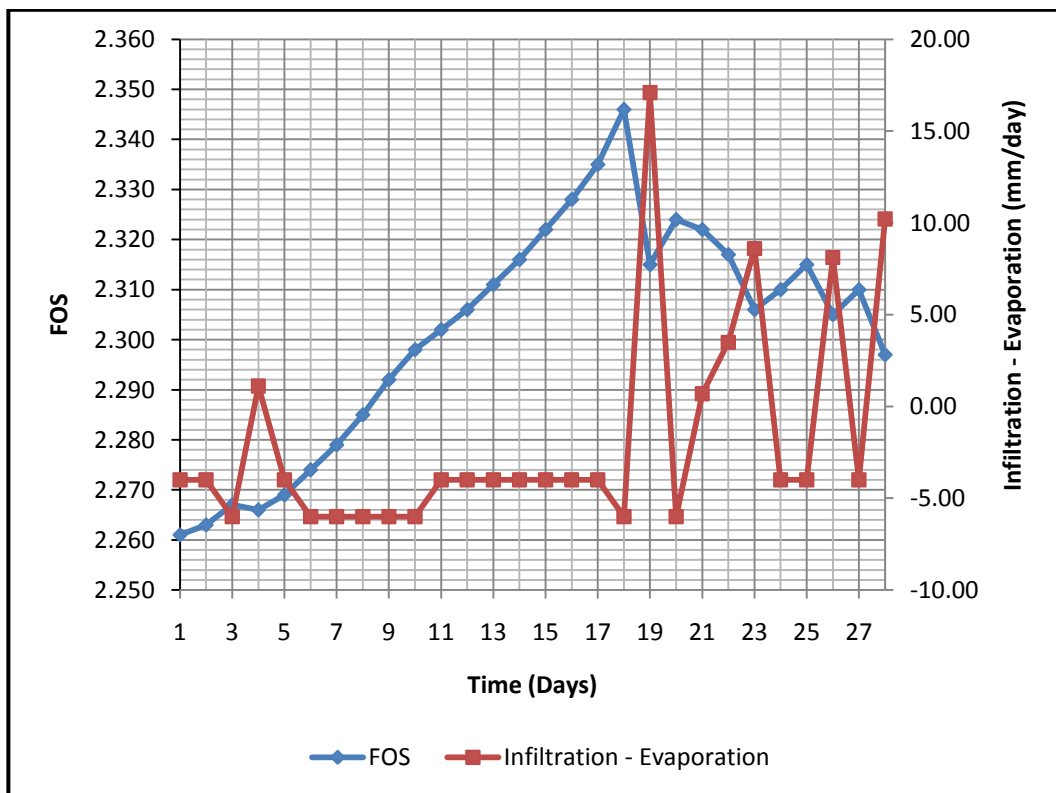
As explained previously, the month of February is one of the dry months considered for the analysis in this project. The results obtained were expressed in terms of factor of safety versus time.

a. Due to Rainfall Infiltration

The variation of FOS and rainfall infiltration with time is presented in Appendix D. Figure 4.24(a) shows the correlation between rainfall infiltration and FOS for this month. From this Figure the FOS decreases with rainfall infiltration due to reduction in soil suction which invariably decreases the shear strength of the soil, and it remain constant on days without rainfall infiltration because the changes in soil suction on those days were negligible. For instance, on 19th February there was rainfall infiltration of 23.1mm/day (highest rainfall infiltration in the month) and this leads to sudden decrease in FOS from 2.257 on a day before (18th February) to 2.248 on 19th February.



(a)



(b)

Figure 4.24: Correlation of Infiltration and Difference and the FOS with time in February

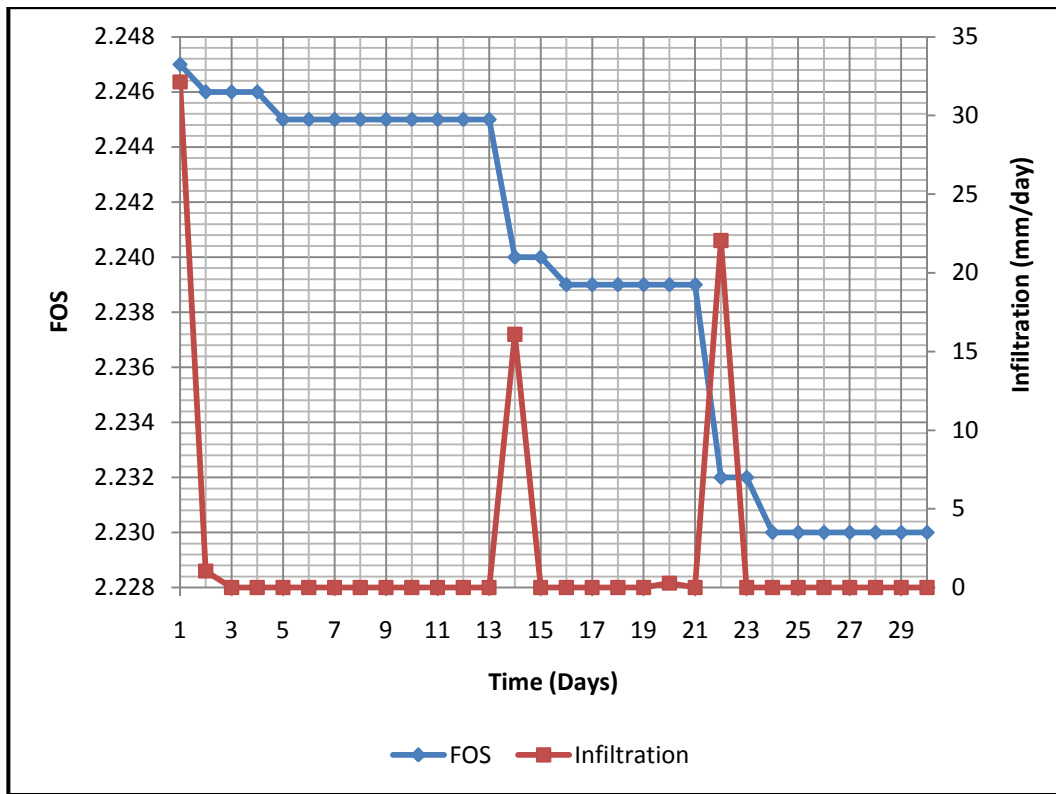
a. Due to Rainfall Infiltration and Evaporation

The variation of FOS and the difference between rainfall infiltration and evaporation with time is presented in Appendix D. Similarly, Figure 4.24(b) shows the correlation between FOS and the differences between rainfall infiltration and evaporation with time for this month. Based on this Figure the FOS increases on the days without rainfall due to continuous drying of the soil mass which leads to increase in soil suction and invariably increases the shear strength of the soil. But where the difference between the rainfall infiltration and evaporation resulted in wetting of the soil mass there was decrease in FOS. For instance, on 19th February, the difference resulted in wetting of the soil mass which reduces the soil suction from 112.31kPa on 18th February to 82.42kPa and this resulted in the decrease in FOS from 2.346 to 2.315.

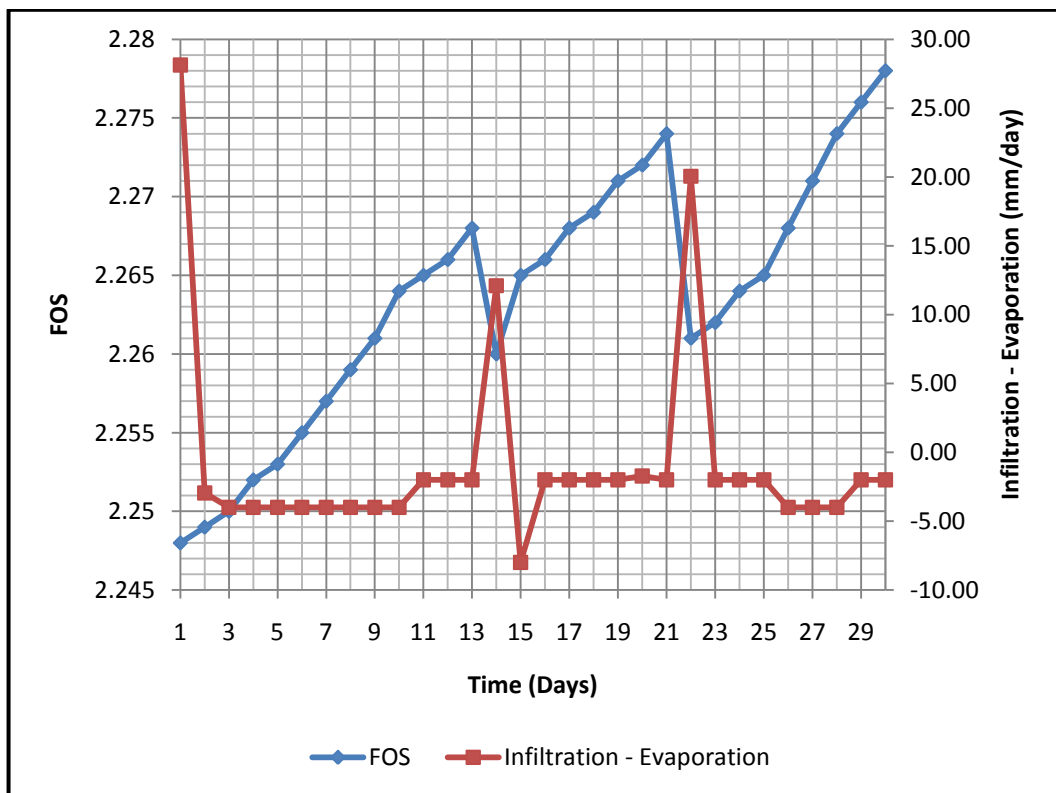
4.4.2 Factor of Safety Variation in June

a. Due to Rainfall Infiltration

June is the second dry month considered for the analysis, the variation of rainfall infiltration and FOS with time is presented in Appendix D. Figure 4.25(a) shows the correlation between the rainfall infiltration and the FOS for this month. From this Figure, the FOS decreases with rainfall infiltration due to decrease in soil suction and became relatively constant on the days without rainfall infiltration (because the changes in soil suction were negligible). For instance, on 22nd June the rainfall infiltration was 22.05mm/day, the suction value was 30.49kPa and the FOS was 2.232 which was less than the FOS of 2.239 recorded a day before (i.e., 21st June) where the rainfall intensity was 0 mm/day and the suction value was 33.47kPa. Therefore, the FOS decreases on days with rainfall infiltration due to reduction in soil suction and remained constant on days without rainfall infiltration.



(a)



(b)

Figure 4.25: Correlation of Infiltration and Difference and the FOS with time in June

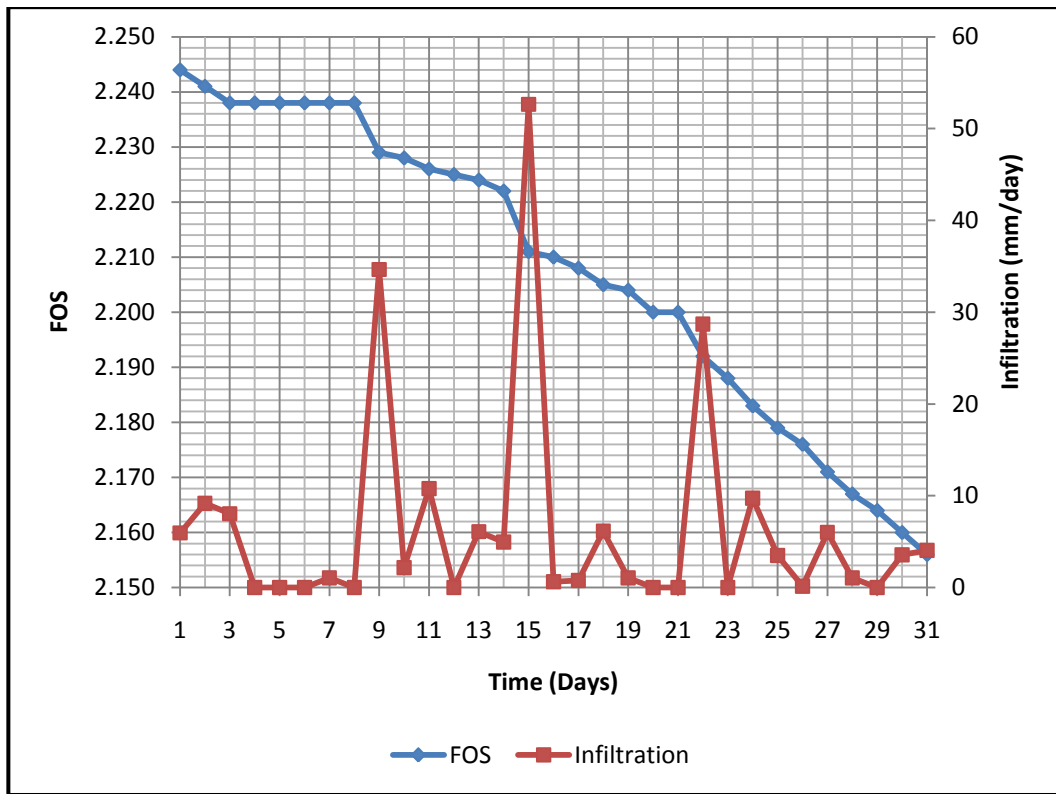
a. Due to Rainfall Infiltration and Evaporation

The variation of FOS and difference between rainfall infiltration and evaporation with time for this month is presented in Appendix D. Figure 4.25(b) shows the correlation between the difference between the rainfall infiltration and evaporation for this month. The FOS generally increases on days where the difference between rainfall infiltration and evaporation resulted in negative value (i.e., drying of the soil mass) which leads to increase in soil suction and it decreases where the difference resulted in a positive value (i.e., wetting of the soil) which leads to decrease in soil suction. For instance, from 2nd June up to 13th June the differences resulted in negative value (i.e., drying of soil mass) and the suction increases from 33.84kPa on 2nd June up to 43.37kPa on 13th June and this leads to increase in FOS from 2.249 on 2nd June to 2.268 on 13th June, but on 14th June the difference resulted in positive value (i.e., wetting of soil mass) and the soil suction decreases 39.70kPa which resulted in decrease in FOS to 2.260.

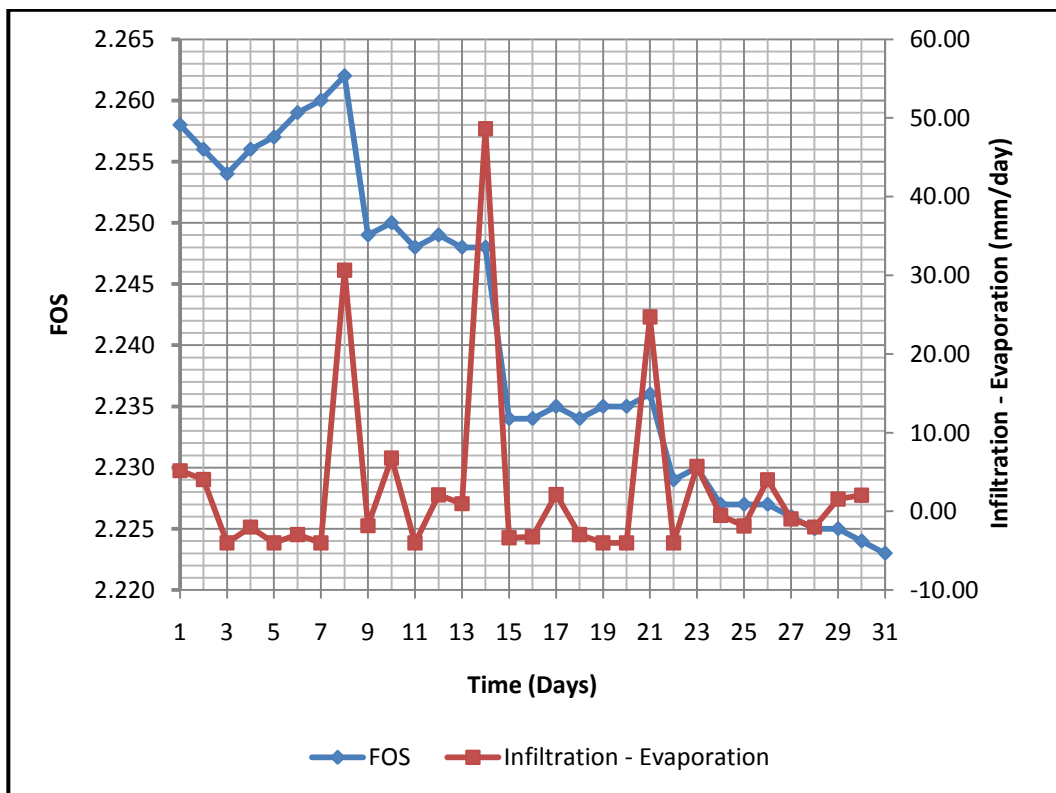
4.4.3 Factor of Safety Variation in March

a. Due to Rainfall Infiltration

March is the first wet months considered for the analysis, the variation of rainfall infiltration and FOS with time is presented in Appendix D. Figure 4.26(a) shows the correlation between the rainfall infiltration and FOS with time for this month. From this Figure; the FOS decreases in the first 3 days of the month due continuous rainfall infiltration on those days because the soil suction on those days decreases due to infiltration, and it remained constant on other days without rainfall infiltration because the changes in suction was relatively constant on those days. Similarly, towards the end of the month because substantial amount of rainfall infiltration has already saturated the soil and there was accumulation of water towards the toe of the slope, the FOS decreases even without rainfall infiltration. The FOS in this month decreases from 2.244 at the beginning of the month to 2.156 at the end of the month.



(a)



(b)

Figure 4.26: Correlation of Infiltration and Difference and the FOS with time in March

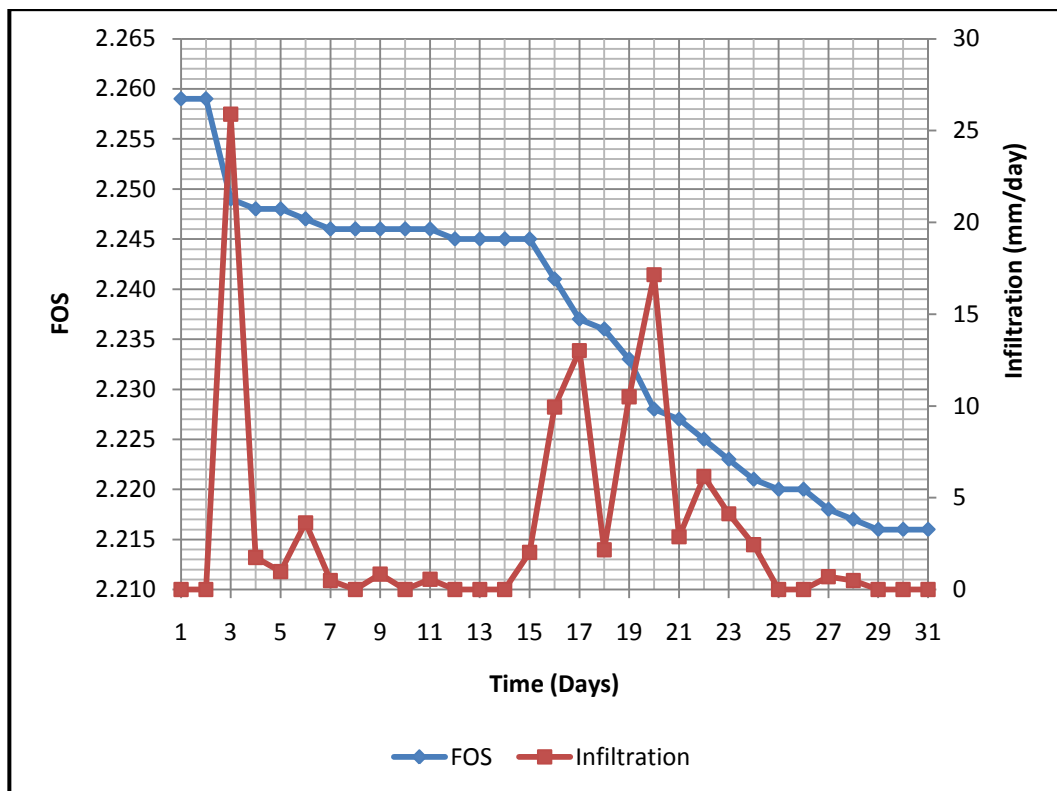
a. Due Rainfall Infiltration and Evaporation

The variation of FOS and the difference between rainfall infiltration and evaporation with time is presented in Appendix D. Figure 4.26(b) shows the correlation between the difference between rainfall infiltration and evaporation and FOS with time for this month. As explained earlier where the difference resulted in negative value it indicates drying of the soil which invariably leads to increase in soil suction and FOS and where the difference resulted in positive value it indicates wetting of the soil and invariably leads to decrease in soil suction and the FOS. That is why from this figure the FOS keeps alternating and decreases substantially where the difference was very high such as 9th, 15th and 22nd of March. The FOS due to the difference between rainfall infiltration and evaporation was 2.258 and 2.223 at the beginning and end of the month respectively which shows decrease in FOS because of heavy rainfall infiltration which leads to wetting of the soil.

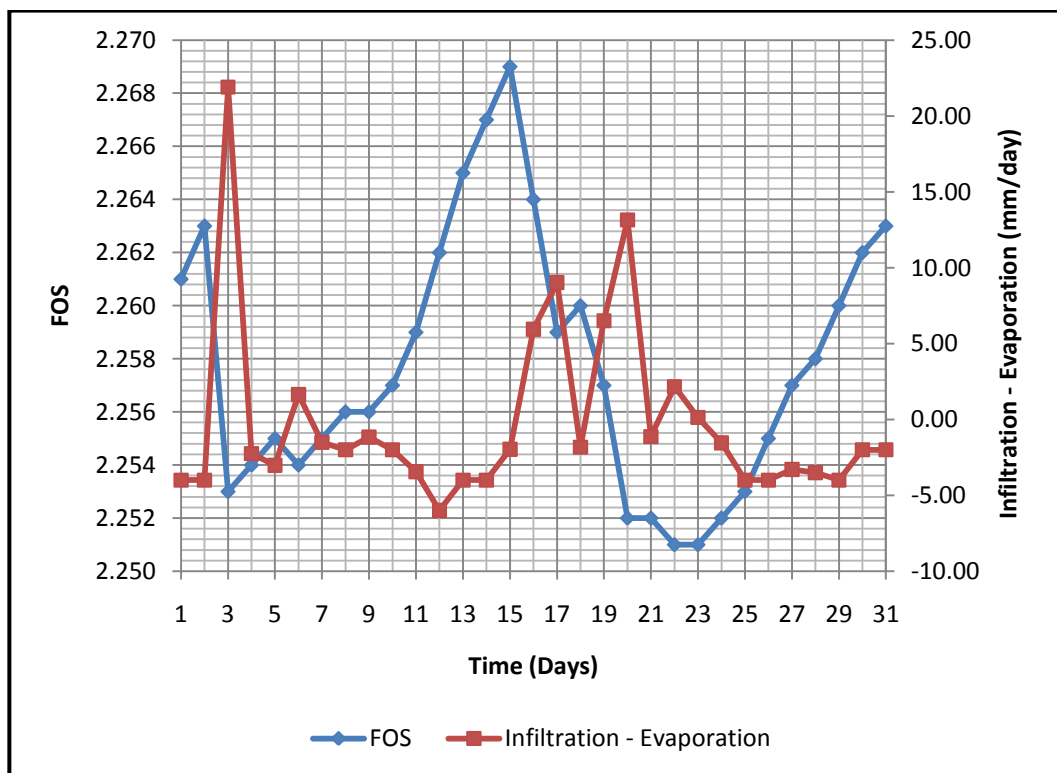
4.4.4 Factor of Safety Variation in December

a. Due to Rainfall Infiltration

December is the second wet months considered for the analysis. The variation of rainfall infiltration and FOS with time for this month is presented in Appendix D. Figure 4.27(a) shows the correlation between the rainfall infiltration and the FOS with time for this month. As explained previously; the FOS decreases with rainfall infiltration as indicated on 3rd December where the rainfall infiltration of 25.90mm/day resulted in decrease of soil suction to 34.63kPa against 40.17kPa on the first 2 days of the month, this leads to decrease in FOS from 2.259 to 2.249. In the same pattern the FOS decrease continuously with rainfall infiltration and remained relatively constant on other days without rainfall infiltration.



(a)



(b)

Figure 4.27: Correlation of Infiltration and Difference and the FOS with time in December

a. Due Rainfall Infiltration and Evaporation

The variation of rainfall infiltration and evaporation and the FOS for this month is presented in Appendix D. Figure 4.27(b) shows the correlation between the difference between the rainfall infiltration and evaporation and the FOS for this month. From this Figure the FOS increases on the days without rainfall infiltration when the difference resulted in negative value (drying of the soil) and it decreases when the difference resulted in a positive value (wetting of the soil).

4.5 Discussion

From the analyses conducted in this study, the results shows that rainfall infiltration (which causes wetting of the soil mass) decreases the soil matric suction and the additional shear strength provided by the soil matric suction decreases and make it more susceptible to failure. On the other hand, the difference between the rainfall infiltration and evaporation can be divided into two; the first one is when the difference is positive which leads to wetting of the soil and this has the same effect as the rainfall infiltration even though the decrease in suction in this case is less than that of rainfall infiltration, this usually happens when the rainfall infiltration is higher than evaporation. The second one is when the difference is negative which leads to the drying of soil mass and invariably leads to increase in soil suction, this usually occur when there is no rainfall infiltration or when the amount of rainfall infiltration is less than that of evaporation. The effect of decrease or increase in the soil suction due to rainfall infiltration or the difference between rainfall infiltration and evaporation is more influence on depths close to the surface of the soil mass and decreases with depths as indicated in Figure 4.6(a) – Figure 4.23(a). That is why the variation of suction due to rainfall infiltration and the difference between rainfall infiltration and evaporation at 0.5m and 1.0m are greater than at 1.7m, 3.3m and 5.0m, even though in some situations the values of suctions at these depths approaches the value of suction at 1.7m or even lower than that due to rainfall infiltration and due to differences between rainfall infiltration and evaporation as well (i.e., in the wet months). Figure 4.28(a) - (d) shows the variation of suction with

depth and from these Figures it is evident that soil suction responded to climatic conditions (rainfall infiltration and evaporation) more quickly at lower depth (0.0m – 1.5m) in this case, and it is almost constant beyond that points. This also shows that the depth of wetting front lies between 1.0m to 1.7m depending on the moisture condition of the soil, that is to say during the wet months the depth will be more closer to the surface than in the driest months.

The relationships between the soil suction due rainfall infiltration and due to differences between rainfall infiltration and evaporation with time at 0.5m and 1.0 depth were shown in Figure 4.29(a), (b), (c) and (d). These points respond to change in suction due to climatic conditions than other points.

From these Figures the soil suction due to the differences between rainfall infiltration and evaporation were higher than that of rainfall infiltration only. Because the former dries the soil mass while the latter wets the soil mass.

The rainfall intensity (i.e., amount of rainfall) has significant effect on reduction of soil suction that is why the response of soil suction due to rainfall infiltration is more significant when the intensity is high such as on 15th of March where the recorded rainfall infiltration was 52.64mm/day and this resulted in decreasing the soil suction to 23.81kPa, 25.08kPa, 27.45kPa, 15.11kPa and 0.87kPa at 0.5m 1.0m, 1.7m, 3.3m and 5.0m respectively. Similar is the case when the difference between rainfall infiltration and evaporation is considered because the difference was high also due the fact that the maximum value of daily evaporation recorded through out the year was 8mm/day.

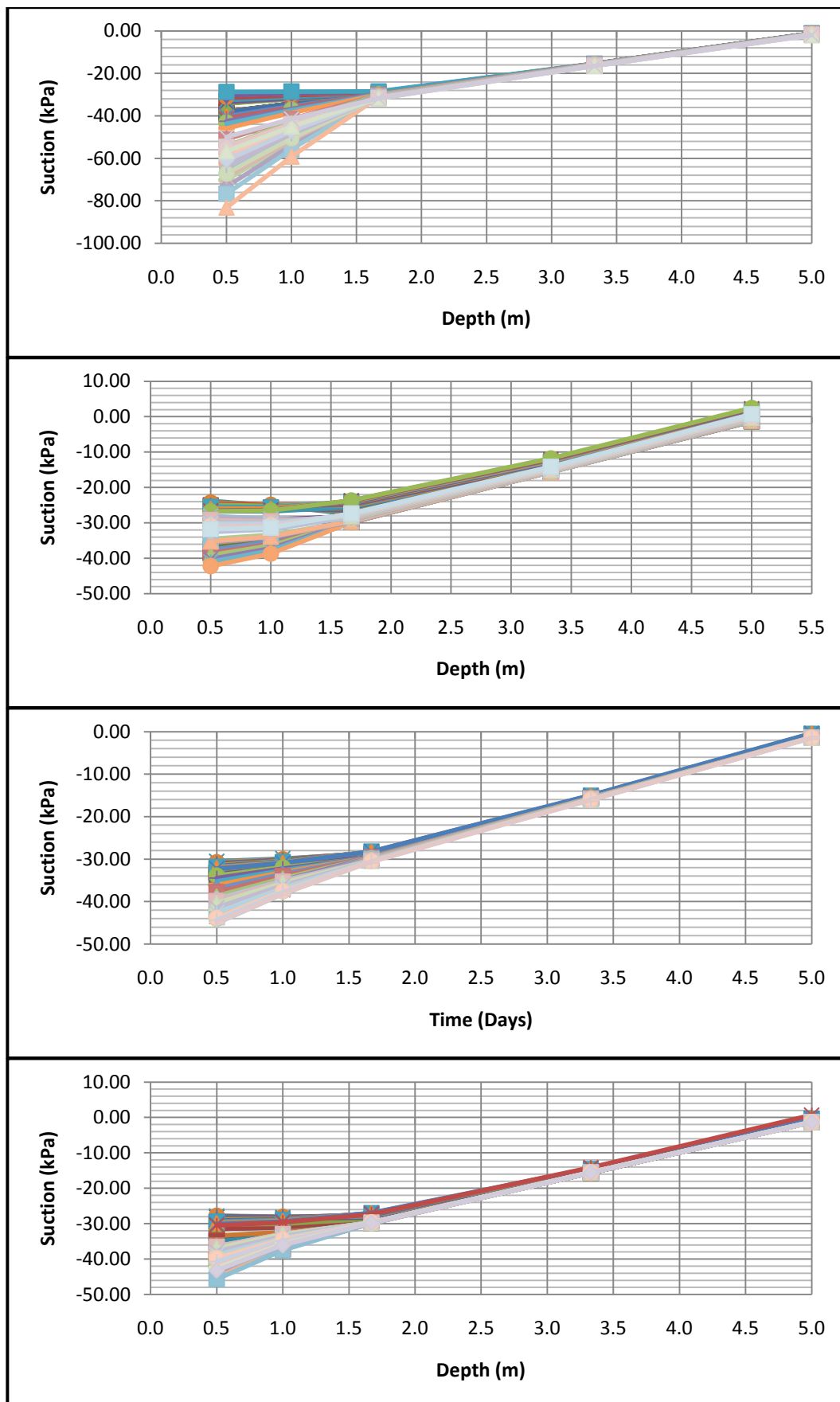


Figure 4.28: Suction distributions with depth due infiltration and infiltration and evaporation, (a) February, (b) March, (c) June and (d) December

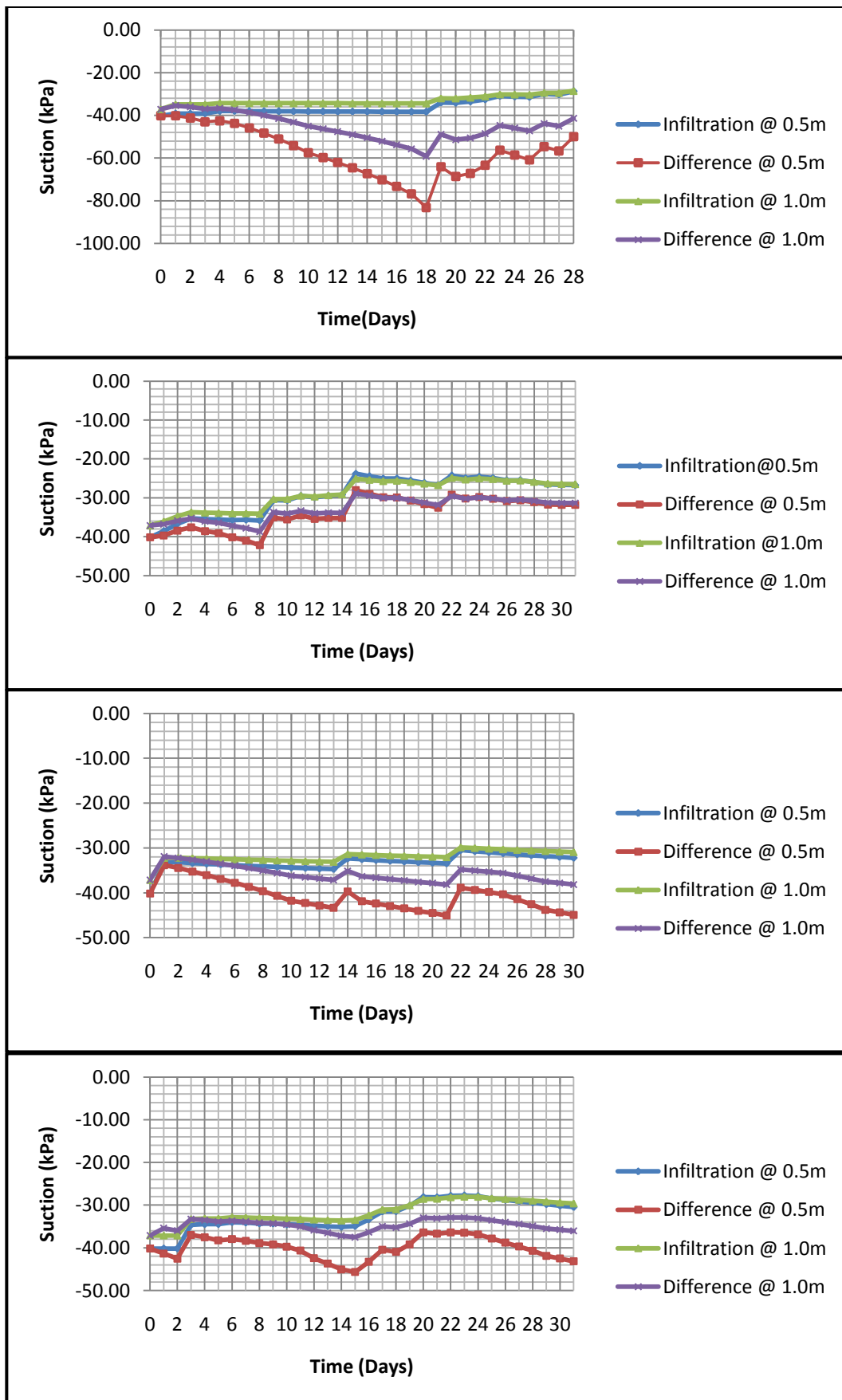


Figure 4.29: Suction distributions due infiltration and infiltration and evaporation, (a) February, (b) March, (c) June and (d) December

When the amount of rainfall infiltrated in to the soil mass is high and occurs frequently, it leads to positive pore-water pressure build up (i.e., perched water table); this condition occurs in the months of March and December (wet months considered for the analysis). In March the pore-water pressure changes to positive on 21st March due to infiltration and 26th March due to the differences between rainfall infiltration and evaporation. Though the changes were noticeable at 5.0m only but as the rainfall continues to infiltrate other depths may be affected depending on the intensity. In December, because the intensity was not up to that of March, the perched water table built up on 31st December and due to rainfall infiltration only, it does not occur due the difference between rainfall infiltration and evaporation this is because some of the rainfall recorded in this month were less than the recorded values of evaporation and of course there are some other days without rainfall infiltration.

From the analysis conducted for the whole four month it was evident that the soil suction varies through out the months depending on level of moisture condition of the soil. Considering the wet months (i.e., March and December) it is clear that the lowest soil suction values were recorded during the month of March due the effect of rainfall infiltration, and the different between the suction variation due to rainfall infiltration and the differences between rainfall infiltration and evaporation has the lowest value in this month. Similarly, by considering the dry months the highest value of soil suction was recorded during the month of February even though it has more number of days of rainfall this is because the intensity of rainfall in February is not up to that of June and also because the month of June started with high rainfall intensity of 32.13mm/day which already saturates the soil mass at the beginning of the month. By considering suction at 0.5m; the lowest suction in the analysis period was 23.81kPa recorded due to rainfall infiltration in the month of March and the highest value of suction in the whole analysis period was 83.17kPa recorded due to differences between rainfall infiltration and evaporation in the month of February.

The slope stability analysis show that the factor of safety of the slope reduces with increase in rainfall infiltration, and it is obvious that rainfall infiltration leads to the reduction in soil matric suction and the reduction in soil matric suction leads to the reduction of additional shear strength of the soil provided by the matric suction, and the factor of safety of a slope depends on the shear strength of the soil. The lowest factor of safety due rainfall infiltration and the differences between rainfall infiltration and evaporation were recorded in the month of March because it has more days with rainfall (both frequency and magnitude) and the lowest soil suction was recorded during this month. Similarly, the difference between the FOS due to rainfall infiltration and rainfall infiltration and evaporation was lowest in this month.

The relationship between the FOS due rainfall infiltration and the difference between rainfall infiltration and evaporation were shown in Figure 4.29(a), (b), (c) and (d).

From these Figures the FOS due difference between rainfall infiltration and evaporation were greater than those due to rainfall infiltration because there were high values of suction due to drying of soil than due to wetting of the soil which resulted in reduction of soil suction.

The highest FOS in the whole analysis period was 2.346 recorded on 18th February, due to the differences between rainfall infiltration and evaporation and this was inline with the fact that the highest suction of 83.17kPa was recorded on the same date (i.e., 18th).

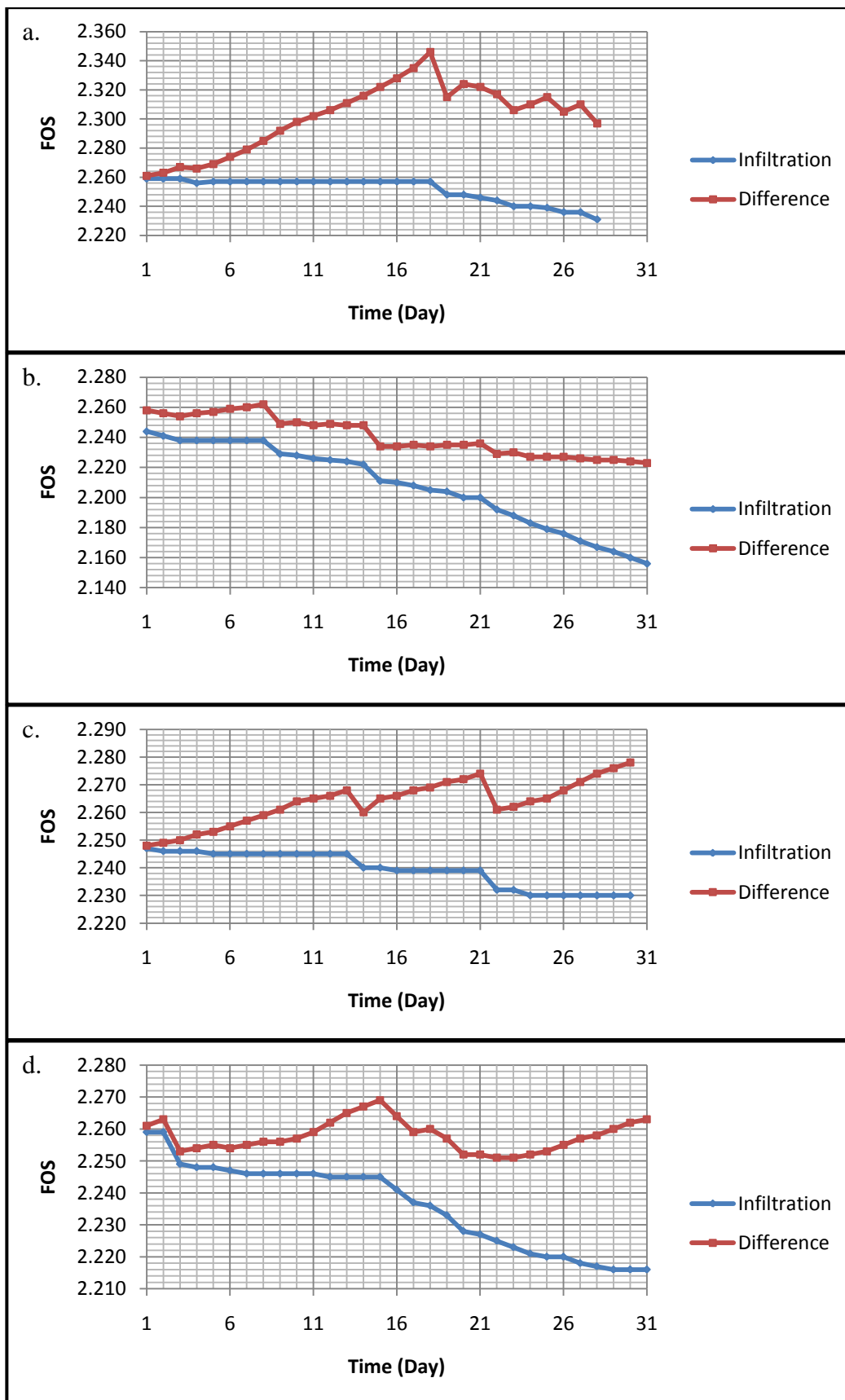


Figure 4.29: Variation of FOS with time due to Infiltration and Infiltration and Evaporation (a) February, (b) March, (c) June and (d) December

CHAPTER 5

CONCLUSIONS AND RECOMMENDATIONS

5.1 Introduction

This study looks at the influence of rainfall infiltration and evaporation on suction distribution and slope stability. Transient seepage analysis using commercial finite element software SEEP/W, (GeoSlope International Ltd., 2007) was conducted and the variations of suction due to rainfall infiltration and the differences between rainfall infiltration and evaporation were evaluated where the former one served as control so that the influence of the latter one can vividly be ascertain. The seepage pattern and pore-water pressure profile obtained from the above analysis were used to obtain the FOS for the slope using software which was based on limit equilibrium, SLOPE/W, (GeoSlope International Ltd., 2007).

5.2 Conclusion

Based on the results obtained from the analyses, the following conclusions can be drawn on the influence of rainfall infiltration and evaporation on suction distribution and slope stability.

1. The rainfall infiltration leads to the reduction of soil suctions with time and the reduction is more prominent when the intensity of the rainfall is high, the soil suction usually remain constant on days without rainfall infiltration more especially at the beginning of the month but it decreases a little as time goes

on due the effect of antecedent moisture in the soil. The differences between rainfall infiltration and evaporation leads to the increase in soil suction if the value is negative (i.e. drying of the soil mass), and it leads to the decrease of the soil suction when the value is positive (wetting of the soil mass) but the decrease in soil suction for this case is less than the decrease due to rainfall infiltration.

2. Due to the differences in total head the seepage pattern is flowing in downward direction i.e., from crest to the toe, and water accumulate at the toe and towards the middle of the slope which leads to the development of perched water table more especially at the bottom surface of the slope.
3. The reduction in soil suction leads to reduction in shear strength of the soil and this leads to the reduction in FOS of the slope, the FOS remain constant on days without rainfall infiltration because the soil suction remain unchanged. Therefore the FOS decreases due to rainfall infiltration and increases due to the differences between rainfall infiltration and evaporation.

5.3 Recommendations

The study has concluded its objectives and the following recommendations were made for future study.

1. The study considers only one soil layer therefore two soil layers are recommended for further study.
2. The study does not consider rainfall duration and the effect of antecedent moisture content of the soil, therefore these are recommended for further study.
3. It is recommended to do the analysis continuously for the four months such as from March to June or from October to December because these periods cover two dry and two wet periods so that the effect can be noticed continuously.

REFERENCES

Ali, M. H., Lee, T. S., Kwok, C. Y. and Eloubaidy. A. F. (2000). *Modelling evaporation and evapotranspiration under temperature change in Malaysia*. *Pertanika J. Sci. & Techno.*, 8(2), 191 – 204.

Cho, S. E. and Lee, S. R. (2001). *Instability of Unsaturated soil slope due to infiltration*. *Computer and Geotechnics* 2001; 28: 185-208.

Duncan, J. M. (1996). *State of the art: Limit equilibrium and finite element Analyses of Slopes*. *Journal of Geotechnical and Geoenvironmental Engineering ASCE* 122(7) 577 - 596.

Fratta, D., Aguetant, J. and Roussel-Smith, L. (2007). *Soil Mechanics Laboratory Testing*, CRC press.

Fredlund, D. G. and Rahardjo, H. (1993): *Soil mechanics for unsaturated soils*, John Wiley and sons, Inc., New York.

Fredlund, D. G., Xing, A. and Huang, S. (1994). *Predictions the permeability function for unsaturated soils using the Soil Water Characteristics Curve*. *Canadian Geotechnical Journal* 31(3) 521 - 532

Fredlund, D. G., Xing, A., Fredlund, M. D. and Barbour, S. L. (2002). *The relationships of the unsaturated soil shear strength function to the soil-water characteristics curve*. *Canadian Geotechnical Journal* 32(3) 40 - 48

Fredlund, M. D., Wilson, G. W., and Fredlund, D. G. (2002): *Use of grain – size distribution for estimation of soil water characteristics curve*. *Canadian Geotechnical Journal* 39(3) 1103 – 1117.

Fredlund, D. G. and Morgenstern, N. R. (1977). *Stress state variables for unsaturated soils*. Journal of Geotechnical Engineering. ASCE 103() 447-466

Gasmo, J. M., Rahardjo, H. and Leong, E.C. (2000): *Infiltration effects on stability of a residual soil slope*, Journal of ScienceDirect Volume 26 issue 2.

GeoSlope International Ltd. (2007): *SEEP/W User's guide for finite element seepage analysis*, GEO-SLOPE International Ltd, Calgary, Alta.

GeoSlope International Ltd. (2007): *SLOPE/W User's guide for slope stability analysis*, GEO-SLOPE International Ltd, Calgary, Alta.

Gofar, N. (2010): *A simple model for evaluation of rainfall induced slope instability*, paper presented at workshop on recent issues and development in geotechnical engineering, Department of Geotechnics and Transportation, Universiti Teknologi Malaysia.

Gofar, N. and Kassim, K. A. (2007): *Introduction to Geotechnical Engineering Part 1*. Pearson Education South Asia Pte. Ltd.

Gofar, N., Lee, M. L. and Asof, M. (2006): *Transient seepage and Slope stability for rainfall induced landslide: A case study*, Malaysian Journal of Civil Engineering.

Gofar, N., Lee, M. L. and Kassim, A. (2006): *Effect of surface boundary condition on rainfall infiltration*, Jurnal Teknologi, Universiti Teknologi Malaysia.

Head, K. H. (2006). *Manual of Soil Laboratory Testing*, Volume 1 third edition, Whittles publishing.

Head, K. H. (1981). *Manual of Soil Laboratory Testing*, Volume 2 first edition, Pentech press, London.

Kassim, A., Gofar, N., Mokhtar, N. and Lee, M. L. (2006): *The effect of transient state rainfall on stability of residual soil slope*, Journal of International Conference on Slope, Malaysia.

Kenneth, G., and Jianfeng, X. (2007): *A Simple method to analyze infiltration into unsaturated soil slopes*, Computer and Geotechnics, 2008; 35: 223-230.

Holtz, R. D. and Kovacs, W. D. (1981). *An introduction to Geotechnical Engineering*. Prentice Hall, Eaglewood Cliffs, New Jersey

Lal, R. and Shukla, M. K. (2004): *Principles of Soil Physics*, 1st edition, Marcel Dekker, Inc. New York

Lambe, T. W., and Whitman, R. V. (1969): *Soil Mechanics*, John Wiley and sons, New York.

Leong, E. C. and Rahardjo, H. (1997). *Permeability functions for unsaturated soils*. Journal of Geotechnical and Geoenvironmental Engineering. ASCE

Lu, N. and Likos, W. J. (2004). *Unsaturated Soil Mechanics*. John Wiley and sons Inc.

Murthy, V. N. S. (2000): *Geotechnical Engineering Principles and practices of soil mechanics and foundation engineering*, Marcel Dekker, Inc 270 Madison Avenue New York 100016.

Ng, C. W. W. and Shi, Q. (1998): *Influence of rainfall intensity and duration on slope stability in unsaturated soils*, Quarterly Journal of engineering Geology.

Ng, C. W.W. and Bruce, M. (2007): *Advanced Unsaturated Soil Mechanics and Engineering*, first edition Taylor & Francis, 2 Park Square, Milton Park, Abingdon, Oxon OX14 4RN.

Rahardjo, H. and Leong, E. C. (2006): *Suction Measurements*, American Society of Civil Engineers, Proceeding of the fourth international conference on unsaturated soils, 2006; 03:81-104.

Rahardjo, H., Leong, E. C., Michael, S. D., Jason, M. G., Tang, S. K. (2000). "Rainfall Induced Slope Failures" *Geotechnical Engineering Monograph 3*, NTU-PWD Geotechnical Research Centre, NTU, Singapore.

Rahardjo, H., Leong, E. C., Rezaur, R. B., Tang, S. K. and Quan, C. N. (2001): *Rainfall induced slope failures: Mechanism and assessment*, CSE Research bulletin No. 14.

Tsaparas, I., Rahardjo, H., Toll, D.G. and Leong, E.C. (2002): *Controlling parameters for rainfall-induced landslides*, Computers and Geotechnics 2002; 29: 1–27

Weeks, B. and Wilson, G.W. (2006): *Prediction of evaporation from soil slopes*, Canadian Geotechnical Journals.

Wei, L., Koutnik, T. and Woodward, M. (2010): *A slope stability case study by limit equilibrium and finite element methods*, GeoFlorida 2010: Advances in analysis, modelling and design (GSP app).

APPENDIX A

RAINFALL AND EVAPORATION DATA

1. Rainfall Data

Daily Rainfall data for February

Days	Rainfall intensity (mm/day)	Rainfall (m/s)	Infiltration (m/s)
1	0.00	0.00E+00	0.00E+00
2	0.00	0.00E+00	0.00E+00
3	0.00	0.00E+00	0.00E+00
4	7.30	8.45E-08	5.91E-08
5	0.00	0.00E+00	0.00E+00
6	0.00	0.00E+00	0.00E+00
7	0.00	0.00E+00	0.00E+00
8	0.00	0.00E+00	0.00E+00
9	0.00	0.00E+00	0.00E+00
10	0.00	0.00E+00	0.00E+00
11	0.00	0.00E+00	0.00E+00
12	0.00	0.00E+00	0.00E+00
13	0.00	0.00E+00	0.00E+00
14	0.00	0.00E+00	0.00E+00
15	0.00	0.00E+00	0.00E+00
16	0.00	0.00E+00	0.00E+00
17	0.00	0.00E+00	0.00E+00
18	0.00	0.00E+00	0.00E+00
19	33.00	3.82E-07	2.67E-07
20	0.00	0.00E+00	0.00E+00
21	6.70	7.75E-08	5.43E-08
22	10.70	1.24E-07	8.67E-08
23	18.00	2.08E-07	1.46E-07
24	0.00	0.00+00	0.00E+00
25	0.00	0.00E+00	0.00E+00
26	17.30	2.00E-07	1.40E-07
27	0.00	0.00E+00	0.00E+00
28	20.30	2.35E-07	1.64E-07

Daily Rainfall data for March

Days	Rainfall intensity (mm/day)	Rainfall (m/s)	Infiltration (m/s)
1	8.50	9.84E-08	6.89E-08
2	13.10	1.52E-07	1.06E-07
3	11.50	1.33E-07	9.32E-08
4	0.00	0.00E+00	0.00E+00
5	0.00	0.00E+00	0.00E+00
6	0.00	0.00E+00	0.00E+00
7	1.50	1.74E-08	1.22E-08
8	0.00	0.00E+00	0.00E+00
9	49.50	5.73E-07	4.01E-07
10	3.10	3.59E-08	2.51E-08
11	15.40	1.78E-07	1.2E-07
12	0.00	0.00E+00	0.00E+00
13	8.70	1.01E-07	7.05E-08
14	7.10	8.22E-08	5.75E-08
15	75.20	8.70E-07	6.09E-07
16	0.90	1.04E-08	7.29E-09
17	1.10	1.27E-08	8.91E-09
18	8.80	1.02E-07	7.13E-08
19	1.50	1.74E-08	1.22E-08
20	0.00	0.00E+00	0.00E+00
21	0.00	0.00E+00	0.00E+00
22	41.00	4.75E-07	3.32E-07
23	0.00	00E+00	0.00E+00
24	13.90	1.61E-07	1.13E-07
25	5.00	5.79E-08	4.05E-08
26	0.20	2.31E-09	1.62E-09
27	8.60	9.95E-08	6.97E-08
28	1.50	1.74E-08	1.2E-08
29	0.00	0.00E+00	0.00E+00
30	5.10	5.90E-08	4.13E-08
31	5.80	6.71E-08	4.70E-08

Daily Rainfall data for June

Days	Rainfall intensity (mm/day)	Rainfall (m/s)	Infiltration (m/s)
1	45.90	5.31E-07	3.72E-07
2	1.50	1.74E-08	1.22E-08
3	0.00	0.00E+00	0.00E+00
4	0.00	0.00E+00	0.00E+00
5	0.00	0.00E+00	0.00E+00
6	0.00	0.00E+00	0.00E+00
7	0.00	0.00E+00	0.00E+00
8	0.00	0.00E+00	0.00E+00
9	0.00	0.00E+00	0.00E+00
10	0.00	0.00E+00	0.00E+00
11	0.00	0.00E+00	0.00E+00
12	0.00	0.00E+00	0.00E+00
13	0.00	0.00E+00	0.00E+00
14	23.00	2.66E-07	1.86E-07
15	0.00	0.00E+00	0.00E+00
16	0.00	0.00E+00	0.00E+00
17	0.00	0.00E+00	0.00E+00
18	0.00	0.00E+00	0.00E+00
19	0.00	0.00E+00	0.00E+00
20	0.40	4.63E-09	3.24E-09
21	0.00	0.00E+00	0.00E+00
22	31.50	3.65E-07	2.55E-07
23	0.00	0.00E+00	0.00E+00
24	0.00	0.00E+00	0.00E+00
25	0.00	0.00E+00	0.00E+00
26	0.00	0.00E+00	0.00E+00
27	0.00	0.00E+00	0.00E+00
28	0.00	0.00E+00	0.00E+00
29	0.00	0.00E+00	0.00E+00
30	0.00	0.00E+00	0.00E+00

Daily Rainfall for December

Days	Rainfall intensity (mm/day)	Rainfall (m/s)	Infiltration (m/s)
1	0.00	0.00E+00	0.00E+00
2	0.00	0.00E+00	0.00E+00
3	37	4.28E-07	3.00E-07
4	2.50	2.89E-08	2.03E-08
5	1.40	1.62E-08	1.13E-08
6	5.20	6.02E-08	4.21E-08
7	0.70	8.10E-09	5.67E-09
8	0.00	0.00E+00	0.00E+00
9	1.20	1.39E-08	9.72E-09
10	0.00	0.00E+00	0.0E+00
11	0.80	9.26E-09	6.48E-09
12	0.00	0.00E+00	0.00E+00
13	0.00	0.00E+00	0.00E+00
14	0.00	0.00E+00	0.00E+00
15	2.90	3.36E-08	2.35E-08
16	14.20	1.64E-07	1.15E-07
17	18.60	2.15E-07	1.51E-07
18	3.10	3.59E-08	2.51E-08
19	15.00	1.74E-07	1.22E-07
20	24.50	2.84E-07	1.98E-07
21	4.10	4.75E-08	3.32E-08
22	8.80	1.02E-07	7.13E-08
23	5.90	6.83E-08	4.78E-08
24	3.50	4.05E-08	2.84E-08
25	0.00	0.00E+00	0.00E+00
26	0.00	0.00E+00	0.00E+00
27	1.00	1.16E-08	8.10E-09
28	0.70	8.10E-09	5.67E-09
29	0.00	0.00E+00	0.00E+00
30	0.00	0.00E+00	0.00E+00
31	0.00	0.00E+00	0.00E+00

1. Evaporation**Daily Evaporation data for February**

Days	Evaporation (mm/day)	Evaporation (m/s)
1	4.00	4.63E-08
2	4.00	4.63E-08
3	6.00	6.94E-08
4	4.00	4.63E-08
5	4.00	4.63E-08
6	6.00	6.94E-08
7	6.00	6.94E-08
8	6.00	6.94E-08
9	6.00	6.94E-08
10	6.00	6.94E-08
11	4.00	4.63E-08
12	4.00	4.63E-08
13	4.00	4.63E-08
14	4.00	4.63E-08
15	4.00	4.63E-08
16	4.00	4.63E-08
17	4.00	4.63E-08
18	6.00	6.94E-08
19	6.00	6.94E-08
20	6.00	6.94E-08
21	4.00	4.63E-08
22	4.00	4.63E-08
23	4.00	4.63E-08
24	4.00	4.63E-08
25	4.00	4.63E-08
26	4.00	4.63E-08
27	4.00	4.63E-08
28	4.00	4.63E-08

Daily Evaporation data for March

Time (Days)	Evaporation (mm/day)	Evaporation (m/s)
1	4.00	4.63E-08
2	4.00	4.63E-08
3	4.00	4.63E-08
4	4.00	4.63E-08
5	2.00	2.31E-08
6	4.00	4.63E-08
7	4.00	4.63E-08
8	4.00	4.63E-08
9	4.00	4.63E-08
10	4.00	4.63E-08
11	4.00	4.63E-08
12	4.00	4.63E-08
13	4.00	4.63E-08
14	4.00	4.63E-08
15	4.00	4.63E-08
16	4.00	4.63E-08
17	4.00	4.63E-08
18	4.00	4.63E-08
19	4.00	4.63E-08
20	4.00	4.63E-08
21	4.00	4.63E-08
22	4.00	4.63E-08
23	4.00	4.63E-08
24	4.00	4.63E-08
25	4.00	4.63E-08
26	2.00	2.31E-08
27	2.00	2.31E-08
28	2.00	2.31E-08
29	2.00	2.31E-08
30	2.00	2.31E-08
31	2.00	2.31E-08

Daily Evaporation data for June

Days	Evaporation (mm/day)	Evaporation (m/s)
1	4.00	4.63E-08
2	4.00	4.63E-08
3	4.00	4.63E-08
4	4.00	4.63E-08
5	4.00	4.63E-08
6	4.00	4.63E-08
7	4.00	4.63E-08
8	4.00	4.63E-08
9	4.00	4.63E-08
10	4.00	4.63E-08
11	2.00	2.31E-08
12	2.00	2.31E-08
13	2.00	2.31E-08
14	4.00	4.63E-08
15	8.00	9.26E-08
16	2.00	2.31E-08
17	2.00	2.31E-08
18	2.00	2.31E-08
19	2.00	2.31E-08
20	2.00	2.31E-08
21	2.00	2.31E-08
22	2.00	2.31E-08
23	2.00	2.31E-08
24	2.00	2.31E-08
25	2.00	2.31E-08
26	4.00	4.63E-08
27	4.00	4.63E-08
28	4.00	4.63E-08
29	2.00	2.31E-08
30	2.00	2.31E-08

Daily Evaporation data for December

Days	Evaporation (mm/day)	Evaporation (m/s)
1	4.00	4.63E-08
2	4.00	4.63E-08
3	4.00	4.63E-08
4	4.00	4.63E-08
5	4.00	4.63E-08
6	2.00	2.31E-08
7	2.00	2.31E-08
8	2.00	2.31E-08
9	2.00	2.31E-08
10	2.00	2.31E-08
11	4.00	4.63E-08
12	6.00	6.94E-08
13	4.00	4.63E-08
14	4.00	4.63E-08
15	4.00	4.63E-08
16	4.00	4.63E-08
17	4.00	4.63E-08
18	4.00	4.63E-08
19	4.00	4.63E-08
20	4.00	4.63E-08
21	4.00	4.63E-08
22	4.00	4.63E-08
23	4.00	4.63E-08
24	4.00	4.63E-08
25	4.00	4.63E-08
26	4.00	4.63E-08
27	4.00	4.63E-08
28	4.00	4.63E-08
29	4.00	4.63E-08
30	2.00	2.31E-08
31	2.00	2.31E-08

APPENDIX B

TEST RESULTS OF SOIL PROPERTIES

Results of Particle size distribution analysis

Sieve Size	Mass retained (g)	% retained	Cumulative mass passing	% passing
5mm	0	0	500	100%
3.35mm	0	0	500	100%
2mm	03	0.60	03/497	$497/500 \times 100 = 99.4\%$
1.18mm	20	4	20/477	$477/500 \times 100 = 95.4\%$
600micron	85	17	85/392	$392/500 \times 100 = 78.4\%$
425micron	54	11	54/338	$338/500 \times 100 = 67.6\%$
300micron	60	12	60/278	$278/500 \times 100 = 55.6\%$
212micron	57	11	57/221	$221/500 \times 100 = 44.2\%$
150micron	57	11	57/164	$164/500 \times 100 = 32.8\%$
63micron	20	4	20/144	$144/500 \times 100 = 28.8\%$

 $m_F = 10$ $m_L = 134$

RESULTS OF FALLING-HEAD PERMEABILITY TEST

Length of Specimen (L) = 120.00mm

Diameter of Specimen (D) = 105.00mm

Area of Specimen (A) = $\frac{\pi D^2}{4} = 8.659 \times 10^{-3} \text{m}^2$

Volume of the Specimen (V) = A x L = $1.039 \times 10^{-3} \text{m}^3$

Weight of Mould = 1.359kg

Weight of Mould + wet Soil = 3.315kg

Weight of wet Soil $W_{ws} = 1.956 \text{kg}$

Diameter of Burette (d) = 6mm

Area of Burette (a) = $2.827 \times 10^{-5} \text{m}^2$

No of Test	Time (s)	$h_1(\text{mm})$	$h_2(\text{mm})$	$K = \frac{2.3026aL}{V} \log_{10}(h_1/h_2)$ m/sec
1	90	1000	868	4.80×10^{-7}
2	115	800	695	4.77×10^{-7}
3	129	600	521	4.79×10^{-7}
Average				4.79×10^{-7}

RESULT OF SOIL WATER CHARACTERISTIC CURVE

Matric Suction (kPa)	Volumetric Water Content
0.01	0.45
4	0.445
8	0.44
10	0.43
14	0.4
21	0.31
30	0.24
40	0.19
60	0.14
100	0.105
1000	0.08
10000	0.062

HYDRAULIC CONDUCTIVITY FUNCTION

Matric suction (kPa)	Hydraulic conductivity (m/sec)
0.1	4.80E-07
1	4.80E-07
10	4.80E-07
70	3.00E-07
300	3.50E-08
600	2.50E-09
1300	8.00E-11
3000	3.00E-12
5000	2.50E-13
10000	2.00E-14

APPENDIX C

RESULTS OF SEEPAGE ANALYSES

1. Rainfall Infiltration only

Suction Distribution with Depth and Time for February

Time (Days)	Suction (kPa)					Infiltration (mm/day)
	Depth (m)					
	0.5	1.0	1.7	3.3	5.0	
0	-40.17	-37.13	-29.82	-15.56	-1.32	-
1	-39.13	-34.85	-29.81	-15.55	-1.3	0
2	-39.13	-34.85	-29.81	-15.55	-1.3	0
3	-39.13	-34.85	-29.81	-15.55	-1.3	0
4	-37.96	-34.22	-29.8	-15.55	-1.32	5.11
5	-37.99	-34.23	-29.79	-15.57	-1.33	0
6	-38.02	-34.24	-29.78	-15.57	-1.32	0
7	-38.05	-34.25	-29.77	-15.57	-1.32	0
8	-38.08	-34.26	-29.76	-15.58	-1.32	0
9	-38.11	-34.27	-29.76	-15.57	-1.32	0
10	-38.14	-34.28	-29.75	-15.57	-1.32	0
11	-38.17	-34.29	-29.74	-15.57	-1.31	0
12	-38.20	-34.30	-29.74	-15.57	-1.31	0
13	-38.22	-34.31	-29.73	-15.56	-1.3	0
14	-38.25	-34.32	-29.73	-15.56	-1.3	0
15	-38.27	-34.33	-29.73	-15.55	-1.3	0
16	-38.29	-34.34	-29.72	-15.55	-1.29	0
17	-38.32	-34.35	-29.72	-15.54	-1.29	0
18	-38.34	-34.36	-29.71	-15.54	-1.29	0
19	-34.04	-32.01	-29.66	-15.54	-1.3	23.1
20	-34.18	-32.05	-29.58	-15.54	-1.3	0
21	-33.56	-31.67	-29.5	-15.55	-1.3	4.69
22	-32.57	-31.09	-29.4	-15.55	-1.3	7.49
23	-30.95	-30.15	-29.27	-15.55	-1.3	12.6
24	-31.20	-30.21	-29.12	-15.54	-1.28	0
25	-31.43	-30.27	-29	-15.53	-1.26	
26	-30.00	-29.42	-28.86	-15.52	-1.24	12.11
27	-30.28	-29.50	-28.71	-15.5	-1.2	0
28	-28.70	-28.56	-28.53	-15.47	-1.16	14.21

Suction Distribution with Time and Depth for March

Time (Days)	Suction (kPa)					Infiltration (mm/day)
	Depth (m)					
	0.5	1.0	1.7	3.3	5.0	
0	-40.17	-37.13	-29.82	-15.56	-1.32	-
1	-38.56	-36.09	-29.77	-15.55	-1.30	5.95
2	-36.68	-34.73	-29.73	-15.54	-1.29	9.17
3	-35.29	-33.72	-29.65	-15.54	-1.29	8.05
4	-35.44	-33.82	-29.59	-15.53	-1.28	0
5	-35.58	-33.92	-29.53	-15.52	-1.27	0
6	-35.73	-34.02	-29.48	-15.50	-1.26	0
7	-35.68	-34.00	-29.43	-15.49	-1.24	1.05
8	-35.83	-34.11	-29.38	-15.47	-1.23	0
9	-30.62	-30.32	-29.17	-15.45	-1.20	34.65
10	-30.64	-30.31	-28.98	-15.42	-1.17	2.17
11	-29.52	-29.46	-28.75	-15.38	-1.13	10.78
12	-29.90	-29.70	-28.55	-15.33	-1.09	0
13	-29.46	-29.35	-28.34	-15.27	-1.03	6.09
14	-29.20	-29.13	-28.13	-15.21	-0.97	4.97
15	-23.81	-25.08	-27.45	-15.11	-0.87	52.64
16	-24.44	-25.41	-26.94	-14.98	-0.75	0.63
17	-25.02	-25.74	-26.54	-14.84	-0.61	0.77
18	-25.02	-25.66	-26.17	-14.68	-0.45	6.16
19	-25.54	-25.98	-25.89	-14.50	-0.27	1.05
20	-26.15	-26.38	-25.68	-14.32	-0.09	0
21	-26.72	-26.77	-25.52	-14.13	0.10	0
22	-24.24	-24.90	-25.15	-13.92	0.31	28.7
23	-24.92	-25.33	-24.88	-13.70	0.53	0
24	-24.57	-25.02	-24.60	-13.46	0.76	9.73
25	-24.88	-25.20	-24.37	-13.21	1.01	3.5
26	-25.50	-25.63	-24.21	-12.97	1.26	0.14
27	-25.46	-25.58	-24.04	-12.72	1.51	6.02
28	-25.96	-25.93	-23.91	-12.47	1.76	1.05
29	-26.54	-26.35	-23.82	-12.22	2.00	0
30	-26.74	-26.51	-23.73	-11.98	2.48	3.57
31	-26.67	-26.45	-23.63	-11.75	2.24	4.06

Suction Distribution with Depth and time for June

Time (Days)	Suction (kPa)					Infiltration (mm/day)
	Depth (m)					
	0.5	1.0	1.7	3.3	5.0	
0	-40.17	-37.13	-29.82	-15.56	-1.32	-
1	-33.2	-32.22	-29.69	-15.54	-1.3	32.13
2	-33.21	-32.19	-29.58	-15.54	-1.3	1.05
3	-33.37	-32.27	-29.49	-15.53	-1.29	0
4	-33.53	-32.36	-29.41	-15.53	-1.29	0
5	-33.68	-32.45	-29.34	-15.52	-1.29	0
6	-33.82	-32.53	-29.28	-15.52	-1.28	0
7	-33.96	-32.62	-29.23	-15.52	-1.27	0
8	-34.10	-32.70	-29.19	-15.51	-1.26	0
9	-34.23	-32.78	-29.16	-15.51	-1.25	0
10	-34.36	-32.86	-29.13	-15.51	-1.23	0
11	-34.49	-32.94	-29.11	-15.51	-1.22	0
12	-34.61	-33.02	-29.09	-15.5	-1.2	0
13	-34.72	-33.09	-29.08	-15.5	-1.18	0
14	-32.35	-31.37	-29.01	-15.49	-1.16	16.1
15	-32.54	-31.48	-28.95	-15.48	-1.13	0
16	-32.71	-31.58	-28.9	-15.46	-1.1	0
17	-32.88	-31.69	-28.85	-15.45	-1.07	0
18	-33.05	-31.79	-28.82	-15.43	-1.03	0
19	-33.21	-31.89	-28.79	-15.41	-1	0
20	-33.32	-31.96	-28.77	-15.39	-0.96	0.28
21	-33.47	-32.06	-28.76	-15.36	-0.92	0
22	-30.49	-29.88	-28.64	-15.33	-0.87	22.05
23	-30.73	-30.02	-28.54	-15.3	-0.82	0
24	-30.97	-30.16	-28.45	-15.26	-0.77	0
25	-31.20	-30.30	-28.39	-15.22	-0.71	0
26	-31.42	-30.44	-28.33	-15.17	-0.65	0
27	-31.63	-30.57	-28.28	-15.12	-0.58	0
28	-31.83	-30.70	-28.25	-15.07	-0.52	0
29	-32.02	-30.82	-28.22	-15.02	-0.45	0
30	-32.21	-30.94	-28.19	-14.97	-0.38	0

Suction Distribution with Time and Depth for December

Time (Days)	Suction (kPa)					Infiltration (mm/day)
	Depth (m)					
	0.5	1.0	1.7	3.3	5.0	
0	-40.17	-37.13	-29.82	-15.56	-1.32	-
1	-40.17	-37.13	-29.81	-15.55	-1.3	0
2	-40.17	-37.14	-29.8	-15.55	-1.32	0
3	-34.63	-33.27	-29.76	-15.56	-1.33	25.9
4	-34.48	-33.15	-29.69	-15.57	-1.34	1.75
5	-34.48	-33.14	-29.64	-15.59	-1.35	0.98
6	-34.01	-32.82	-29.59	-15.6	-1.35	3.64
7	-34.12	-32.89	-29.55	-15.61	-1.35	0.49
8	-34.31	-33.03	-29.52	-15.62	-1.35	0
9	-34.35	-33.07	-29.46	-15.63	-1.34	0.84
10	-34.54	-33.21	-29.41	-15.63	-1.34	0
11	-34.62	-33.28	-29.36	-15.63	-1.31	0.56
12	-34.80	-33.41	-29.32	-15.61	-1.29	0
13	-34.98	-33.53	-29.28	-15.6	-1.27	0
14	-35.14	-33.64	-29.25	-15.57	-1.25	0
15	-34.93	-33.49	-29.12	-15.55	-1.24	2.03
16	-33.37	-32.39	-29	-15.52	-1.2	9.94
17	-31.50	-31.08	-28.87	-15.48	-1.17	13.02
18	-31.46	-31.00	-28.73	-15.43	1.12	2.17
19	-30.17	-30.06	-28.59	-15.38	-1.08	10.5
20	-28.11	-28.57	-28.41	-15.33	-1.03	17.15
21	-28.18	-28.53	-28.22	-15.26	-0.97	2.87
22	-27.80	-28.18	-27.99	-15.19	-0.91	6.16
23	-27.73	-28.05	-27.79	-15.11	-0.83	4.13
24	-27.88	-28.07	-27.59	-15.02	-0.75	2.45
25	-28.50	-28.42	-27.34	-14.86	-0.6	0
26	-28.79	-28.58	-27.23	-14.77	-0.51	0
27	-29.11	-28.76	-27.14	-14.67	-0.42	0.7
28	-29.43	-28.95	-27.07	-14.57	-0.33	0.49
29	-29.80	-29.19	-27.01	-14.48	-0.24	0
30	-30.14	-29.41	-26.97	-14.39	-0.18	0
31	-30.47	-29.62	-27.34	-14.15	0.69	0

2. Difference between Rainfall infiltration and Evaporation

Suction Distribution with Depth and Time for February

Time (Days)	Suction (kPa)					Infiltration - Evaporation
	Depth (m)					
	0.5	1.0	1.7	3.3	5.0	
0	-40.17	-37.13	-29.82	-15.56	-1.32	
1	-40.13	-35.40	-29.82	-15.55	-1.3	-4
2	-41.21	-35.99	-29.84	-15.55	-1.32	-4
3	-43.00	-36.98	-29.87	-15.57	-1.33	-6
4	-42.51	-36.73	-29.91	-15.59	-1.35	1.11
5	-43.74	-37.42	-29.96	-15.61	-1.37	-4
6	-45.88	-38.60	-30.02	-15.64	-1.38	-6
7	-48.30	-39.94	-30.09	-15.67	-1.4	-6
8	-51.05	-41.46	-30.17	-15.7	-1.42	-6
9	-54.14	-43.17	-30.26	-15.73	-1.45	-6
10	-57.53	-45.04	-30.36	-15.77	-1.47	-6
11	-59.73	-46.27	-30.46	-15.81	-1.49	-4
12	-62.08	-47.58	-30.55	-15.85	-1.52	-4
13	-64.58	-48.97	-30.65	-15.9	-1.55	-4
14	-67.26	-50.46	-30.75	-15.94	-1.57	-4
15	-70.16	-52.06	-30.84	-15.98	-1.6	-4
16	-73.30	-53.79	-30.93	-16.03	-1.63	-4
17	-76.74	-55.69	-31.02	-16.07	-1.66	-4
18	-83.17	-59.20	-31.1	-16.12	-1.69	-6
19	-64.08	-48.87	-31.18	-16.16	-1.71	17.1
20	-68.63	-51.36	-31.26	-16.2	-1.74	-6
21	-67.15	-50.58	-31.33	-16.25	-1.77	0.69
22	-63.36	-48.55	-31.4	-16.29	-1.79	3.49
23	-56.31	-44.75	-31.47	-16.33	-1.82	8.6
24	-58.51	-45.96	-31.53	-16.37	-1.85	-4
25	-60.85	-47.24	-31.59	-16.42	-1.87	-4
26	-54.57	-43.85	-31.65	-16.46	-1.9	8.11
27	-56.69	-45.02	-31.7	-16.5	-1.92	-4
28	-50.01	-41.41	-31.74	-16.54	-1.95	10.21

Suction Distribution with Depth and Time for March

Time (Days)	Suction (kPa)					Infiltration - Evaporation
	Depth (m)					
	0.5	1.0	1.7	3.3	5.0	
0	-40.17	-37.13	-29.82	-15.56	-1.32	
1	-39.66	-36.77	-29.81	-15.56	-1.32	1.95
2	-38.43	-35.91	-29.79	-15.56	-1.32	5.17
3	-37.59	-35.33	-29.76	-15.57	-1.31	4.05
4	-38.56	-36.02	-29.75	-15.58	-1.3	-4
5	-39.09	-36.41	-29.75	-15.58	-1.29	-2
6	-40.16	-37.19	-29.76	-15.59	-1.27	-4
7	-40.99	-37.81	-29.78	-15.6	-1.26	-2.95
8	-42.18	-38.70	-29.82	-15.61	-1.24	-4
9	-35.06	-33.70	-29.74	-15.61	-1.22	30.65
10	-35.57	-34.07	-29.69	-15.61	-1.19	-1.83
11	-34.50	-33.34	-29.62	-15.6	-1.16	6.78
12	-35.41	-33.98	-29.57	-15.59	-1.13	-4
13	-35.19	-33.85	-29.52	-15.58	-1.09	2.09
14	-35.19	-33.87	-29.48	-15.56	-1.05	0.97
15	-28.04	-28.87	-29.15	-15.53	-0.99	48.64
16	-28.97	-29.45	-28.91	-15.49	-0.92	-3.37
17	-29.84	-30.02	-28.73	-15.43	-0.85	-3.23
18	-29.91	-30.05	-28.57	-15.37	-0.76	2.16
19	-30.71	-30.58	-28.45	-15.3	-0.67	-2.95
20	-31.64	-31.23	-28.37	-15.23	-0.58	-4
21	-32.55	-31.88	-28.32	-15.16	-0.48	-4
22	-29.23	-29.56	-28.14	-15.07	-0.38	24.7
23	-30.20	-30.22	-28.01	-14.99	-0.27	-4
24	-29.76	-29.90	-27.87	-14.89	-0.16	5.73
25	-30.22	-30.21	-27.76	-14.79	-0.04	-0.5
26	-30.86	-30.65	-27.68	-14.69	0.08	-1.86
27	-30.62	-30.49	-27.58	-14.59	0.21	4.02
28	-31.11	-30.83	-27.51	-14.48	0.33	-0.95
29	-31.74	-31.28	-27.45	-14.37	0.45	-2
30	-31.80	-31.34	-27.4	-14.26	0.58	1.57
31	-31.80	-31.35	-27.34	-14.15	0.69	2.06

Suction Distribution with Depth and time for June

Time (Days)	Suction (kPa)					Infiltration - Evaporation
	Depth (m)					
	0.5	1.0	1.7	3.3	5.0	
0	-40.17	-37.13	-29.82	-15.56	-1.32	
1	-33.84	-31.94	-29.71	-15.54	-1.3	28.13
2	-34.45	-32.23	-29.63	-15.54	-1.31	-2.95
3	-35.24	-32.64	-29.58	-15.55	-1.31	-4
4	-36.05	-33.07	-29.56	-15.55	-1.32	-4
5	-36.89	-33.51	-29.55	-15.56	-1.32	-4
6	-37.76	-33.98	-29.56	-15.57	-1.32	-4
7	-38.68	-34.49	-29.58	-15.59	-1.32	-4
8	-39.65	-35.02	-29.62	-15.6	-1.33	-4
9	-40.67	-35.59	-29.67	-15.62	-1.33	-4
10	-41.77	-36.21	-29.73	-15.64	-1.34	-4
11	-42.29	-36.51	-29.79	-15.66	-1.34	-2
12	-42.82	-36.82	-29.85	-15.68	-1.35	-2
13	-43.37	-37.13	-29.92	-15.7	-1.36	-2
14	-39.70	-35.15	-29.94	-15.72	-1.36	12.1
15	-41.87	-36.34	-29.99	-15.74	-1.37	-8
16	-42.40	-36.64	-30.04	-15.77	-1.37	-2
17	-42.94	-36.95	-30.1	-15.79	-1.38	-2
18	-43.48	-37.26	-30.16	-15.81	-1.39	-2
19	-44.04	-37.58	-30.22	-15.83	-1.39	-2
20	-44.50	-37.84	-30.28	-15.86	-1.4	-1.72
21	-45.07	-38.17	-30.34	-15.88	-1.41	-2
22	-38.88	-34.80	-30.34	-15.9	-1.42	20.05
23	-39.36	-35.06	-30.35	-15.92	-1.42	-2
24	-39.85	-35.32	-30.36	-15.94	-1.42	-2
25	-40.35	-35.59	-30.38	-15.95	-1.43	-2
26	-41.42	-36.18	-30.41	-15.97	-1.43	-4
27	-42.57	-36.81	-30.46	-15.99	-1.43	-4
28	-43.80	-37.50	-30.51	-16	-1.43	-4
29	-44.36	-37.82	-30.56	-16.02	-1.44	-2
30	-44.94	-38.15	-30.62	-16.04	-1.44	-2

Suction Distribution with Time and Depth for December

Time (Days)	Suction (kPa)					Infiltration - Evaporation
	Depth (m)					
	0.5	1.0	1.7	3.3	5.0	
0	-40.17	-37.13	-29.82	-15.56	-1.32	
1	-41.33	-35.40	-29.82	-15.55	-1.3	-4
2	-42.53	-35.99	-29.84	-15.55	-1.3	-4
3	-36.97	-33.26	-29.82	-15.55	-1.3	21.9
4	-37.53	-33.52	-29.78	-15.55	-1.3	-2.25
5	-38.27	-33.87	-29.75	-15.55	-1.3	-3.02
6	-37.95	-33.70	-29.72	-15.55	-1.3	1.64
7	-38.36	-33.89	-29.7	-15.54	-1.3	-1.51
8	-38.88	-34.14	-29.69	-15.54	-1.29	-2
9	-39.20	-3.429	-29.68	-15.53	-1.29	-1.16
10	-39.73	-34.55	-29.69	-15.53	-1.28	-2
11	-40.67	-35.01	-29.69	-15.52	-1.28	-3.44
12	-42.44	-35.88	-29.72	-15.52	-1.28	-6
13	-43.70	-36.51	-29.76	-15.52	-1.27	-4
14	-45.06	-37.19	-29.8	-15.52	-1.27	-4
15	-45.67	-37.51	-29.85	-15.52	-1.28	-1.97
16	-43.28	-36.37	-29.88	-15.53	-1.28	5.94
17	-40.44	-34.99	-29.89	-15.53	-1.28	9.02
18	-40.94	-35.24	-29.89	-15.54	-1.29	-1.83
19	-39.19	-34.38	-29.88	-15.54	-1.29	6.5
20	-36.37	-32.96	-29.83	-15.54	-1.3	13.15
21	-36.70	-33.10	-29.78	-15.54	-1.3	-1.13
22	-36.37	-32.91	-29.72	-15.54	-1.29	2.16
23	-36.45	-32.92	-29.67	-15.54	-1.29	0.13
24	-36.87	-33.10	-29.63	-15.53	-1.28	-1.55
25	-37.80	-33.55	-29.6	-15.53	-1.29	-4
26	-38.80	-34.02	-29.59	-15.53	-1.3	-4
27	-39.69	-34.44	-29.6	-15.54	-1.3	-3.3
28	-40.68	-34.91	-29.62	-15.55	-1.31	-3.51
29	-41.89	-35.47	-29.66	-15.56	-1.31	-4
30	-42.52	-35.76	-29.7	-15.58	-1.32	-2
31	-43.17	-36.06	-29.75	-15.6	-1.33	-2

APPENDIX D

RESULTS OF SLOPE STABILITY ANALYSIS

Variation of Infiltration and Infiltration and Evaporation with FOS for February

Days	Infiltration (mm/day)	FOS	Difference (mm/day)	FOS
1	0.00	2.259	-4.00	2.261
2	0.00	2.259	-4.00	2.263
3	0.00	2.259	-6.00	2.267
4	5.11	2.256	1.11	2.266
5	0.00	2.257	-4.00	2.269
6	0.00	2.257	-6.00	2.274
7	0.00	2.257	-6.00	2.279
8	0.00	2.257	-6.00	2.285
9	0.00	2.257	-6.00	2.292
10	0.00	2.257	-6.00	2.298
11	0.00	2.257	-4.00	2.302
12	0.00	2.257	-4.00	2.306
13	0.00	2.257	-4.00	2.311
14	0.00	2.257	-4.00	2.316
15	0.00	2.257	4.00	2.322
16	0.00	2.257	-4.00	2.328
17	0.00	2.257	-4.00	2.335
18	0.00	2.257	-6.00	2.346
19	23.10	2.248	17.10	2.315
20	0.00	2.248	-6.00	2.324
21	4.69	2.246	0.69	2.322
22	7.49	2.244	3.49	2.317
23	12.60	2.240	8.60	2.306
24	0.00	2.240	-4.00	2.310
25	0.00	2.239	-4.00	2.315
26	12.11	2.236	8.11	2.305
27	0.00	2.236	-4.00	2.310
28	14.21	2.231	10.21	2.297

Variation of Infiltration and Infiltration and Evaporation with FOS for March

Days	Infiltration (mm/day)	FOS	Difference (mm/day)	FOS
1	5.95	2.244	1.95	2.258
2	9.17	2.241	5.17	2.256
3	8.05	2.238	4.05	2.254
4	0	2.238	-4.00	2.256
5	0	2.238	-2.00	2.257
6	0	2.238	-4.00	2.259
7	1.05	2.238	-2.95	2.260
8	0	2.238	-4.00	2.262
9	34.65	2.229	30.65	2.249
10	2.17	2.228	-1.83	2.250
11	10.78	2.226	6.78	2.248
12	0	2.225	-4.00	2.249
13	6.09	2.224	2.09	2.248
14	4.97	2.222	0.97	2.248
15	52.64	2.211	48.64	2.234
16	0.63	2.210	-3.37	2.234
17	0.77	2.208	-3.23	2.235
18	6.16	2.205	2.16	2.234
19	1.05	2.204	-2.95	2.235
20	0	2.200	-4.00	2.235
21	0	2.200	-4.00	2.236
22	28.7	2.192	24.70	2.229
23	0	2.188	-4.00	2.230
24	9.73	2.183	5.73	2.227
25	3.5	2.179	-0.50	2.227
26	0.14	2.176	-1.86	2.227
27	6.02	2.171	4.02	2.226
28	1.05	2.167	-0.95	2.225
29	0	2.164	-2.00	2.225
30	3.57	2.160	1.57	2.224
31	4.06	2.156	2.06	2.223

Variation of Infiltration and Infiltration and Evaporation with FOS for June

Days	Infiltration (mm/day)	FOS	Difference (mm/day)	FOS
1	32.13	2.247	28.13	2.248
2	1.05	2.246	-2.95	2.249
3	0.00	2.246	-4.00	2.250
4	0.00	2.246	-4.00	2.252
5	0.00	2.245	-4.00	2.253
6	0.00	2.245	-4.00	2.255
7	0.00	2.245	-4.00	2.257
8	0.00	2.245	-4.00	2.259
9	0.00	2.245	-4.00	2.261
10	0.00	2.245	-4.00	2.264
11	0.00	2.245	-2.00	2.265
12	0.00	2.245	-2.00	2.266
13	0.00	2.245	-2.00	2.268
14	16.10	2.240	12.10	2.26
15	0.00	2.240	-8.00	2.265
16	0.00	2.239	-2.00	2.266
17	0.00	2.239	-2.00	2.268
18	0.00	2.239	-2.00	2.269
19	0.00	2.239	-2.00	2.271
20	0.28	2.239	-1.72	2.272
21	0.00	2.239	-2.00	2.274
22	22.05	2.232	20.05	2.261
23	0.00	2.232	-2.00	2.262
24	0.00	2.230	-2.00	2.264
25	0.00	2.230	-2.00	2.265
26	0.00	2.230	-4.00	2.268
27	0.00	2.230	-4.00	2.271
28	0.00	2.230	-4.00	2.274
29	0.00	2.230	-2.00	2.276
30	0.00	2.230	-2.00	2.278

Variation of Infiltration and Infiltration and Evaporation with FOS for December

Days	Infiltration (mm/day)	FOS	Difference (mm/day)	FOS
1	0.00	2.259	-4.00	2.261
2	0.00	2.259	-4.00	2.263
3	25.90	2.249	21.90	2.253
4	1.75	2.248	-2.25	2.254
5	0.98	2.248	-3.02	2.255
6	3.64	2.247	1.64	2.254
7	0.49	2.246	-1.51	2.255
8	0.00	2.246	-2.00	2.256
9	0.84	2.246	-1.16	2.256
10	0.00	2.246	-2.00	2.257
11	0.56	2.246	-3.44	2.259
12	0.00	2.245	-6.00	2.262
13	0.00	2.245	-4.00	2.265
14	0.00	2.245	-4.00	2.267
15	2.03	2.245	-1.97	2.269
16	9.94	2.241	5.94	2.264
17	13.02	2.237	9.02	2.259
18	2.17	2.236	-1.83	2.260
19	10.50	2.233	6.50	2.257
20	17.15	2.228	13.15	2.252
21	2.87	2.227	-1.13	2.252
22	6.16	2.225	2.16	2.251
23	4.13	2.223	0.13	2.251
24	2.45	2.221	-1.55	2.252
25	0.00	2.220	-4.00	2.253
26	0.00	2.220	-4.00	2.255
27	0.70	2.218	-3.30	2.257
28	0.49	2.217	-3.51	2.258
29	0.00	2.216	-4.00	2.260
30	0.00	2.216	-2.00	2.262
31	0.00	2.216	-2.00	2.263